



Discrete reaction waves: Gasless combustion of solid powder mixtures

A.S. Mukasyan^{a,*}, A.S. Rogachev^b

^aDepartment of Chemical and Biomolecular Engineering, Center for Molecularly Engineered Materials, University of Notre Dame, Notre Dame, IN 46556, USA

^bInstitute of Structural Macrokinetics and Materials Science, Russian Academy of Sciences, Chernogolovka 123432, Russia

Received 4 April 2007; accepted 10 September 2007

Available online 26 November 2007

Abstract

This review considers a specific domain in combustion science, so-called *discrete* combustion waves, which have been observed in a variety of processes including combustion synthesis of materials, burning of solid propellants, coals and biomass. The main objective of this work is to discuss the relevant experimental and theoretical results and to bring to light the fundamental nature of this phenomenon. The criteria for distinguishing between the homogeneous and discrete combustion waves based on the analysis of local and global behavior of the reaction systems have been discussed. Different theoretical models that account the discrete nature of the process are critically overviewed and compared with experimental results. It was concluded that combustion occurs in quasi-homogeneous or discrete modes depending on the ratio of characteristic times of chemical reaction and heat transfer in the heterogeneous medium.

© 2007 Elsevier Ltd. All rights reserved.

Keywords: Heterogeneous combustion wave; Mechanisms of flame propagation; Self-propagating high-temperature synthesis; Combustion synthesis; Discrete and quasi-homogeneous models

Contents

1. Introduction	378
2. Experimental results.	379
2.1. Combustion velocity	380
2.2. Temperature–time history	383
2.3. Global and local behavior of combustion waves: relation to microstructure of the reaction media	385
3. Theoretical models for discrete combustion	388
3.1. Discrete combustion waves: evolution of ideas.	388
3.2. Contemporary theoretical models of discrete combustion	390
3.2.1. One-dimensional discrete models with zero-order Arrhenius-type kinetics	391
3.2.2. One-dimensional discrete models with stepwise kinetics	393
3.2.3. Two-dimensional discrete models	394
3.2.4. Discrete models with homogeneous heat transfer.	396
3.3. Summary of the theoretical models.	398
4. Comparison of experimental and theoretical results	399
4.1. Microscopic aspects.	399
4.2. Thermal and chemical heterogeneity of the reaction media	400
4.3. Global characteristics of combustion processes	404
4.4. Combustion in model heterogeneous systems.	407

*Corresponding author. Tel.: +1 574 631 9825; fax: +1 574 631 8366.

E-mail address: amoukasi@nd.edu (A.S. Mukasyan).

5. Concluding remarks. 410
 Acknowledgments 412
 References 412

1. Introduction

A combustion wave represents a self-organized system where a chemical reaction, localized in the vicinity of the reaction front, propagates throughout the reaction media, converting initial reactants into combustion products. Depending on the nature of reaction media, we can distinguish homogeneous combustion processes, such as premixed gas flames, and heterogeneous combustion, when the reaction medium consists of several phases. Analysis of works published in the last decade in the field of heterogeneous combustion leads to the conclusion that a “critical mass” of experimental and theoretical data has been accumulated, which may initiate a new domain in combustion science, so-called *discrete* combustion waves. This phenomenon has been observed in a variety of processes including combustion synthesis of materials [1–4], burning of solid propellants [5–7], coals and biomass [8–10], forest fires [11–13], reaction propagation in fluidized beds [14–16] and in clouds of solid particles or spray combustion [17–19]. The main objective of this work is to discuss the relevant experimental and theoretical results and to bring to light the fundamental nature of this phenomenon. It is worth noting that in this review we primarily focus on gasless combustion of solid powder mixtures, which represents a typical example of discrete combustion waves.

To differentiate continuous and discrete combustion waves, let us first recall some basic concepts of combustion wave propagation. It is commonly accepted that steady-state combustion represents an important class of auto-wave processes, where invariable space distributions of temperature, concentrations, density, etc., propagate with constant velocity, U , through the reactive medium [20]. For example, in a one-dimensional (1D) case, this means that the temperature at any random point with coordinate, x_1 , and instantaneous time, t_1 , can be related to the temperature of any other point x_2 (see Fig. 1a) by the following equation:

$$T(x_1, t_1) = T(x_2, t_1 + (x_2 - x_1)/U). \tag{1}$$

Note that values of x_1 and x_2 can be taken randomly only if the medium is a strictly homogeneous continuum. Taking into account the discrete atomic nature of matter, one can admit that no real media fits this requirement for an arbitrarily small volume. As the scale of the region under consideration is gradually decreased, at some step, when the media heterogeneity becomes noticeable, the selection of x_i points influences relation (1), and thus the process cannot be described as homogeneous. The critical dimension can be as small as the size of a molecule

(combustion of gas mixtures) or as large as the size of a tree (forest fire).

In general, a homogeneous approach can be applied to describe combustion processes with high accuracy when the critical size of heterogeneity is small compared to the thickness of the combustion wave. In this case, the spatial fluctuations of temperature and concentration can be neglected. In classical works [21,22], it was shown that the continuous approach is applicable for describing premixed gas flame propagation based on the following experimental observations: (a) the thickness of the preheated zone far exceeds the free path of molecules in the gas and (b) the characteristic time of chemical reaction (t_{cr}) is much larger than the time of heat transfer in gas phase media (t_{ht}). The latter is explained by the fact that the energy exchange occurs during any collision between molecules, but only a small fraction of these collisions results in chemical conversion.

In turn, heterogeneous condensed systems, such as powder mixtures, solid propellants, clouds of coal particles, and many others, are characterized by relatively large scales of heterogeneity (usually comparable with the particle size of the reactants). In addition, such media involves not only particles, but also boundary regions between them. These elements (particles and boundaries) typically have different physical and chemical properties and as a rule, auto-wave solutions cannot be used to

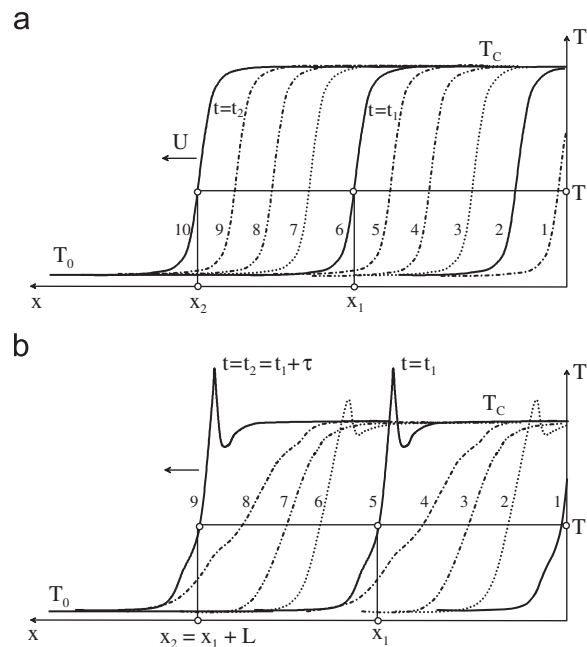


Fig. 1. Typical temperature time profiles for different combustion regimes: (a) homogeneous and (b) discrete.

describe the combustion process on a scale comparable with the scale of media heterogeneity. Nevertheless, combustion reactions propagate through such media in a wave-like manner, and average combustion velocity (measured for a scale much larger than the particle size) can be considered as approximately constant.

Does this mean that the homogeneous approach can be used as a proper approximation for describing combustion in all heterogeneous condensed systems? At first glance, the answer is straightforward: the smaller the particle size (down to the size of molecules), the better the approximation provided by the homogeneous model. However, similar to a gas flame, one of the main criteria for applicability of the continuum approximation is not the reactant size, but the ratio of the characteristic times for chemical reaction and energy (heat) transfer. Recall that the homogeneous approximation works well if the time of heat exchange (t_{ht}) in the heterogeneous medium is much less than the time of chemical reaction (t_{cr}) in the considered system, i.e. $t_{cr} \ll t_{ht}$. In the opposite limiting case, when $t_{cr} \gg t_{ht}$, it should be expected that propagation of the combustion front occurs as an intermittent sequence of discrete local “explosions”, which correspond to rapid exothermic reaction within some elementary reaction cell. Evidently, such a process cannot be described as a steady-state propagation of the invariable temperature profile, as shown in Fig. 1a for the homogeneous combustion wave. Rather, the self-sustained propagation of “explosions” should exhibit oscillatory-type T-profiles (see Fig. 1b), where the “super-adiabatic peak” corresponds to rapid reaction within the cell followed by relatively slow heat dissipation into the neighboring cells until their “ignition”. We designate this kind of reaction propagation as a *discrete* combustion wave.

For example, in the case of combustion of a 1D chain of elemental chemical cells, the temperature profile undergoes periodic oscillations with some period, $\tau = L/\langle U \rangle$, where L is the size of a reaction cell, and $\langle U \rangle$ is the average combustion velocity, measured during a period of time much longer than τ . With this, condition (1) can be rewritten as follows:

$$T(x_1, t_1) = T(x_1 + nL, t_1 + n\tau), \quad (2)$$

where $n = 1, 2, 3, \dots$ (i.e. natural numbers). This means that if any spatial temperature distribution $T(x)$ takes place at time t_1 , a similar temperature profile will be reproduced only after discrete time- and space-intervals.

Various heterogeneous media give a wide variety of reaction cells with different sizes, ranging from microns in powder mixtures to meters for a forest fire (where the reaction cell is the crown of a tree). As noted above, in this review we focus on micro-heterogeneous systems, with a scale of heterogeneity on the order of 1–100 μm . These, for example, include powder mixtures for combustion synthesis of materials, pyrotechnical systems, and some solid propellants.

In Section 2 of this work, recent experimental results that illustrate the specifics of discrete waves are discussed. Most of the data on microstructure and thermal structure of the combustion waves was obtained by means of high-speed micro-video recording, as well as micro-pyrometry, and thermal vision techniques. In Section 3, theoretical models and results of computer simulations of discrete wave propagation in gasless powder media are reviewed, and evolution of the related ideas is traced from the classical works of the end of the 19th century to the present day. Section 4 is devoted to a comparison of theoretical predictions and experimental results. The objective of this section is to describe criteria for distinguishing between the homogeneous and discrete combustion waves based on the analysis of local and global behavior of the reaction systems.

2. Experimental results

The velocity of the reaction front propagation and the temperature–time history for any random point of the reaction medium are two major macroscopic parameters that define the combustion wave behavior in different systems [23,24]. One of the main tasks is to establish a relation between these parameters and to define the specific regions for different combustion regimes (e.g. steady-state, pulsating, spin, chaotic, etc.). According to homogeneous theory, in the case of steady-state propagation the combustion velocity is strictly constant, and the temperature profile simply shifts with this velocity, maintaining its shape and values. Observation of the non-steady state (by the above description) combustion waves may be explained either by the loss of reaction front stability (pulsations, extinction, etc.) or by manifestation of the discrete combustion mode. The specific experimental approaches were used to define the differences between these two cases.

The temperature profiles of combustion processes are measured by thermocouples, point and linear pyrometers, and 2D thermal video systems [25–31]. The combustion front velocity is commonly determined by photo-registration method, frame-by-frame treatment of the movie and video recordings, or from data obtained by sets of thermocouples (photo-diodes) located at fixed distance intervals along the burning sample [32–35]. It is well recognized that in order to obtain reliable data on the investigated phenomenon, the researcher needs to use experimental techniques with certain scales of space and time resolutions, which in turn are determined by the characteristic scales of the considered process. For example, it was shown that to obtain an accurate *thermal structure* of the combustion wave in heterogeneous systems, such as Nb–B, Ti–Si and Ti–C powder mixtures, the thickness of the thermocouple used for recording temperature profiles should be less than the width of the reaction front (i.e. $< 10 \mu\text{m}$) [26]. Also the characteristic *scale of heterogeneity* in such reaction systems is on the

order of the precursors dimensions (i.e. a few microns). For example, powders with a wide range of particle sizes (i.e., $d \sim 1\text{--}10^2 \mu\text{m}$) are used for combustion synthesis of advanced materials [14–16]. Under typical conditions, $d \sim 10 \mu\text{m}$ and $U_c \sim 1 \text{cm/s}$, the reaction front travels the distance of one particle in $\sim 10^{-3} \text{s}$. Thus, for in-situ studies of the phenomenon, an apparatus that allows the process to be observed with a spatial resolution on the micron level and time scale on the order of microseconds must be used. In the past 10–15 years, several methods that permit the measurement of combustion parameters with such time and spatial resolutions have been developed. Let us overview some recent results obtained through the use of such unique diagnostics to study the process of combustion wave propagation in porous powder mixtures.

2.1. Combustion velocity

High-speed micro-video recording (HSMVR) is the most effective technique that provides the required characteristics for observation of the combustion wave propagation in heterogeneous media. Beginning with high-speed film recording [36,37], development of the method progressed by utilizing analog [38–40] and digital [41,42] cameras, as well as further enhancement of lighting conditions and optical systems [43].

The scheme of an HSMVR set-up is shown in Fig. 2. Propagation of the reaction wave is observed through a quartz window in the reactor by using a long-focus microscope attached to a digital high-speed video camera and processor. The spatial resolution of the microscope (e.g. K-2, Infinity Photo-Optical, Boulder, CO) can be as high as $1.7 \mu\text{m}$ with magnification up to $1000\times$. These values are probably close to the physical limits of the method. Achieving higher resolution could be possible by using short-focus objective lenses (as is typical for metallographic microscopes); however, the severe conditions near the combustion wave do not allow one to decrease the distance between the burning sample and the lens. Perhaps,

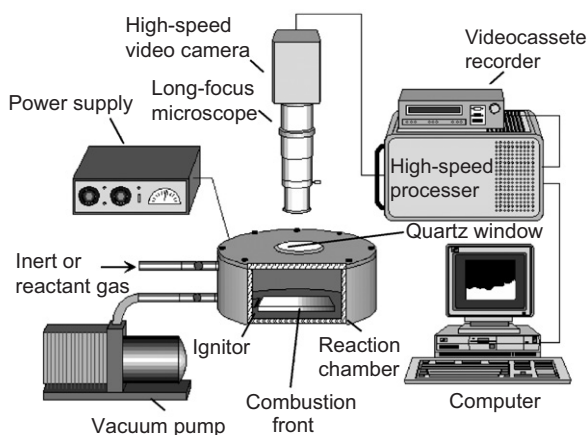


Fig. 2. Experimental setup for microscopic high-speed video recording of the combustion wave propagation (adopted from Ref. [2]).

development of novel optical methods, such as scanning laser microscopy etc., can help to overcome this obstacle.

The high-resolution, high-speed video camera attached to the microscope records the events, and the images are transferred to the intermediate digital processor or directly to the computer memory. The recording rate depends on the desired size and quality of the picture. For example, for black-and-white recording, with a frame size of about 768×512 pixels, the recording rate is in the range of 300–1000 frames/s. Rate up to 50,000 frames/s can be achieved by decreasing the frame size. Additionally, strong illumination (highlighting) of the surface allows one to monitor both initial reaction media and the reacted part of the sample. In contrast to space resolution, the time resolution (recording rate) of digital video cameras has increased rapidly, and high-speed cameras are becoming more available for routine combustion experiments.

Digital images, transferred to the computer memory, can be processed and analyzed to yield quantitative characteristics of the reaction wave structure by utilizing specially developed or commercially available software packages for image analysis. The latter gives state-of-the-art imaging and analysis capabilities, which includes measuring object attributes such as: area, diameter, aspect ratio, as well as object numbers and center-to-center distance between them [44,45]. Typically, in conjunction with the HSMVR method, a conventional video camera (24–30 frames/s) is used, which provides a macroscopic view of the process.

A variety of reaction processes were investigated by high-speed recording, including combustion of propellants, coals, metal–nonmetal (e.g. Ti–C, Ti–Si), metal–metal (e.g. Ni–Al, Ti–Al), thermite (Al–Fe₂O₃), and metal–gas (e.g. Ti–N₂) systems [46–51]. Among several important observations, let us consider those which are related to the measurement of the combustion front velocity. These results are critical for understanding the fundamental concept of combustion wave propagation in heterogeneous systems.

For a majority of the above-mentioned systems (e.g. Ti–C, Ti–Si, Ni–Al, Ti–N), the existence of an essentially flat combustion front, which under certain experimental conditions propagates in a steady-state manner (i.e. with constant velocity), is a well-established experimental fact. However, this conclusion was made based on phenomenon observation by conventional video camera (i.e. a spatial resolution $\Delta_r \sim 0.1 \text{mm}$ and time scale $\Delta_t \sim 10^{-1} \text{s}$, Fig. 3a). Monitoring of the same processes using HSMVR with $\Delta_r \sim 10^{-4} \mu\text{m}$ and $\Delta_t \sim 10^{-4} \text{s}$ (Fig. 3b) unequivocally revealed that on the microscopic scale, the reaction front has an irregular shape and propagates in a sequence of rapid “jumps” and long-term hesitations (i.e. with chaotic oscillations in local velocity) [37–45].

The local random perturbations of the combustion front cause some difficulties in the precise measurement of combustion velocity. In the case of strictly homogeneous steady-state combustion, any point of the reaction front with some chosen value of temperature (within the range

$T_0 < T < T_C$) can be used as a marker for measuring its velocity. In the presence of local perturbations, different points of the temperature profile move with different

velocities. Therefore, determination of the combustion front position and its propagating velocity becomes a nontrivial task. Methods for determining the combustion front position, its roughness, instantaneous local velocity, etc. are discussed in several publications [39–42,45].

Fig. 4 illustrates one of the possible ways for determining the location of the combustion front. The original image (Fig. 4a) is converted to a matrix of brightness intensity levels (Fig. 4b). The intersection of the matrix with the threshold intensity (see [53] for the algorithm for finding the threshold) separates the reacted and unreacted parts of the sample and corresponds to the instantaneous location, $F(x,y)$, of the combustion front (Fig. 4c). Another way is to determine the point of maximum gradient of the temperature (or brightness) at the combustion front and monitor movement of this point [54]. At first glance, the value of the chosen temperature (or its gradient) may influence the obtained value of combustion velocity leading to uncertainty in experimental results. However, the thickness of the combustion front is usually very small and comparable with the space resolution of the optical systems used in experiments. Thus, the exact selection of the marker point, while it is within the width of combustion front (preheating + reaction zones), does not significantly affect the measurements.

An average combustion front profile $\bar{F}(t)$ was introduced (see Fig. 4d) based on the relation:

$$\bar{F}(t) = \frac{\int_0^{y_0} F(y, t) dy}{y_0},$$

where y_0 is the width of the investigated sample surface.

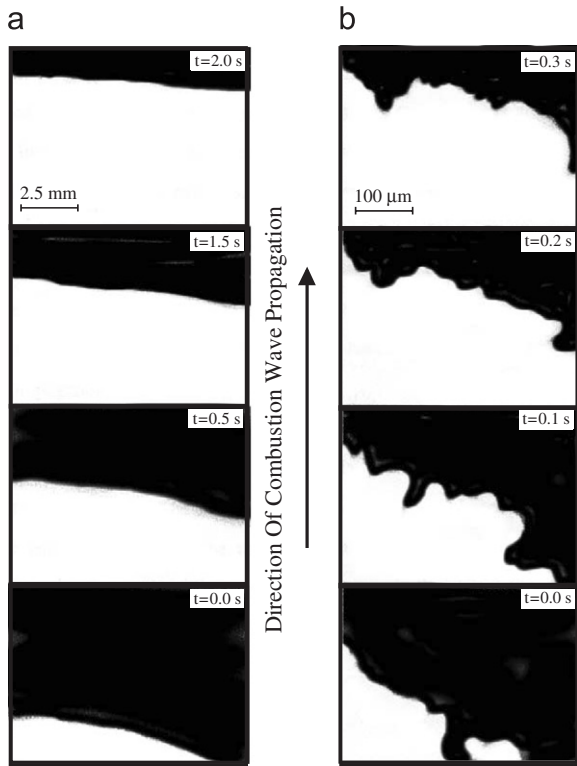


Fig. 3. Frames of the combustion front propagation for the 5Ti–3Si system obtained with different magnifications and imaging rates: (a) 4 × and 30 frames/s and (b) 100 × and 1000 frames/s (adopted from Ref. [52]).

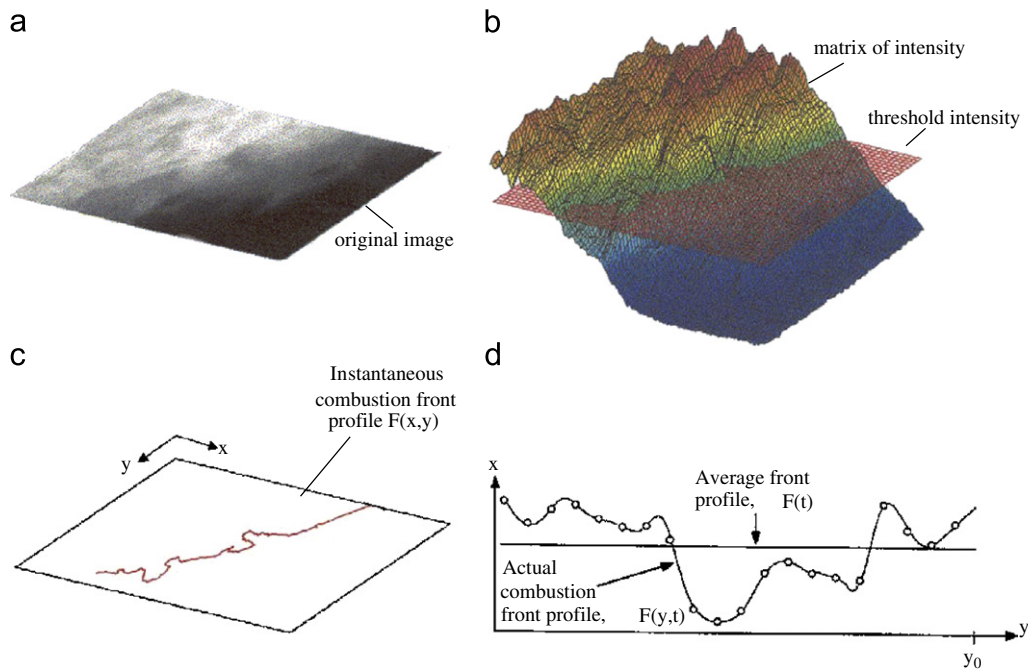


Fig. 4. Estimation of the combustion front location: (a) original image; (b) matrix of the brightness level; (c) subsequent wave front and (d) average front (adopted from Ref. [42]).

Once $F(x,y)$ and $\bar{F}(t)$ are found for the series of video images, the heterogeneity of the combustion front can be characterized in many ways. For example, a set of parameters that characterizes the combustion front *shape* (e.g. average front length (l) and its dispersion (s_F, σ_F)) were suggested (see Table 1). A group of functions that describe the combustion front *propagation* were also introduced (Table 2). Specifically, the instantaneous velocity of the combustion front, $U_{inst}(y,t)$, projected along lines parallel to the macroscopic direction of the wave propagation, is determined by measuring the distance the combustion front moves along the axis in one time step:

$$U_{inst}(y, t) = \frac{\partial F(y, t)}{\partial t} = \frac{F(y, t_j) - F(y, t_{j-1})}{t_j - t_{j-1}}.$$

By conducting a statistical treatment on the video frames obtained by the HSMVR technique, it was shown that the transition from the steady-state to the jump-hesitation regime can be achieved by changing sample density [39–42]. To illustrate this important observation, let us compare experimental results obtained on combustion in the Ni–Al system [55]. Fig. 5 represents the distributions of the instantaneous combustion velocities, U_{inst} , for samples with relatively high (Fig. 5a) and low (Fig. 5b) initial densities. It can be seen that for dense reaction media, the

U_{inst} distribution is *unimodal*, narrow ($\Delta U_{1/2}/U_{max} < 5\%$) and its maximum exactly coincides with the average value of the combustion velocity, U_c^{av} , which was measured by conventional video camera. However, in the case of less dense samples, this distribution is noticeably different and involves two maxima (Fig. 5b). It is important that the most prevalent velocity (U_{max}^I) *approaches zero*, i.e. the combustion front is momentarily stationary. It means that most of the time the reaction front *hesitates!* The second peak (U_{max}^{II}) is wide and its maximum value *exceeds* the average macroscopic combustion velocity. Interesting that observation of the same process by conventional video camera (time scale $\sim 5 \times 10^{-2}$ s) gives an unconditional illusion of the steady-state process!

These experimental data led to the formulation of a new mechanism for combustion wave propagation in gasless heterogeneous media. This concept affirms that the process of reaction front propagation possesses a jump-hesitation (discrete) character and involves two stages: (a) *rapid burning* ($t_b \sim 10^{-4}$ s) of the specific local area (so-called elemental reaction cells), and (b) a relatively *long* ($t_{ind} \sim 10^{-2}$ s) *ignition delay* stage during which the next reaction cell is preheated. Since in this case one region successively ignites the other, this mechanism has been named *relay-race* [39,40]. The existence of such phenomena

Table 1
Characterization of combustion front shape (adopted from Refs. [132,157])

Characteristics	Value at time t	Over experimental duration
Range	$R_F(t) = \max_y[F(y, t)] - \min_y[F(y, t)]$	$\bar{R}_F(t) = \frac{\int_{t_0}^{t_f} R_F(t') dt'}{t_f - t_0}$
Dispersion	$s_F(t) = \sqrt{\frac{\int_0^{y_0} [\bar{F}(t) - F(y, t)]^2 dy}{y_0}}$	$\sigma_F(t) = \sqrt{\frac{\int_{t_0}^{t_f} \int_0^{y_0} [\bar{F}(t) - F(y, t)]^2 dy dt}{y_0(t_f - t_0)}}$
Length	$l(t) = \frac{1}{y_0} \int_0^{y_0} \sqrt{\left\{ 1 + \left(\frac{\partial F(y, t)}{\partial t} \right)^2 \right\}} dy$	$\bar{l} = \frac{\int_{t_0}^{t_f} l(t') dt'}{(t_f - t_0)}$

Table 2
Characterization of combustion wave propagation (adopted from Refs. [132,157])

Characteristics	Value at time t	Over experimental duration
Range	$R_U(t) = \max_y[U(y, t)] - \min_y[U(y, t)]$	$\bar{R}_U(t) = \frac{\int_{t_0}^{t_f} R_U(t') dt'}{t_f - t_0}$
Average	$\bar{U}(t) = \frac{\int_0^{y_0} U(y) dy}{y_0}$	$\bar{\bar{U}}(t) = \frac{\int_{t_0}^{t_f} \int_0^{y_0} U(y) dy dt}{y_0(t_f - t_0)}$
Dispersion	$s_U(t) = \sqrt{\frac{\int_0^{y_0} [\bar{U}(t) - U(y, t)]^2 dy}{y_0}}$	$\sigma_U(t) = \sqrt{\frac{\int_{t_0}^{t_f} \int_0^{y_0} [\bar{U}(t) - U(y, t)]^2 dy dt}{y_0(t_f - t_0)}}$

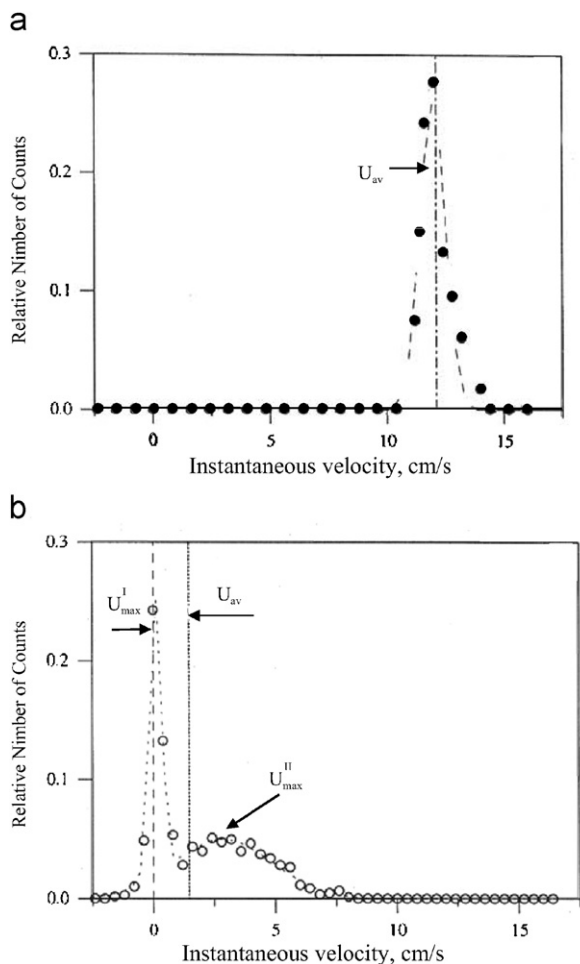


Fig. 5. Typical distribution of the instantaneous combustion velocities in a heterogeneous system for different combustion modes: (a) homogeneous and (b) heterogeneous (adopted from Ref. [55]).

was explained by the micro-heterogeneous nature of the reaction media that consists of reaction particles with a varying “quality” of inter-particle contacts, which is discussed in details below.

2.2. Temperature–time history

Qualitative consideration of the brightness maps obtained by micro-video recording with high magnification, assuming that in general the brighter areas have a higher temperature compared to the darker regions, brought other unusual observations [2]. For example it was shown that in many systems (e.g. Ti–Si, Ni–Al, Ti–C, etc.) temperature is not uniformly distributed in the combustion front. More specifically, relatively small (10–100 μm) bright (“hot”) spots randomly appear in the vicinity of the reaction front, indicating local (discrete) regions of very high temperatures (Fig. 6). Some of these spots tarnish, and dissipate, others initiate the reaction in the neighboring areas, leading to a virtual propagation of the high temperature spots *along the lateral direction* of the front. It was also shown that the front moves forward as a consequence of the appearance of

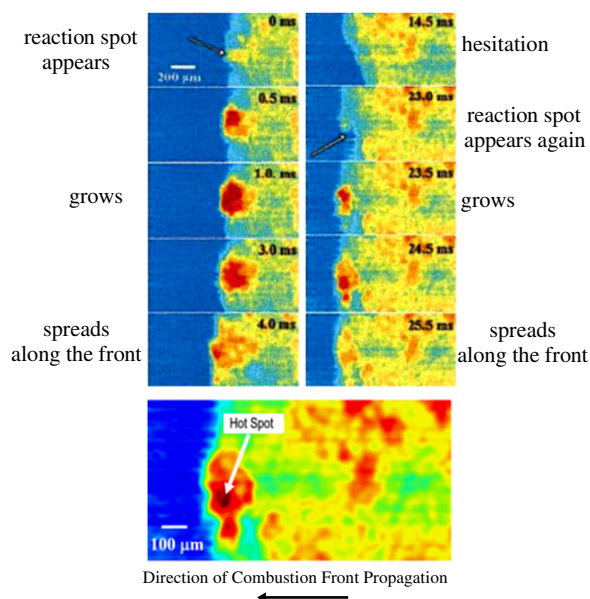


Fig. 6. Frames of the combustion front propagation illustrating the scintillating character of the reaction wave (adopted from Ref. [2]).

hot spots and the overall progress of the front occurs only locally in the vicinity of such high temperature regions [2,43,45]. It means that during the periods of time when the hot spots are absent, the reaction front hesitates. Taking into account all of these features, this mode was designated as a “*scintillating reaction wave*” (SRW).

Typical 2D and 3D representations of thermal structures in the Ti–Si system are shown in Fig. 7. It is worth noting that the temperature of the hot regions *exceeds* the average temperature of the reaction front. Based on this observation, it was concluded that in these local overheating (scintillation) zones, the reaction rate is so high that the characteristic reaction time is much less than the time required for heat dissipation into the surrounding media. Similar, hot spot type, temperature maps were obtained for combustion of solid fuels [3]. For example, Fig. 8 shows the thermal heterogeneity of the combustion wave in the Fe–KMnO₄ system.

More accurate methods to obtain data on the combustion wave thermal structure are related to the utilization of thermocouples and pyrometers. In the former case, because of the high-temperature gradients occurring in the combustion wave, very thin thermocouples (with diameter less than width of the reaction front, i.e. 7–10 μm) with a small relaxation time should be used [26]. A variety of systems were investigated by this method and the obtained results contributed to a deeper understanding of the reaction mechanisms [56,57]. Analysis of such temperature profiles by applying, for example, the Boddington–Laye method, allow one to extract the kinetics parameters of rapid combustion reactions [27,58,59]. However, the reliability and reproducibility of this technique is not always sufficient [60], especially in the case of monitoring the stochastic distribution of high temperature regions along the sample surface.

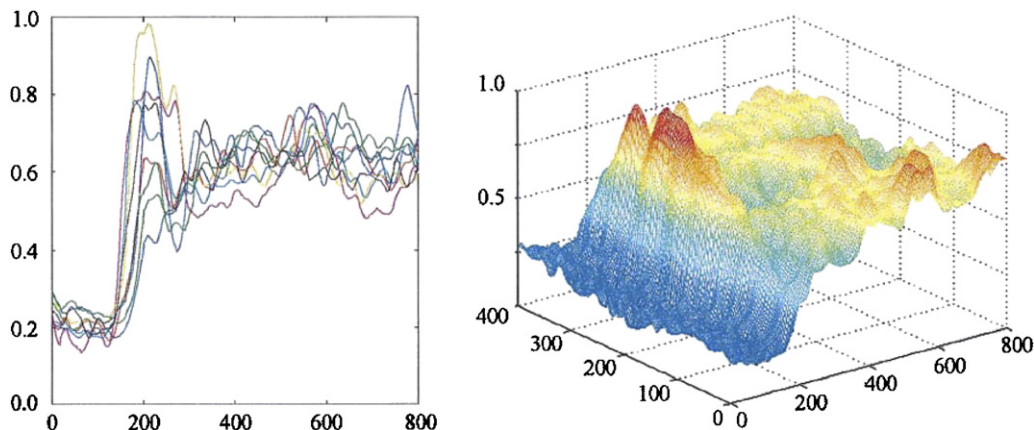


Fig. 7. Thermal structures of a scintillating reaction wave (adopted from Ref. [2]).

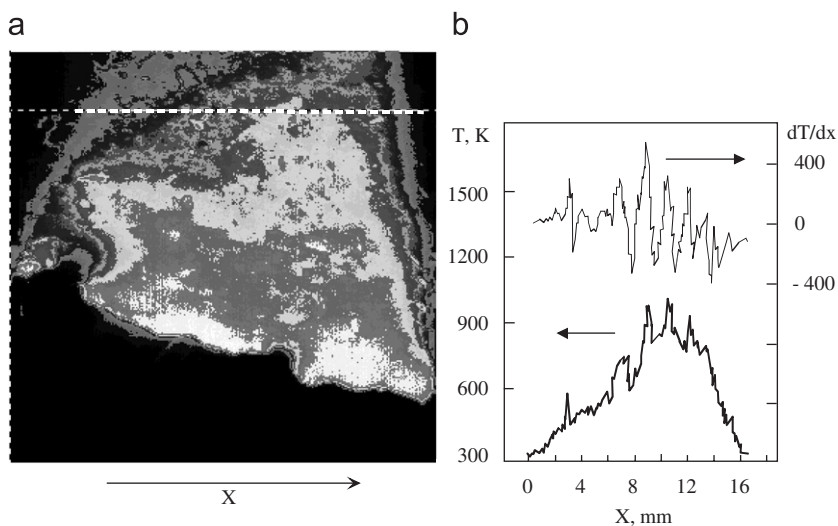


Fig. 8. (a) 2D-temperature map of combustion front propagation and (b) temperature and temperature gradient distributions along selected cross section (adopted from Ref. [3]).

Recently, rapid high-resolution optical pyrometers were developed to meet the specific need for studying propagation of high-temperature heterogeneous reactions. For example, a two-color linear 2D array device, built on the basis of high-resolution CCD light detectors, allow one to reach spatial resolution of $1\ \mu\text{m}$ and monitor the combustion wave propagation every $10^{-2}\ \text{s}$ [61]. The scheme of the experimental apparatus is shown in Fig. 9. The linear detectors consist of 1024 sensing elements, $13 \times 13\ \mu\text{m}$ each. The two wavelengths (750 and 850 nm) were selected by using narrow-band (10 nm) interference filters (Fig. 9b). An even faster apparatus, (time scale $10^{-6}\ \text{s}$) however, with lower spatial resolution ($100\ \mu\text{m}$) was designed and constructed by another group [62].

Examples of temperature profiles obtained during the combustion of a Zr+CoO system using a CCD-based pyrometer are presented in Fig. 10. It can be seen that the sharp temperature peaks are present at the beginning of each profile (Fig. 10a). Analysis of such data revealed that some of these peaks are attributed to the formation of small cracks on the sample surface. However, the others

are directly related to the existence of the “hot” spot regions described above.

Another example of temperature profiles captured by a high-speed pyrometer for the Ni–Al mixture is shown in Fig. 11 [62]. It was statistically proven that complex temperature–time dependencies characterize the interaction in this system. While inflection points and saturated regions can be explained based on the analysis of the system phase diagram [29], the observed temperature peaks are a direct confirmation of the “hot” spot appearances, followed by the process of energy dissipation to the neighboring regions.

Further, it was suggested that hot spots form in the locations of the most refractory reactant (e.g. Ti in Ti–Si system) at the melting point of the other reactant (Si) [2,50]. Indeed, in initial solid porous media (Ti+Si), the contact area between the particles is small, which leads to relatively slow heat conduction and negligible reaction rates. A significant intensification of chemical interaction occurs at the melting point of the less refractory reactant (e.g. Si). For example, when temperature in the vicinity of a Ti particle reaches $1410\ ^\circ\text{C}$, silicon melts and rapidly

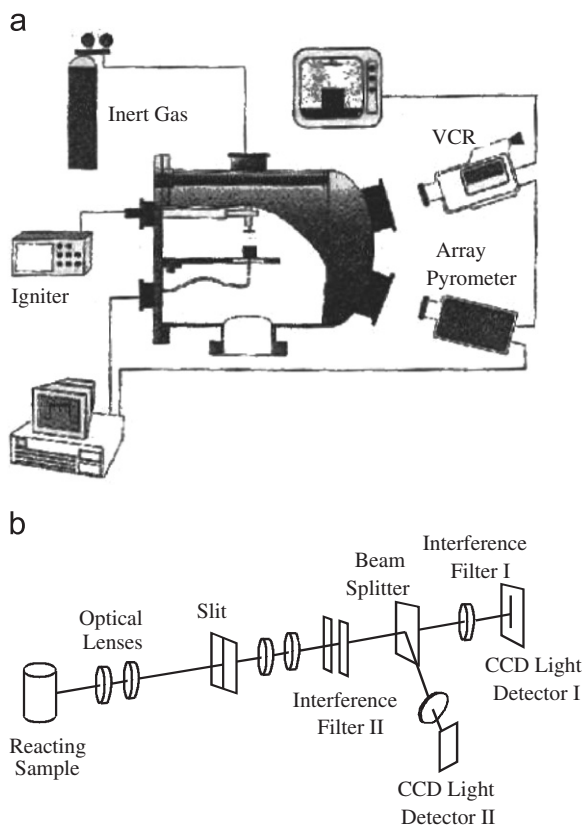


Fig. 9. Schematic representations of (a) experimental apparatus and (b) the two-color array pyrometer (adopted from Ref. [61]).

spreads over the surface of a solid Ti particle with simultaneous chemical reaction (so-called “reaction-spreading”). Hence, the reactant melting point is indicative of the ignition temperature (T_{ig}), which is much smaller than the maximum combustion temperature, T_c . Since the temperature of the media just before “ignition” is much greater than T_0 , and the reaction time is so small, the generated heat does not have enough time to dissipate from the local area, causing a maximum temperature in the hot spot that can be significantly higher than the “adiabatic” combustion temperature.

In conclusion, recent experimental observations conducted by means of different time-resolved techniques, show that, when observed on time scales of $\sim 10^{-3}$ – 10^{-4} s and at spatial resolutions on the order of the scale of heterogeneity of the discrete system, the combustion front moves as a sequence of rapid jumps and hesitation with random formation of localized high-temperature regions, which stimulate the reaction propagation. It became clear that the aforementioned features are related to the microstructural characteristics of the initial reaction media, and thus it was critical to find out these relations.

2.3. Global and local behavior of combustion waves: relation to microstructure of the reaction media

A considerable amount of published experimental data on the dependencies of combustion parameters (i.e. U_c and

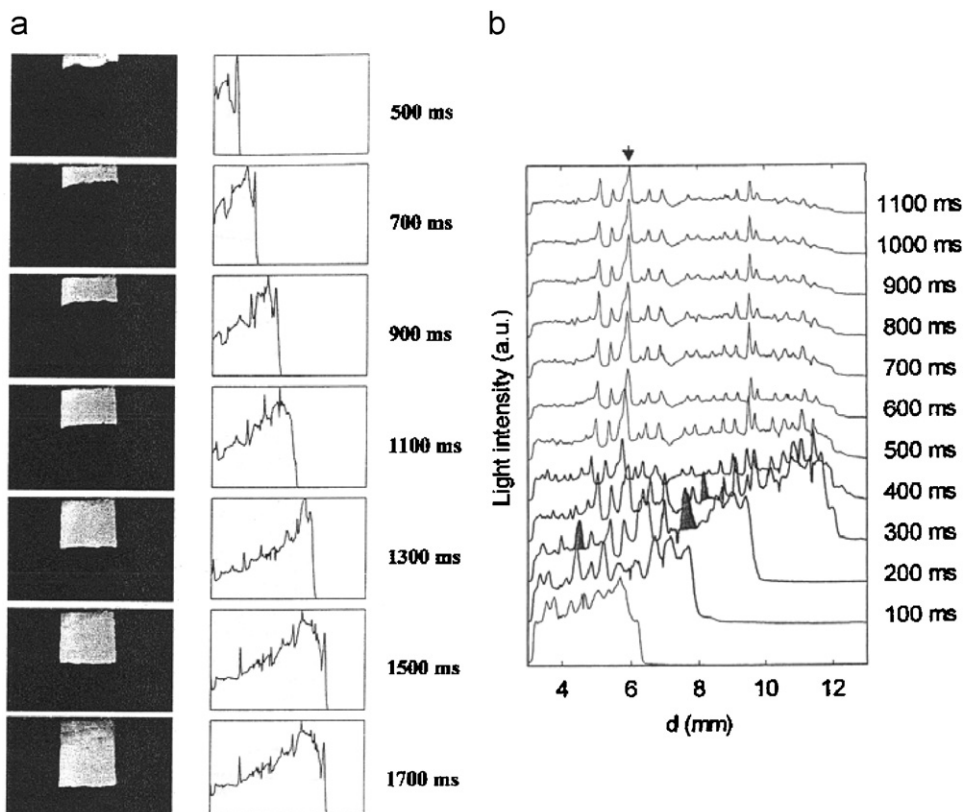


Fig. 10. (a) Video images and instantaneous light-intensity profiles (LIPs) for reaction front propagation in the Zr + NiO system and (b) set of LIPs over the experimental duration (adopted from Ref. [61]).

$T(t)$) versus different process factors (e.g. reaction media composition, its porosity, reactant particle size, etc.) are difficult to explain based on the classical concepts of combustion phenomena. For example, Fig. 12a represents the burning rates for amorphous and crystalline boron with

different oxidizers as a function of boron/oxidizer ratio. It can be seen that no common trend can be attributed to these data. However, an accurate statistical analysis of the initial mixture microstructure revealed the parameter that makes sense of this complex “irregular” picture. It was shown that the contact surface area between boron and oxidizer per volume (S) is a parameter that is responsible for the variation of combustion velocity. Indeed, the same data for U_c re-plotted versus S gives a straight line (Fig. 12b). Similar relations were found for other systems such as Al-AP-PMMA and Zr-AP-PMMA [3] (where AP is ammonium perchlorate and PMMA is polymethyl methacrylate).

Also, detailed studies demonstrate that in many systems (e.g. solid rocket propellants, pyrotechnic mixtures, and spray combustion) the combustion limits are defined by the formation of the percolation cluster, i.e. a continuous net of contacting reactants on the burning surface [63–66]. For example, it was shown that at some critical volume concentration of metal in different heterogeneous condensed systems, a sharp change of combustion velocity occurs (see Fig. 13). It was also reported that for a variety of systems (metal-metal, metal-AP/PMMA, etc.) the critical concentration of metal component is essentially constant (~ 16 vol%). Statistical treatment of the samples

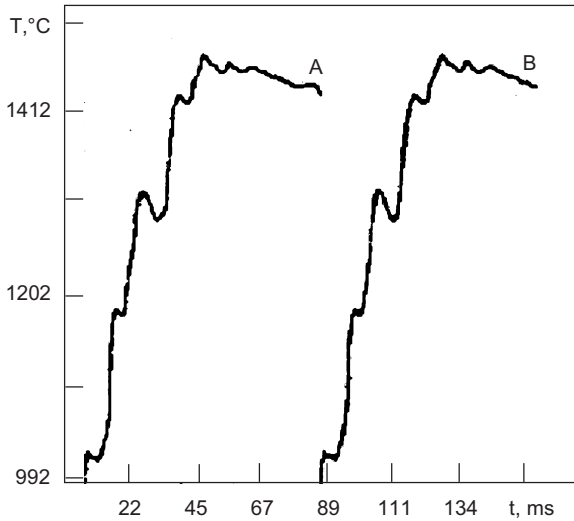


Fig. 11. Temperature profiles of combustion wave propagation in the Ni-Al system at two points 1 mm apart (adopted from Ref. [62]).

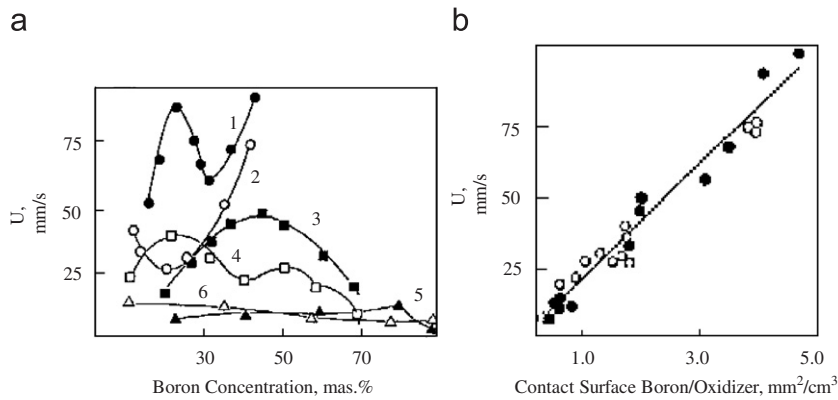


Fig. 12. Combustion velocity in different boron-oxidizer systems as a function of (a) boron concentration and (b) contact surface between boron and oxidizer (adopted from Ref. [3]).

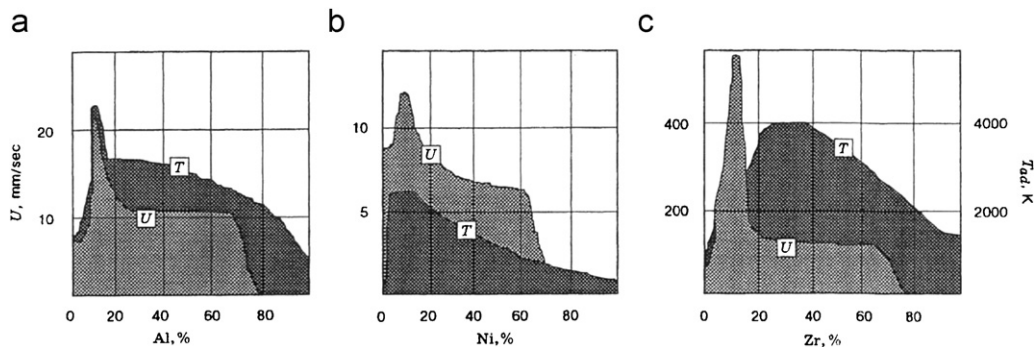


Fig. 13. Dependencies of combustion velocity and temperature as a function of relative volume content of the metal in the different systems: (a) Al/AP/PMMA; (b) Ni/AP/PMMA and (c) Zr/AP/PMMA (adopted from Ref. [64]).

cross section revealed that at this specific concentration, percolation clusters are formed in the reactive heterogeneous media [3,64]. These results suggest that the observed thermal heterogeneity of the reaction front should correlate with the microstructure of the reaction media.

To verify this hypothesis, microstructural parameters of the reaction media should be quantitatively compared with the suitable features of the combustion wave [44,45]. While microstructural characteristics of heterogeneous media (such as average particle and pore sizes, their distributions, contact surface area, etc.) are well known, the microstructural parameters of the combustion wave should be defined.

Let us consider an example. Typical backscattering electron images of the microstructures for initial reaction media in the Ti–Si system with different Ti particle size are presented in Fig. 14 (light phase: Ti; gray: Si; black: pore) [48]. It can be seen that the microstructure consists of relatively large Ti particles surrounded by smaller particles of Si as well as many fine pores (1–2 μm) and a few randomly distributed coarse pores ($\sim 10 \mu\text{m}$). The corresponding values of different parameters, which are characteristics of these structures and obtained by computer analysis of images using the IMAGE-PROPLUS package, are presented in Table 3.

In turn, the sequences of video micro-images of combustion wave propagation in such media (see Fig. 6),

were also statistically analyzed. The microstructural features of the SRW were described through many parameters including a size distribution of the hot spots and the distance between them, their lifetime (the period between the appearance of a bright spot and the moment when its brightness equals that of the combustion product), and time intervals between the appearance of hot spots (for some predetermined area or along an arbitrarily selected line). Some of these data are also presented in Table 3.

Comparison of the obtained results demonstrates a good correlation between the microstructural characteristics of the initial reaction media and those for the combustion wave. Indeed, for coarse powders ($> 40 \mu\text{m}$), the specific number of Ti particles approximately equals the number of hot spots observed during the combustion process. This essentially means that every Ti particle forms a hot spot. However, for finer Ti particles, the average hot spot is formed by several (3–5) such particles (a cluster). It can also be seen that several parameters of SRW, such as the number and size of hot spots, and the average distance between their appearances, strongly correlate with the number, size and location of titanium particles. It is important that the typical lifetime of the hot spots in the local area is at least ten times shorter than the time between consecutive appearances of hot spots in the same area. It was found that this “delay” time increases with increasing

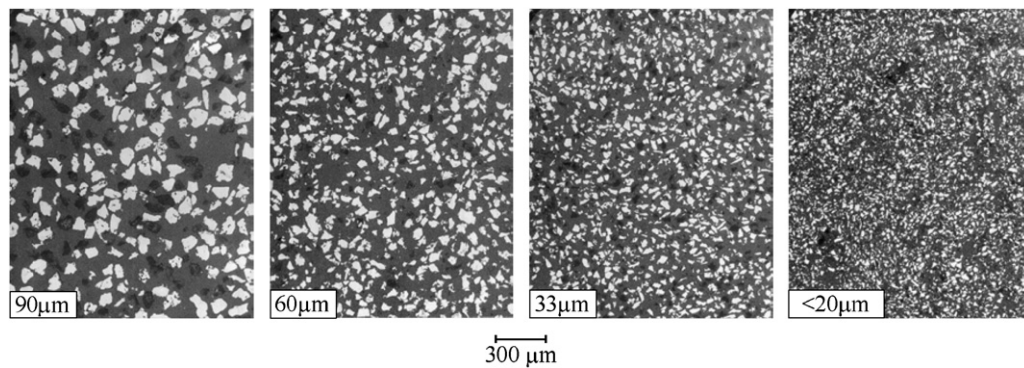


Fig. 14. Typical microstructure of initial sample cross sections (Ti–Si system) with different titanium particle size (adopted from Ref. [45]).

Table 3
Microstructural characteristics: initial reaction medium and combustion wave (adopted from Ref. [48])

Parameters	Values		
Range of Ti particles size, μm (sieving)	20–45	45–75	75–106
Average Ti particles size, μm (sieving)	33	60	90
Number of Ti particles per unit volume, mm^{-3} (sieving)	14,990	2490	740
Number of Ti particles per unit cross section area, mm^{-2}	332	169	82
Number of hot spots per unit cross section area, mm^{-2}	100	92	76
Number of Ti particles per unit volume, mm^{-3}	10,060	2815	907
Number of hot spots per unit volume, mm^{-3}	3030	1533	844
Approximate number of Ti particles per hot spot	3.3	1.8	1.1
Average c–c distance between Ti particles, μm	39	45	53
Average c–c distance between hot spots, μm	38	40	52
Average time between hot spots appearance along line, ms	5.8	9	11
Average lifetime of hot spot, ms	2.2	1.5	1.6

Ti particle size (Table 3). Apparently, preheating of larger particles up to the reaction initiation temperature requires more time compared to smaller particles. When the reaction is initiated, it proceeds within a small local volume in a relatively short time, independent of the Ti particle size. Finally, it was also demonstrated [45] that the hot spot size does not change, while its average lifetime slightly decreases with increasing reaction media density. The latter was explained by an increasing rate of energy dissipation within the media for higher densities.

Thus, it was concluded that thermal micro-heterogeneity of the combustion wave, which manifests itself through characteristic roughness of the reaction front and chaotic local oscillations of the instantaneous propagation velocity and formation of the short-lived hot spots along the front surface, is strongly correlated and even defined by the heterogeneity of the reaction media [41,45].

Let us summarize the experimental findings. For many heterogeneous gasless and gas–solid systems including, Ti–C, Ti–Si, Ni–Al, Ti–N, etc., it was shown that combustion waves, which look steady-state and planar when they are observed with the time scale of $\Delta t \sim 10^{-1}$ s and spatial resolution of $\Delta r \sim 0.1$ mm, under more precise examination (i.e. $\Delta t \sim 10^{-4}$ – 10^{-3} s and $\Delta r \sim 1$ μ m) show a discrete (jump-hesitation) manner of propagation with non-uniform temperature distribution along the reaction front. Such waves possess a complex temperature structure that is correlated with the microstructure of the reaction media.

While the specific experimental conditions for each system are different (see corresponding references), it was proven that above behavior is observed when the characteristic reaction rate is much faster than the rate of heat transfer in the considered reaction media. Analysis shows (see also Section 4) that this requirement is fulfilled over a wide range of typically used experimental parameters (density, particle size, etc.).

In the above context, to switch from relay-race to a quasi-homogeneous mode of combustion wave propagation, one needs to significantly increase the thermal conductivity of the reaction media, e.g., using samples with very high initial density (> 75%) and/or to slow down the intrinsic kinetics of the chemical reaction. The latter can be achieved, for example, in a gas–solid system by using low gas pressure or in a gasless system by diluting the reaction mixture with an inert substance. As noted above, in general a decrease in reactant particle size does not lead to the quasi-homogeneous combustion mode, but rather causes the opposite effect.

3. Theoretical models for discrete combustion

3.1. Discrete combustion waves: evolution of ideas

It is shown below that all major features of the discrete combustion wave discussed in Section 2 may be described

based on two assumptions:

- (A) Reaction medium consists of clearly distinguishable reaction cells.
- (B) Reaction time within the cell is shorter than the time of heat transfer between the neighboring cells.

These simple statements lead to the theoretical models for discrete combustion wave propagation; however the route for developing such models was not straightforward. Let us briefly overview some aspects of combustion theory from the viewpoint of the discrete reaction wave.

It is interesting that the early theory of flame propagation developed in pioneer works of Mallard and Le Chatelier [21], as well as Mason and Wheeler [22], exhibit some features of the discrete approach. First, the temperature profile of the combustion wave, considered in these classical papers, involves a discontinuity in the derivative at some “ignition” point (T_{ig}) and a super-adiabatic peak (T_m) (see Fig. 15). Second, when they described a small movement of the combustion front (on distance ds , Fig. 15), it was assumed that heat, generated by the chemical reaction of source F , was used for preheating of the ds layer from the initial temperature (T_0) up to the ignition temperature T_{ig} :

$$c(T_{ig} - T_0) ds = F(T_m, T_{ig}) dt.$$

Note that these features are similar to those for the combustion of a chain of reaction cells with size ds , which have high thermal conductivity and are separated by highly thermal resistive contacts (i.e. conditions of step-like temperature distribution on the boundary between the cells). Also, while the assumption of a fixed ignition temperature (T_{ig}) typically does not hold for gaseous reaction mixtures (see below) it may have physical meaning for combustion in a condensed system. Indeed, it can be related to the system characteristic temperature of phase transformation, such as melting or dissociation, as discussed above. Finally, as noted by Garner [67], the equation for combustion velocity

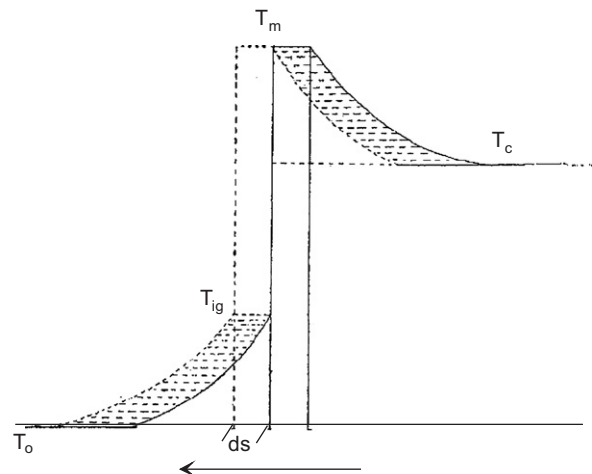


Fig. 15. Temperature profile with super adiabatic peak (adopted from Ref. [22]).

obtained in this earliest theory is

$$U = \frac{F(T, t)}{c(T_{\text{ig}} - T_0)} = \frac{F'(T_m, T_{\text{ig}})\lambda(T_m - T_{\text{ig}})}{c(T_{\text{ig}} - T_0)} = \frac{F'(T_m, T_{\text{ig}})\lambda Q}{c' c(T_{\text{ig}} - T_0)}, \quad (3)$$

where Q is the heat of reaction, λ is heat conductivity of the reaction media, "...holds exactly only for the *limiting* case where the speed of reaction in the flame is very rapid compared with the rate of conduction of heat to the cold gas, but it is of general service for all but the slowest burning mixtures".

Later, Zeldovich, Frank-Kamenetskii, and co-workers [20,24] showed that the above physical model could not be applied to the combustion of premixed gases. In their theory of the thermal propagation of flame, it was proven that for a homogeneous, steady state propagation regime, it is necessary to take into account not only the heat conservation law, but also the continuity of heat flow at any point. As a result, a novel equation for the combustion velocity was derived:

$$U = \frac{(2\lambda \int F dT)^{1/2}}{\rho Q}, \quad (4)$$

where ρ is reaction media density.

In the suggested approach the continuity of heat flow means that in the steady-state propagation regime the rate of heat transfer from reaction to the preheating zone cannot be slower than the rate of heat generation in the reaction zone, which in some sense denies the aforementioned note of Garner [67]. Nevertheless, the Zeldovich–Frank-Kamenetskii model serves as a basis for modern combustion theories and it was further adapted to describe different phenomena such as combustion of condensed matters, gasless combustion, SHS, and other processes.

However, condensed combustibles (gun powders, explosives, composite and homogeneous propellants, etc.) possess quite different thermal properties and reaction kinetics in comparison with gas mixtures. For example, many solid propellants consist of two phases (fuel particles and oxidizing binder, or fine oxidizer particles embedded in a fuel matrix), which allow reaction cells to be outlined and define media heterogeneity. Nevertheless, under certain conditions, the homogeneous theory describes the burning of solid matter well. The experimental basis for understanding why combustion of essentially heterogeneous systems can be described by a homogeneous model was first provided by Belyaev [68]. He showed that a gap exists between the surface of the burning solid explosive and the flame. Based on this observation, a conclusion was made that combustion primarily occurs in a gas phase and heat flux from the reaction zone cause further evaporation of the solid explosive.

These experimental results allowed Zeldovich to develop a theory for combustion of gunpowders and explosives [69], where gas-phase reactions play a controlling role in

the complex burning process, while reactions in the condensed phase are neglected. Later, it was shown [70] that with increasing temperature, the "leading" combustion stage transfers from gas to the condensed phase. This effect occurs because at sufficiently high temperatures, the rate of the condensed phase reaction becomes greater than the rate of gas phase combustion. Note that increasing ambient pressure also leads to the dominating role of reaction in the condensed phase in such systems. Upon analyzing different possible limiting stages in propellant combustion, Williams [71] came to the conclusion that a complete theory must take into account the heterogeneity of composite propellants.

An attempt to develop a novel, essentially discrete, combustion model for the burning of composite propellants and other exothermic mixtures was made by Fur [72,73]. The model was named a "relaxation mechanism" of combustion propagation. The main features of this model are: (1) the reaction medium consists of a cubic lattice with fuel particles located on the lattice points and small oxidizer particles are distributed between them; (2) a layer of such cubic lattice cells is considered to be an elementary layer of the mixture; (3) heat flow from the reaction zone preheats the elementary layer to some ignition temperature, T_{ig} , at which the reaction initiates (inflames); (4) the inflammation time is much less than the preheating time. The preheating process is treated as thermal relaxation, lending to the name of the model. Comparison of these conditions with the previously formulated criteria for discrete combustion shows that Fur's relaxation mechanism represents a kind of discrete combustion process. Based on the heat balance between reaction and preheating layers, the following equation for the combustion velocity was suggested:

$$U = \frac{k_1 \lambda}{c \rho \Delta} \frac{T^* - k_2 T_{\text{ig}} - k_3 T_0}{k_4 (T_{\text{ig}} - k_5 T_0) + \frac{Q}{c} + \frac{4\varepsilon}{c \rho d}}, \quad (5)$$

where k_i ($i=1, \dots, 5$) are numerical coefficients, Δ is a dimension of the elementary cell, ε is a coefficient of thermal emission. Note that Eq. (5) is a complicated version of the Mallard and Le Chatelier formula (3). Fur's works were subjected to severe criticism [74], in which the model was characterized as a deteriorated variant of Mallard and Le Chatelier's theories. The main points for the criticism were the following:

- (1) It is not correct to introduce ignition temperature (T_{ig}) as a constant value, because according to fundamental theory [75], T_{ig} is determined by the balance between reaction heat evolution and heat losses, which can vary for the same system from one experiment to the next.
- (2) Fur's formula does not provide the proper dependence of combustion velocity on gas pressure.
- (3) A reciprocal proportion between combustion velocity and particle size, $U \sim 1/\Delta$, "has no serious experimental ground", and if it finds experimental confirmation in

the future, it will be “more natural to explain this dependence by a diffusion combustion mode” [75].

While today, these arguments look less unquestionable than 45 years ago, they led to a long pause in further development of discrete combustion models.

Failure of the early discrete combustion models can also be explained by the lack of understanding of the systems to which they should be applied. The following types of combustible condensed phase systems can be outlined: (i) homogeneous; (ii) initially heterogeneous, but all of its components melt and mix at the molecular level in the preheating zone (i.e. before the reaction starts); (iii) heterogeneous, in which at least one component remains solid (completely or partially) to the point of reaction initiation. Thermal homogeneous theory [20,24,76] can be adapted to describe the features of combustion wave propagation for the first two cases [77,78]. A comprehensive analysis of these models can be found in the monographs and review [71,79–81]. The third case, where a heterogeneous reaction leads the combustion process, is of the most interest from the viewpoint of a discrete model. As it was shown in Section 2, many experimental results clearly indicate the existence of a discrete combustion wave in such systems. However, the experimental techniques that permitted this evidence to be obtained were not available at the beginning of the 1970s, when the combustion theory of heterogeneous mixtures was being established. Probably for this reason, a *quasi-homogeneous* approach was used as the basis for the development of such models.

The principle of thermal homogeneity for reaction media was introduced in several works [82,83] as follows: “...regardless of the particle size, a condensed mixture may be considered as thermally homogeneous, because heat release in such mixtures (controlled by inter-diffusion of the components) is much slower as compared to heat relaxation in the particles. Chemical heterogeneity, which is intrinsic for such mixtures, reveals itself only through special types of kinetic functions, which defines heat evolution in the effectively homogeneous medium”.

Since this postulate has been the basis for thousands of publications on combustion of heterogeneous mixtures during the last 30 years, it is worthwhile to consider the evidence for such a statement. First, it was assumed that heterogeneous reactions occur by diffusion of the components through the solid layer of product formed along the boundary between the reactants. Thus, solid-state diffusion was admitted to be a limiting stage of the process. Second, thermal conductivity in the bulk solid material was considered to be a main mechanism of heat transfer in such media. Based on these assumptions and Arrhenius-type kinetic laws, a parameter that characterizes a mixture thermal homogeneity was derived [84]:

$$\zeta = \frac{D}{a\gamma},$$

where D and a are the maximum values of reaction diffusion coefficient and thermal diffusivity of the medium, respectively; $\gamma = RT_c^2/E(T_c - T_0)$. If ζ is small, the reaction medium may be considered as thermally homogeneous, while if $\zeta \geq 1$ it is important to account for the media heterogeneity. Upon substitution of common values, according to assumed mechanisms ($D \sim 10^{-6} - 10^{-8} \text{ cm}^2/\text{s}$, $a \sim 10^{-1} - 10^{-2} \text{ cm}^2/\text{s}$ and $\gamma \sim 0.1$), one finds $\zeta \leq 1$. Thus, it was accepted as indisputable fact that combustion processes in all chemically heterogeneous combustible mixtures can be considered as thermal homogeneous.

Recent experimental results (see Section 2) have shown that the above assumptions fit only a small portion of the investigated heterogeneous powder systems. For example, let us consider combustion when mass transfer is controlled by liquid-phase diffusion ($D \sim 10^{-5} \text{ cm}^2/\text{s}$) and take into account high thermal resistances between the contacts of particles (thermal diffusivity of real powder mixtures $\sim 10^{-3} - 10^{-4} \text{ cm}^2/\text{s}$). It is obvious that, in this case $\zeta \sim 1$, and the above stated principles of media thermal homogeneity could not be applied. In the next paragraph we briefly discuss several important theoretical models, which were developed to account for the thermal heterogeneity of reaction media during combustion in such systems.

3.2. Contemporary theoretical models of discrete combustion

As it was shown in Section 2, the microstructure of real heterogeneous media is rather complicated (Fig. 14). In an attempt to account for this complexity, a variety of theoretical approaches have been developed, which are based on different assumptions and contain various governing parameters. However, the common feature in all such discrete models is the consideration of a distinguishable element in the structure, a so-called elementary *reaction cell*. Typically, the elementary reaction cell is defined as the smallest volume of the combustible media, which contains all components (fuel, oxidizer, etc.) in the same proportion as the whole mixture. This concept was initially formulated for thermite combustible mixtures with all molten components in the reaction zone [85]. However, it may be applied to most known heterogeneous mixtures [86]. For example, in binary systems (A + B) in which the particle size of one reactant (e.g. A = metal: Ti, Al, Mg) is much larger than the other (e.g. B = nonmetal: carbon, boron, oxides), the reaction cell is composed of one large metal particle surrounded by a defined number of fine non-metal particles. If the reactants in a mixture have comparable sizes (e.g. Ni + Al, Ti + Ni), then two neighboring particles of different reagents may constitute the reaction cell. Thus, the inner structure of the elementary reaction cell may be different for different mixtures. However, the common property of all considered cellular media is that mass transfer and heterogeneous reaction occur inside each cell, while only heat transfer takes place

between the cells. This assumption is of critical importance for all theoretical models discussed below.

Strictly speaking, the geometry of the reaction cell influences the kinetics of heterogeneous reaction. Solid products can appear at the contact boundary between the reactants and thus may retard further reaction. This aspect was analyzed in numerous works, including the classical combustion models with strong retardation [78,79], and further summarized in several reviews [60,81,86]. However, a specific form of the reaction rate function plays a governing role only in the quasi-homogeneous combustion mode, when the reaction heat evolution is a limiting stage of the process. In the discrete mode, propagation of the combustion front is limited by heat transfer between the cells, while heat release inside each reaction cell occurs relatively rapidly. For this reason, the simplest kinetic laws, e.g., stepwise kinetics or zero-order reactions, are widely used in the discrete models considered below.

3.2.1. One-dimensional discrete models with zero-order Arrhenius-type kinetics

One of the simplest discrete models of heterogeneous media is a 1D chain of reaction cells shown in Fig. 16. The state of each cell at any moment in time can be fully described by two variables: temperature, T_i , and degree of conversion, $\eta_i = 1 - m/m_0$ (where m_0 and m are initial and instantaneous fuel contents in the cell). In addition, each cell is characterized by a few invariable parameters: $c \times M$ (where c is the specific heat capacity and M is the mass of the cell, $M = \varepsilon \rho d^3$, ρ and d are density and size of the cell, ε is a shape factor, e.g., $\varepsilon = 1$ for cube, $\varepsilon = \pi/6$ for sphere, etc.), and the heat of reaction Q . Contacts between the cells are defined by a contact surface, S , and heat exchange coefficient, α . A system of equations to describe the combustion wave propagation in i -cell can be written as follows [87]:

$$cM \frac{\partial T_i}{\partial t} = \alpha S(T_{i-1} - 2T_i + T_{i+1}) + Q \frac{\partial \eta_i}{\partial t}, \quad (6)$$

$$\frac{\partial \eta_i}{\partial t} = F(\eta_i, T_i), \quad (7)$$

where $F(\eta_i, T_i)$ is a kinetic function of heterogeneous reaction within the cell presented in the most general form. Further, more accurate, definition of this function can be done to denote the specifics of the reaction mechanism,

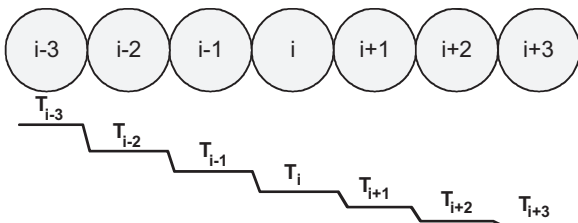


Fig. 16. Schematic representation of the one-dimensional cell model of the reaction media (adopted from Ref. [87]).

e.g., reaction- or diffusion-controlled interaction, dissolution-precipitation, etc.

It should be emphasized that Eq. (6) is valid only if one can neglect temperature distribution within the cell, i.e. assuming that temperature variation inside each cell is much smaller than the temperature “jump” at its boundaries. This means that the Biot number for the single cell should be small, $Bi = \alpha d/\lambda \ll 1$ (where λ is effective thermal conductivity inside the cell). This assumption is based on experimental data, which show that λ of the bulk particle is much higher than the thermal conductivity of the contacts between particles [88]. For example, comparison of experimentally measured values of thermal conductivity for $Ti + xC$ mixtures with the thermal conductivity of Ti , gives $Bi \sim 0.03$.

The influence of radiation heat transfer can be taken into account if, instead of a constant value for α , an effective heat transfer coefficient is introduced [89]:

$$\alpha_{\text{eff}} = \alpha + 4\gamma\sigma T_*^3,$$

where γ is emittance, σ is the Stefan–Boltzmann constant, T_* is a scaled temperature selected from additional considerations (as a first approximation, T_* can be taken as the middle point between initial and maximum combustion temperatures).

Several types of kinetic functions, $F(\eta_i, T_i)$ have been considered in Eq. (7). For example, zero-order Arrhenius-type kinetics was investigated in work [90]. Computational experiments led to the conclusion that a dimensionless Semenov’s number:

$$Se = \frac{Qd}{\alpha_{\text{eff}}} \frac{E}{RT_*^2} k_0 \exp\left(-\frac{E}{RT_*}\right)$$

can be used as a criterion to determine the regime of combustion wave propagation. It was shown that when Se is small, propagation occurs in a quasi-homogeneous regime, while with increasing Se , combustion propagation switches to the heterogeneous (discrete) regime. Note that the Semenov number defines a ratio of characteristic heat exchange time between reaction cells and time of chemical reaction in the cell at some specific temperature (T^*). Therefore, the above conclusion is qualitatively similar to condition B, which was formulated in Section 3.1 based on experimental observations.

However, it is difficult to make a quantitative comparison of the theoretical results obtained in the form suggested in [90] with the experimental data. Analysis has shown that it is not easy to establish a direct relation between dimensionless variables used in the model and physical parameters that can be controlled in the experiments. In order to make such a comparison, other dimensionless variables were suggested [87]:

- temperature $\vartheta_i = T_i - T_0/T_C - T_0$, where $T_C = T_0 + Q/cM$ and
- time $\tau = (\alpha S/cM)t = t/t_T$, where $t_T = cM/\alpha S$ is a characteristic time of heat transfer between the cells.

By using these variables, the Eqs. (6) and (7) with standard initial and boundary conditions can be rewritten as follows:

$$\begin{cases} \frac{\partial \vartheta_i}{\partial \tau} = \vartheta_{i-1} - 2\vartheta_i + \vartheta_{i+1} + \frac{\partial \eta_i}{\partial \tau}, \\ \frac{\partial \eta_i}{\partial \tau} = \Phi(\eta_i, \vartheta_i), \end{cases}$$

$$\tau = 0: \quad \vartheta_i = 0, \quad \eta_i = 0, \quad i = 1 \dots N,$$

$$\tau > 0: \quad \vartheta_1 = \vartheta_{\text{ign}}, \quad \vartheta_N = 0, \quad (8)$$

where N is the total number of reaction cells in the sample.

At $t=0$, the temperature of the first cell $\vartheta_1 = \vartheta_{\text{ign}}$ is high enough to initiate the reaction (e.g. $\vartheta_{\text{ign}} = 1$), while the last cell always remains at the initial temperature ($\vartheta_N = 0$).

It can be seen that system (8) contains only one arbitrary function ($\Phi(\eta_i, \vartheta_i)$), which determines the combustion regime. For example, for Arrhenius-type kinetics:

$$\begin{cases} F(\eta_i, T_i) = k_0 \exp\left(-\frac{E}{RT_i}\right), & 0 \leq \eta_i < 1, \\ F(\eta_i, T_i) = 0, & \eta_i \geq 1, \end{cases} \quad (9a)$$

$\Phi(\eta_i, \vartheta_i)$ can be presented as follows:

$$\begin{cases} \Phi(\eta_i, \vartheta_i) = p \exp\left(-\frac{1}{\text{Ar}_0 + \text{Ar}_c \vartheta_i}\right), & 0 \leq \eta_i < 1, \\ \Phi(\eta_i, \vartheta_i) = 0, & \eta_i \geq 1, \end{cases} \quad (9b)$$

where

$$p = \frac{cM}{\alpha S} k_0$$

$$= t_T k_0 \sim \frac{t_T}{t_r} \quad (t \text{ is a characteristic reaction time}),$$

$$\text{Ar}_0 = \frac{RT_0}{E},$$

$$\text{Ar}_c = \frac{R(T_c - T_0)}{E}. \quad (9c)$$

The dimensionless parameters (9c) have lucid physical meanings and are directly related to the experimental conditions. Parameter p indicates the ratio of characteristic times for heat transfer (t_T) and reaction (t_r). It can be varied in experiment by changing: (i) density of the powder mixture, thus affecting the contacts between particles, which primarily influence t_T ; or (ii) the particle size of the reactants, which governs t_r . The Arrhenius number at the initial temperature, Ar_0 , can be controlled by preheating the reaction mixture. Finally, parameter Ar_c can be varied in experiments by dilution of the reactive mixture with inert additives (e.g. final product), thus changing the combustion temperature, T_c .

Fig. 17 represents the typical structure of a combustion wave computed according to the model (9a) with the kinetic function (9c). It can be seen that if $p \leq 1$, (Fig. 17a), the temperature profile and heat release function are similar to those for a homogeneous combustion wave, as predicted by classical theory [20,79]. However, for $p \gg 1$ (Fig. 17b), the

reaction wave structure is different. The temperature profile involves several inflection points (due to the influence of reaction in neighboring cells) and a “super-adiabatic” peak. Such thermal explosion type profiles are typical for the discrete regime of combustion wave propagation (compare with Figs. 7 and 11). Also note that there is no fixed temperature of reaction initiation in this model. However, by analogy with the theory of thermal explosion [75], some temperature value, ϑ^* , can be considered as critical for reaction initiation in the cell. This critical temperature (ϑ^*) can be defined from the following equation [87]:

$$\frac{\partial \eta_i}{\partial \tau} = \vartheta_{i-1} - 2\vartheta_i^* + \vartheta_{i+1}, \quad (10)$$

which describes conditions when in the i th cell, the rate of heat evolution (owing to chemical reaction) equals the rate of heat accumulation (due to heat exchange between the cells).

When cell temperature is less than the critical value, $\vartheta < \vartheta^*$, it is heated primarily by the thermal flow from the reacted part of the sample, while reaction within the cell is negligible. On the contrary, when $\vartheta > \vartheta^*$, exothermic self-sustained reaction becomes a main source for further increase in the cell temperature. Calculated values of critical temperature for different p are shown on the temperature profiles in Fig. 17c. It can be seen that in the quasi-homogeneous mode ($p \sim 1$), the critical temperature is very close to the maximum combustion temperature, ϑ_m , which is in good agreement with the results of classical Zeldovich–Frank–Kamenetskii theory. In the discrete combustion regime ($p \gg 1$), ϑ^* is much lower than ϑ_m .

Another important characteristic that defines the temperature sensitivity of the process is a temperature coefficient of combustion velocity:

$$K_T = \frac{\partial(\ln U)}{\partial T_0}. \quad (11)$$

In terms of variables used in (8) this parameter can be presented as follows:

$$K_{\text{Ar}(0)} = \frac{\partial(\ln U)}{\partial \text{Ar}_0} = \frac{E}{R} K_T. \quad (12)$$

Temperature coefficients are commonly measured in various combustion experiments and traditionally associated with the temperature dependence of reaction rates. The discrete model of combustion suggests an alternative interpretation for this value. Results of theoretical calculation, by using the above simple discrete model [87], are shown in Fig. 18. When p is small (quasi-homogeneous mode) the temperature coefficient fits the value obtained from Zeldovich homogeneous theory [24]. As p increases, $K_{\text{Ar}(0)}$ first slightly drops, but then slowly increases (e.g. when p grows by one million, $K_{\text{Ar}(0)}$ increases only about two times).

The same model allowed the development of a map for different combustion regimes as shown in Fig. 19. Note that the region of steady-state combustion expands toward smaller values of Ar_c (i.e. more strongly activated

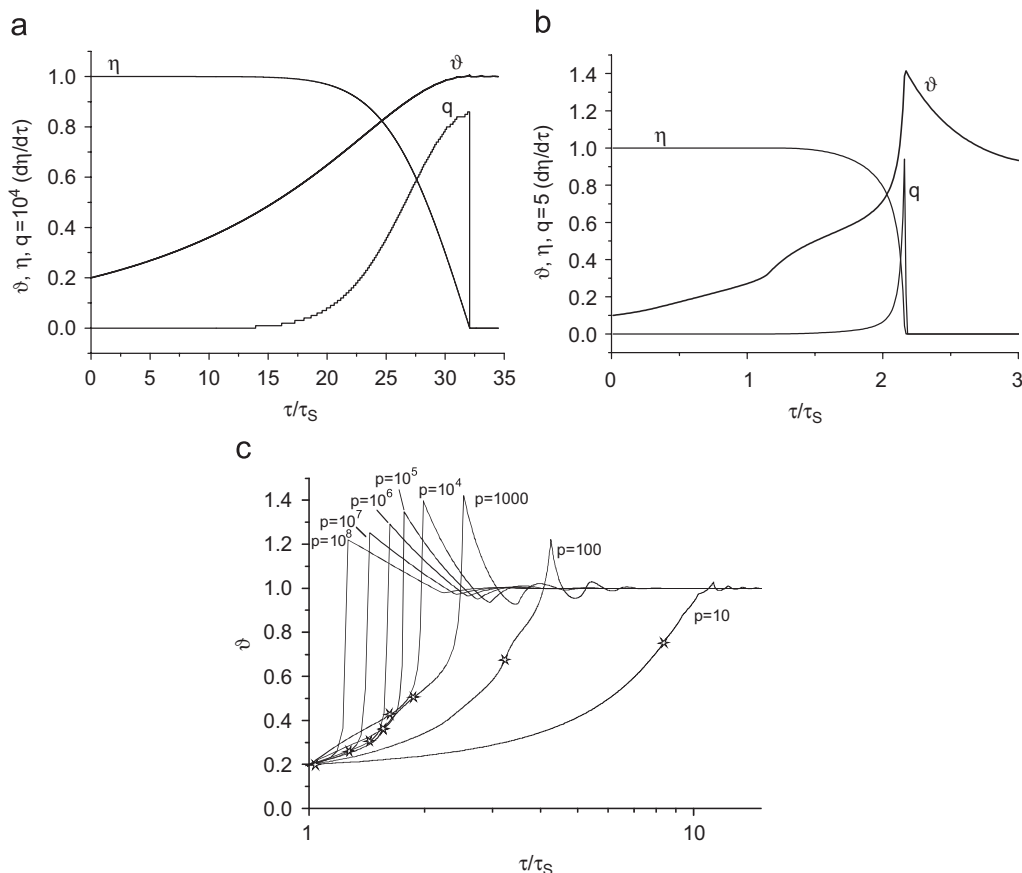


Fig. 17. Temperature (ϑ) and conversion (η) profiles as well as heat release function (q) calculated according to one dimensional cell model for different values of parameter p (Eq. (9b)): (a) $p < 1$; (b) $Pp \gg 1$ and (c) temperature profiles of the discrete combustion wave at different values of the parameter p . Asterisks indicate critical temperatures (Eqs. (10)) (adopted from Ref. [87]).

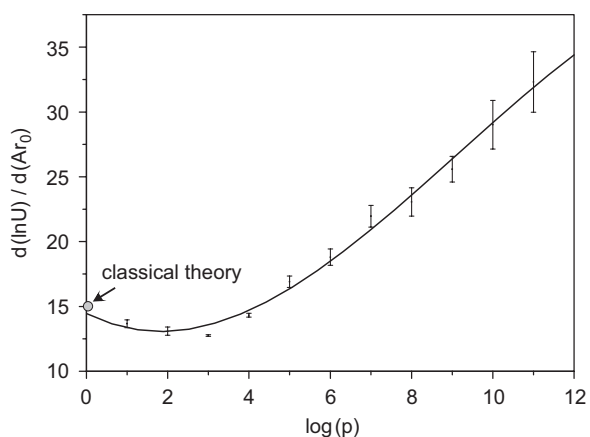


Fig. 18. Dependence of combustion temperature coefficient $K_{Ar(0)}$ (Eqs. (12)) on parameter p (adopted from Ref. [87]).

reactions) with increasing p . It can also be seen that the quasi-homogeneous combustion wave ($p < 10$), becomes oscillating if $Ar_c < 0.15$, while discrete waves ($p \gg 1$) remains stable up to $Ar_c = 0.03$. It is important that the results presented in Figs. 17–19 can be utilized for direct comparison with experimental data (see Section 4).

Besides the zero-order Arrhenius-type function, various stepwise kinetics laws with a pre-determined constant

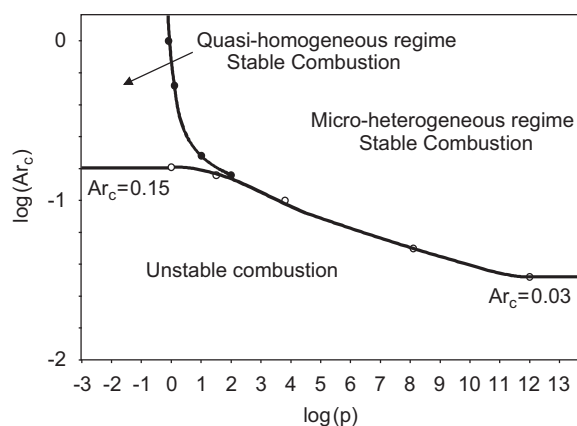


Fig. 19. Parametric (Ar_0-p) map of combustion regimes obtained by one-dimensional cell model (adopted from Ref. [87]).

temperature of reaction initiation have been considered in discrete models and are discussed below.

3.2.2. One-dimensional discrete models with stepwise kinetics

A stepwise kinetic law means that the reaction rate remains zero up to some pre-determined constant temperature, T_{in} . Once the temperature reaches this value the

reaction initiates and proceeds at a significant rate. As mentioned above, the presumption of a fixed temperature of reaction initiation was made in the earliest works on gas combustion [21,22], as well as in the relaxation model [72,73], and was subjected to criticism by creators of modern homogeneous combustion theory [74].

It is worth noting that the concept of reaction initiation at some constant temperature has no direct links to discrete combustion theory. As it is discussed in Section 3.2.1, the discrete heterogeneous models can be established based on conventional Arrhenius-type kinetics, i.e. without the assumption of a fixed critical initiation point. Moreover, detailed analysis of combustion front propagation with stepwise kinetics was for the first time made by Daniel using a homogeneous combustion model [91]. It was shown that in this case, a steady state flame propagation velocity can be calculated from the following equation:

$$\frac{T_{in} - T_0}{T_C - T_0} = \frac{1 - e^{-\chi}}{\chi}, \quad \text{where } \chi = \frac{U^2}{aw}, \quad (13)$$

where $a = \lambda/c\rho$ is the thermal diffusivity of the reaction media, and w is rate of chemical reaction, which is assumed to be constant above the initiation temperature T_{in} . There is one more complication that arises during analysis of Eq. (13). The propagating velocity approaches infinity when $T_0 \rightarrow T_{in}$. However, for condensed phase reactions it was concluded that temperatures of phase transformations (T_{ft}), such as a reactant melting point, which is typically much less than T_m , plays the role of ignition temperature [92]. In turn, as it was pointed out in [93], singularity at $T_0 = T_{in}$ can be overcome by accounting for the heat of phase transformation at $T_{in} = T_{ft}$. Therefore, consideration of step-wise kinetics for heterogeneous systems has a clear physical basis.

Discrete 1D models based on step-like kinetics were developed in the works [85,94]. It was assumed that the dimensionless reaction rate (9a) can be written as follows:

$$\Phi(\eta_i, \vartheta_i) = \frac{d\eta_i}{d\tau} = \begin{cases} 0, & \vartheta_i < \vartheta_{in}, \quad \eta_i < 1, \\ \Phi_1(\eta_i, \vartheta_i), & \vartheta_i \geq \vartheta_R, \quad \eta_i < 1, \\ 0, & \eta_i = 1, \end{cases} \quad (14)$$

where $\vartheta_{in} = T_{in} - T_0/T_C - T_0$. Two types of Φ_1 function were analyzed: $\Phi_1 = \text{const}$ [94] and $\Phi_1 = p \exp(-1/(Ar_0 + Ar_C\vartheta_i))$ [87].

It was shown that in the discrete combustion mode, because the time of reaction is much shorter than the time of heat transfer, a specific form of kinetic function does not influence the combustion wave behavior. The dependencies of the calculated combustion velocity on the reaction initiation temperature are presented in Fig. 20. The role of ϑ_{in} is clarified by comparison of this value with the temperature of thermal explosion ϑ^* (10). Analysis revealed that if $\vartheta_{in} < \vartheta^*$, then the combustion velocity does not depend on ϑ_{in} (curves 2–4, for $\vartheta_{in} < 0.2$). In the opposite case, when $\vartheta_{in} > \vartheta^*$, regardless of considered conditions, all calculated values of combustion velocity, U_c , fit the same

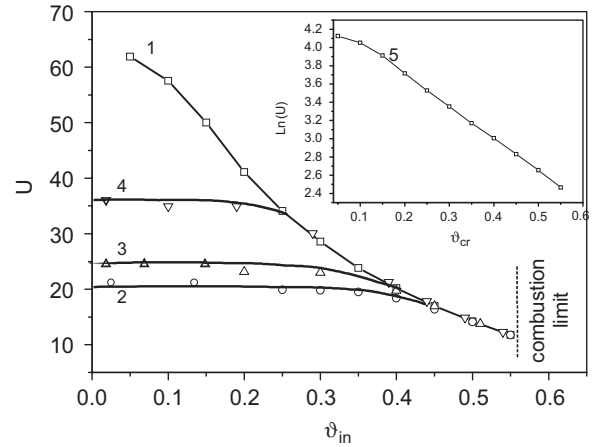


Fig. 20. Dependencies of calculated combustion velocities as a function of the initiation temperature for different parameters Ar_m and p : for curves (1), (5) $Ar_c = 1.0$ and $p = 100$; for curves (2), (3), (4) $Ar_c = 0.2$ and $p = 100, 10^5, 10^7$, respectively (adopted from Ref. [93]).

curve ($\vartheta_{in} > 0.35$). This curve also remains invariant for all types of kinetic functions, because under the considered conditions, the propagation velocity is controlled solely by the heat transfer process.

Note that a semi-logarithmic plot of this curve (curve 5 in Fig. 20), for the region $0.15 < \vartheta_{in} < 0.56$, indicates a linear relationship. This allows for the calculation of a temperature coefficient for combustion velocity:

$$K_R = \frac{\partial(\ln U)}{\partial \vartheta_{in}}, \quad (15)$$

which is linked to the conventional temperature coefficient (11) by the relation:

$$K_T = -\frac{K_R}{T_C - T_0}. \quad (16)$$

Using the least-squares method, values of $K_R = -3.6$ for Arrhenius-type kinetics and $K_R = -3.9$ for stepwise reaction with a constant reaction rate, were found. These values match well with experimental data (see Section 4 for details). Another feature, which is illustrated in Fig. 20, is a combustion limit for discrete reaction waves. Propagation of the reaction becomes unstable when ϑ_{in} approaches 0.56, and combustion is not possible for $\vartheta_{in} > 0.6$.

3.2.3. Two-dimensional discrete models

Describing the combustion process in 2D heterogeneous systems inevitably results in more complicated models. However, the concept of the elementary reaction cell is also utilized. Typically, temperature is assumed to be uniform inside the cell, while heat transfer is limited by heat conduction from one cell to another through contacts between the cells and gas in the pores.

One of the first 2D-micro-heterogeneous cell models was developed in the works [55,95]. It was assumed that the structure of the reaction media is a regular 2D matrix of

circular elements with diameter, d , equal to the diameter of the reactive particles (Figs. 21a and b). Some fraction of the circular elements is randomly removed, so that ratio of voids to total number of cells represents pre-required media porosity. Next, this randomized medium is divided into

square reaction cells by superimposing a rectangular net as illustrated in Fig. 21a. The mesh size of this net, l , was taken to be $d/2$. This procedure creates three basic types of cells, presented in Fig. 21b: “cores” (1), “interstices” (2), and “edges” (3). The cores have the highest thermal conductivity, which equals that of the bulk solid, while interstices possess the lowest value, owing to a large fraction of gas. The edges have some intermediate value of thermal conductivity depending on the properties of thermal contact between particles. An elastic contact model [96] was used to describe contact regions between cells, which accounts for the loading pressure and mechanical properties of the reactants.

The three types of reaction cells correspond to three methods of heat transfer, by volume solid state heat conduction, by heat transfer across the contacts, and heat transfer through the gas filled pore (the latter includes conduction and convection in gas and also radiation heat transfer). A discrete heat balance equation for the cell i, j (horizontal and vertical indices) can be written as follows [95]:

$$[c\rho]^{(i,j)} \frac{\partial T^{(i,j)}}{\partial t} = \left(k_x \frac{\partial T}{\partial x} \Big|^{(i+1/2,j)} - k_x \frac{\partial T}{\partial x} \Big|^{(i-1/2,j)} \right) \frac{1}{\Delta x} + \left(k_y \frac{\partial T}{\partial y} \Big|^{(i,j+1/2)} - k_y \frac{\partial T}{\partial y} \Big|^{(i,j-1/2)} \right) \frac{1}{\Delta y} + Q\rho \frac{\partial \eta}{\partial t} \Big|^{(i,j)},$$

where

$$k_x \Big|^{(i+1/2,j)} = \frac{2k_x^{(i+1,j)}k_x^{(i,j)}}{k_x^{(i+1,j)} + k_x^{(i,j)}},$$

$$\frac{\partial T}{\partial x} \Big|^{(i+1/2,j)} = \frac{2(T^{(i+1,j)} - T^{(i,j)})}{d}, \tag{17}$$

and similarly for k_y and $\partial T/\partial y$.

It is important to note that due to the randomized microstructure of the medium, each square reaction cell has its own coefficient of heat conductivity, k (in “ x ” or “ y ” direction) that is different from the other cells. Among a wide variety of reaction kinetic laws, applicable for this model, a simple stepwise function was chosen for computer simulation. It was assumed that the reaction in the cell starts when the cell reaches a pre-determined temperature, T_{in} , and then runs with constant velocity until full conversion:

$$\frac{\partial \eta}{\partial t} = k_0 H(T - T_{in}) H(1 - \eta), \tag{18}$$

where $k_0 = 1/t_r = \text{const}$, $H(x)$ is a Heaviside function.

Parametric maps of the combustion modes were obtained by computer simulation as shown in Fig. 22 [95]. For high densities, combustion proceeds by the quasi-homogeneous mechanism. As the density decreases, the structure of the reaction medium becomes more heterogeneous, resulting in the appearance of the relay-race (discrete) mechanism. The transition from the quasi-homogeneous to

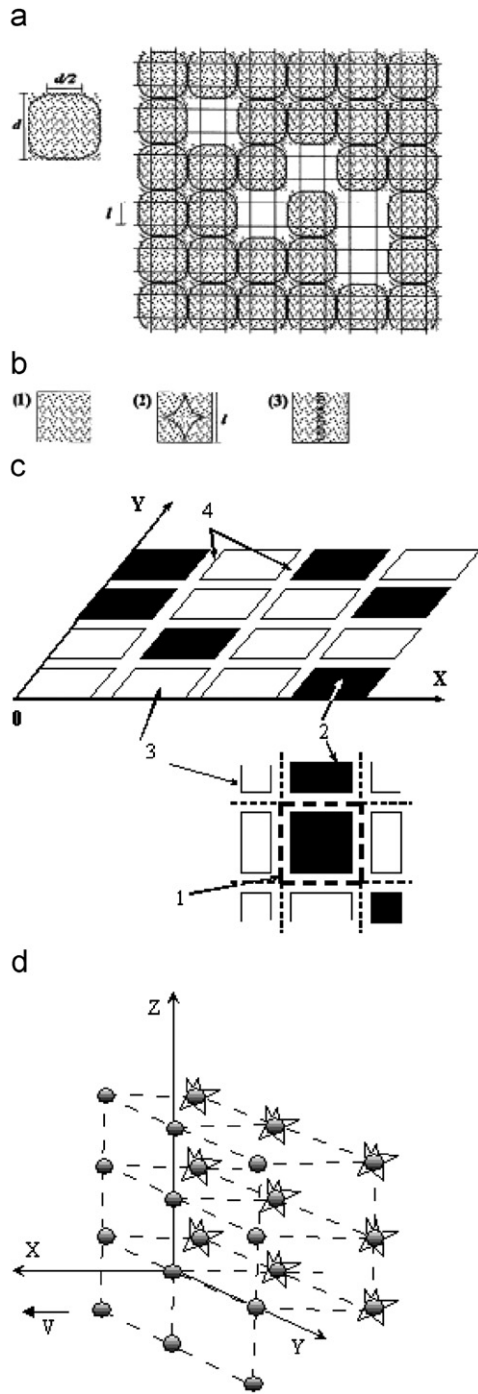


Fig. 21. Schematic representation of the different cell model structures of the reaction medium: (a) 2D model overall view of particle matrix; (b) different cell structures: (1) particle “cores”; (2) interstices; (3) particle “edges” (adopted from Ref. [55]); (c) 2D model: (1) elementary cell; (2) combustible particles (dark cells); (3) inert particles (light cells); (4) gas inter-layers (adopted from Ref. [97]); and (d) 3D model: geometric scheme and coordinate system (adopted from Ref. [152]).

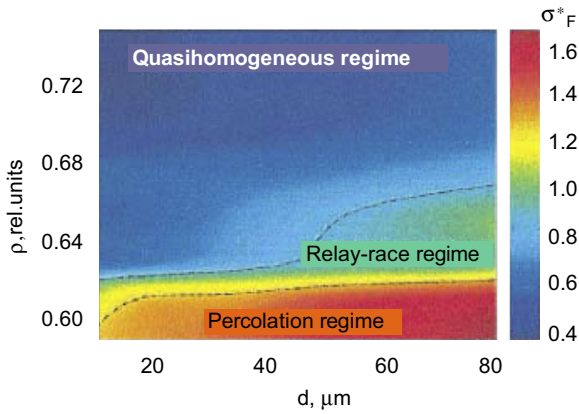


Fig. 22. Parametric density (ρ)–particle size (d) map for different combustion regimes developed based on the two-dimensional cell model (adopted from Ref. [95]).

the relay-race mechanism is more gradual for a larger particle size. At the same time, when relative density is less than 60% (porosity exceeds 40%), only the discrete combustion mode exists for all ranges of considered particle sizes. At this threshold, authors [95] presume that the percolation limit in the heat conduction mechanism is reached, when connectivity of the solid matrix becomes a limiting factor.

Another 2D discrete model was suggested; in works [97,98] composed of reaction cells lined up in a rectangular grid and separated by thin gas-filled gaps, as shown in Fig. 21c. All cells possess similar size, shape and properties (thermal conductivity, density, etc.), except for initial fuel concentration, which may vary from one cell to another. Again, some pre-determined fraction of the cells contains no fuel and plays the role of inert particles in the mixture. The system of heat balance and chemical kinetic equations, used in this model [98], coincides with the previous model with step-like kinetics:

$$c\rho \frac{\partial T_{ij}}{\partial t} = \lambda \left(\frac{\partial^2 T_{ij}}{\partial x^2} + \frac{\partial^2 T_{ij}}{\partial y^2} \right) + p_{ij} Q\rho \frac{\partial \eta_{ij}}{\partial t},$$

$$\frac{d\eta_{ij}}{dt} = W(T_{ij}),$$

$$W(T, \eta) = \frac{1}{\tau_r} H(T - T_{ig}) H(1 - \eta).$$

Factor p_{ij} indicates the relative fuel content in the cell (when $p_{ij} = 0$, the cell is inert; cells with $p_{ij} = 1$ are the most exothermic).

A specific feature of this model is that it does not consider the reaction cell like a point, but rather takes into account the internal temperature distribution within the cell. For this purpose, each cell is considered as a matrix of 49 points (7×7 in a rectangular grid), while the whole sample consists of 2500 such cells (50×50). Two types of systems have been investigated in detail: (a) regular

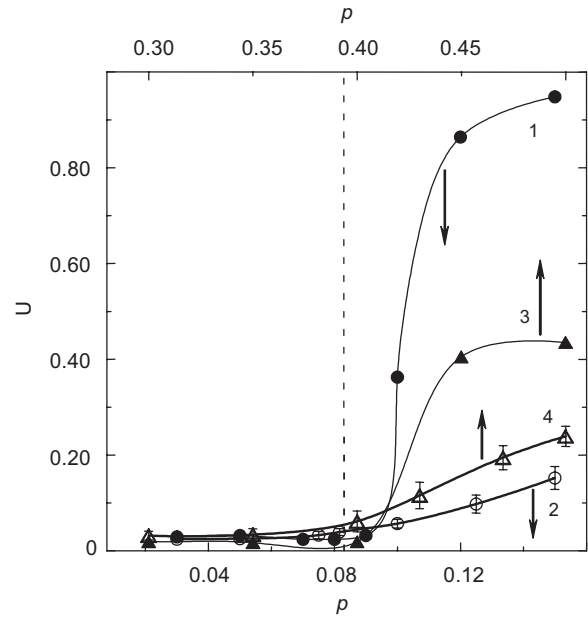


Fig. 23. Mean velocity of the combustion wave versus the concentration of combustible particles: curves 1 and 3 refer to the regular system and curves 2 and 4 refer to the disordered system; the dashed line is the critical concentration for disordered systems: $T_{ig} = 0.05\Delta T_{ad}$ (curves 1 and 2), $T_{ig} = 0.25\Delta T_{ad}$ (curves 3 and 4) (adopted from Ref. [98]).

systems, where all cells have the same fuel concentration equal to the mean concentration of the fuel across the sample, $p_{ij} = p$; (b) disordered (randomized) systems, where some randomly selected cells have $p_{ij} = 0$, all others have $p_{ij} = 1$, so that the average concentration for the sample is equal to a predetermined value, P .

It was found that in the vicinity of some critical value of P , combustion characteristics, such as average velocity, degree of conversion and critical heat loss, undergo abrupt changes. Examples of plots for average velocities are shown in Fig. 23. A conclusion was made that such behavior is a “geometrical phase transition”, which is related to the percolation limit. If P is taken as a variable parameter, then randomization of the system structure leads to a decrease in the combustion limits, compared to a system with ordered structure.

3.2.4. Discrete models with homogeneous heat transfer

The model considered above represents two limiting cases for the description of combustion in heterogeneous systems. The quasi-homogeneous approach is based on the assumption that both heat transfer and heat evolution can be described in terms of continuous functions of space coordinates, and only a particular form of reaction kinetics denotes the specifics of the heterogeneous reaction. On the contrary, the discrete approach assumes that heat sources are located inside reaction cells and that the cells are separated by regions of very low thermal conductivity (contacts, gas gaps), which means that both heat evolution and heat conduction are quantified by discrete functions of

space coordinates. Between these two “poles”, there is a spectrum of models, which combine continuous equations to describe the heat transfer process and essentially heterogeneous (sometimes even discrete) patterns of heat sources. In this section, we will briefly overview the main concepts of such models.

A model proximal to the homogeneous approach was developed in the works [84,99]. Ordered (e.g. layered) or randomly distributed solid reactants generate heat due to the diffusion-controlled heterogeneous reaction, while thermal conductivity is presumed to be uniform throughout the medium. Comprehensive analysis of this model, made in [99], involved three different characteristic length scales. The largest scale is attributed to the preheating zone (thermal conduction). The intermediate scale, under the assumption of a diffusion-limited reaction, is associated with the reaction zone. The smallest scale is identified with the size domain over which mass diffusion takes place (i.e., the typical size domain of the alloyable constituent). Several cases were analyzed: (a) reactant lamina stacked parallel to the flame propagation direction, (b) reaction domain perpendicular to the flame propagation direction; (c) reactants are randomly distributed in the space. In each of these cases, the flame velocity was found to be inversely proportional to the square root of the time for mass diffusion multiplied by the thermal diffusivity. Note that this diffusion time plays the role of the reaction time which typically appears in the common asymptotic solutions for premixed, gas-phase flames. In other words, it was shown that Arrhenius-type diffusion-controlled processes lead to the same flame speed function as premixed gas-phases, but instead of activation energy of chemical reaction, the activation energy for mass diffusion should be used. As it followed from the relations between the characteristic length scales, in this model the thermal relaxation time is always assumed to be much smaller than any other characteristic time of the process (e.g. reaction, diffusion, etc.), which makes this approach close to the homogeneous ones.

Several theoretical models have been developed, taking into consideration more-or-less realistic microstructures for the reaction cells, e.g. spherical particle of one reactant surrounded by a melt of the other reactant. The list of interaction mechanisms is as follows: (a) a continuous layer of solid product appears on the surface of the particle, this layer grows or diminishes depending on the temperature rise in the combustion front and phase diagram of the reacting system [100]; (b) a thin film of intermediate solid product with constant thickness separates the reactants along their border [101–103]; (c) both reactants are molten and interact through the layer of liquid product [85]. As a rule, analysis of diffusion-limiting heterogeneous reactions inside the reaction cells in conjunction with the continuum heat transfer equation lead to a reciprocal dependence of the propagating velocity on particle size, d [85,104,105]. In the case of the product layer thickness, δ , having no direct links with the particle size, d , both of these parameters may

be included in the velocity equation [106]:

$$U = \left[\frac{1}{d} \left(\frac{2}{d} + \frac{1}{\delta} \right) \right]^{1/2} F(T).$$

Sophisticated three-scale models, which have been proposed in works [107,108], take into account the random space distribution of particles, dispersion of their sizes, and melting of one of the reactants. It also assumes that product is formed through a diffusion-controlled heterogeneous reaction at the surface of the refractory reactant. The inter-particle diffusion is modeled with two regimes: an initial primary-diffusion regime followed by a slower secondary-diffusion regime. The availability of reactants depends on the inter-particle diffusion from the melt-rich regions to the melt-lean regions and this transport is influenced by the particle-size distribution. Based on these assumptions, computer modeling was carried out for the Ti–Al system, and good agreement with experimental data was reported [108]. However, too many governing parameters in the model make the generality and significance of such comparisons doubtful.

The examples considered above do not cover all possible reaction mechanisms. Indeed, such important cases as direct dissolution of solid reactant in melts with volumetric product precipitation and reactive coalescence of molten reactants have not been adequately analyzed in combustion theories. Unfortunately, the widely used assumption that diffusion mass transfer controls the reaction restricts the scope of applicability for these models. The appearance of new experimental data on real processes taking place at the microscopic level of reaction media (inside the reaction cells) stimulate development of models based on alternative reaction mechanisms (not on the diffusion-reaction). Recently a continuum-discrete model was suggested that is based on the dissolution/precipitation reaction route [109]. A few works were published taking into account flows of melts in the combustion wave [110–112]; however, no accomplished model has been suggested.

An interesting approach for describing combustion processes in stochastic mixtures was suggested in [113]. A 2D model was composed of square reaction cells characterized by temperature and degree of conversion. The model assumes that reaction in the cell is a random process, while degree of conversion changes with some probability depending on the temperature of the cell. This assumption causes a continuous permanent generation of disturbances, which results in roughness of the combustion front, the appearance of hot spots, and other effects which make the computed patterns look quite similar to the microscopic video records of real micro-heterogeneous combustion waves. Nevertheless, a physical basis for the model assumptions remains questionable.

The distinguishing features of the discrete model were formulated in the work [114] for flame propagation in particulate suspension. A comparison of continuous heat sources and discrete heat sources was performed, always

assuming a homogeneous mechanism of heat transfer which is controlled by thermal diffusivity in the gas phase. For the discrete model, it was assumed that point heat sources (particles) were regularly distributed in space, so that they form a cubic lattice, as shown in Fig. 21d. The particles ignite when the gas temperature of the flame front reaches some constant prescribed value, T_{ig} (step-like kinetics). The distance between particles is much larger than their sizes, and, therefore, the reacting particle is actually a δ -function heat source in spatial coordinates. The flame front is flat and propagates in the x direction (Fig. 21d). It was shown that the combustion velocities obtained from the continuous and discrete models coincide if the burning time of each particle is much longer than the characteristic time of heat transfer between them. In the opposite case, for a rapid burning fuel, the flame speed in the discrete system is a weak function of the particle size and is an explicit function of the distance between the particles. This conclusion is equivalent to the condition (B) from Section 3.1, which indicates a sign of the discrete combustion mode.

A similar approach has been developed for so-called solid flame processes [115]. The following assumptions were used: the heat sources (combustible particles) are located on some regular lattice (e.g. hexagonal), whereas heat transfer is still assumed to be uniform. Stepwise kinetics similar to (14) is attributed to the particles. The combustion wave propagation manifests itself as a process of sequential ignition and burning of the particles. It was found that propagation of a combustion wave in this periodic medium possesses a complex behavior inherent in nonlinear discrete dynamic systems. In particular, so called period doubling bifurcations were found in the vicinity of the steady/non-steady boundary. A similar phenomenon was also reported for the discrete combustion model in the work [116].

Several studies were made for the case of homogeneous media with periodic variations in its composition [117–119]. For example, oscillating propagation of the combustion wave in a lamellar microstructure composed of reactive and inert layers oriented normally to the combustion propagation direction (i.e., parallel to the flat combustion front) was investigated. It was shown that the combustion regime depends on the ratio between the layers width, L , and thickness of reaction zone, l . If $L \ll l$, a quasi-homogeneous regime is realized (similar to the case considered in [99]), in the opposite situation, when $L \gg l$, nearly steady-state homogeneous combustion occurs in the

combustible layers, whereas too thick inert layer may result in extinction of the combustion process. The most interesting case is $L \sim l$, where non-linear interactions between the inherent oscillations of the combustion wave and spatial periodicity of the medium is observed. In this instance, the combustion process has features which are typical for the discrete mode: depression periods of preheating of the inert barrier, alternate with periods of non-stationary over-adiabatic rapid reaction in the reactive layers. The detailed consideration of such oscillating regimes is out of the scope of current review.

Complicated 3D models of heterogeneous reaction mixtures are developed for propellants ([120,121] and related works). A random pack of solid spherical particles of different compositions and sizes generated by computer represents an adequate approximation of the real 3D microstructure of the heterogeneous propellants. Excellent agreement between the model and experimental data has been achieved due to the 3D random pack model of the propellant, complete coupling of the gas-phase combustion processes and the solid-phase heat conduction across the unsteadily regressing non-planar propellant surface. Application of this approach to combustion synthesis systems is limited by the lack of knowledge about real microstructures, mechanisms of heat transfer, and interaction between particles in such systems.

3.3. Summary of the theoretical models

Summarizing the discussion of Section 3, we suggest a classification of the combustion models for reaction wave propagation in heterogeneous powder gasless systems as shown in Table 4. Note that the only difference between homogeneous and quasi-homogeneous models is the type of kinetic law, while in both cases the heat source is described as a continuous function of coordinates, temperature, and degree of conversion. Semi-discrete models (Section 3.2.4) account for the discrete nature of heat evolution, but assume uniform thermal conductivity throughout the medium. It is important that the discrete models (Sections 3.2.2 and 3.2.3) involve a difference in thermal conductivities in the reaction cell (bulk) and between the cells.

As stated above, *the ratio of characteristic reaction and heat transfer times is a main criterion for applicability of the above models*. When the reaction time is much smaller than the time of heat transfer from one cell to another ($t_r \ll t_h$), the kinetics of chemical reaction does not influence the

Table 4
Classification of the combustion models

Model	Nature of heat transfer	Heat sources	Reaction kinetics
Homogeneous	Continued	Continued	Homogeneous
Quasi-homogeneous	Continued	Continued	Heterogeneous
Semi-discrete	Continued	Discrete	Any type
Discrete	Heterogeneous	Discrete	Any type

process of combustion wave propagation. In this case, in heterogeneous gasless systems one has to account for the discrete nature of the combustion phenomena and a stepwise kinetic function is a good approximation for process analysis. In the opposite situation, when $t_r \gg t_h$ the homogeneous approach can be used to describe combustion of such a heterogeneous system. A relation between the reaction cell size and the thickness of the reaction zone results from the above ratio of the characteristic times: if $t_r \gg t_h$ the reaction zone includes many cells; at $t_r \ll t_h$ the sizes of the reaction zone and reaction cells are comparable. It is important to outline that the criterion is not directly defined by the reactant particle size. Therefore, decreasing the particle size does not necessarily result in homogenization of the combustion process.

4. Comparison of experimental and theoretical results

Two general aspects should be discussed when comparing discrete theories with the experimental results. First, the experimentally observed microstructural features of a combustion wave, (such as the appearance of hot spots, their size and lifetime, super-adiabatic temperature peaks, chaotic oscillations of the local propagation velocity, distance of the combustion front jumps, etc.), must be compared with corresponding results predicted by theoretical models. However, comparison of the local, microscopic characteristics is not enough, because most experimental data, accumulated up to now, describe global (average), macroscopic behavior of the combustion wave. Thus, the macroscopic parameters (i.e. average combustion velocity, limits of combustion stability, temperature coefficients of the propagation speed, etc.) must also find their proper explanations in the discrete model. Below, analysis of both aspects is presented, with special attention paid to macroscopic features of the process, which help to distinguish homogeneous and essentially heterogeneous combustion mechanisms.

4.1. Microscopic aspects

It can be understood why the local behavior of the combustion front predicted by discrete theoretical models *qualitatively* correlates with the experimental results obtained by high-speed micro-video recording (Sections 2.1 and 2.3) and temperature–time measurements by optical pyrometers (Section 2.2). Indeed, heterogeneity either of a real mixture or a virtual 2D lattice leads to similar results: (a) deviations of the combustion front from planar, (b) random oscillations of the propagating velocity, (c) existence of hot spots, etc. For example, study of flame propagation in random media [122,123] led to 2D temperature field patterns, which looked very similar to the experimentally observed scintillating mode of gasless combustion. Akin results were obtained when irregularities were attributed not to the medium, but to the kinetic law [113].

It is important to reiterate that not all theoretically obtained features, which qualitatively look similar to the experimental observations, prove a models reliability. For example, the theoretically predicted existence of hot spots [113] or oscillating behavior of the temperature profile with a pronounced super-adiabatic peak [115] cannot be considered as indisputable proof for the discrete nature of the described phenomenon. Only *quantitative* congruence of the theoretical and experimental results can prove that the model adequately depicts the real process. Unfortunately, analysis of publications allows us to conclude that most of the developed theoretical models do not provide sufficient results for *quantitative* comparison with existing experimental data. Also, not all experimental studies provide numerical values, which can be compared with theoretical predictions. Therefore, this task should be solved from both sides, i.e. by development of experimental approaches that allow formalizing of the data, as well as by adapting theoretical models in order to make them comparable with experiments.

Elaboration of the microstructural characteristics of combustion front propagation was made in [42]. Definitions of main parameters are given in Tables 2 and 3 (see Section 3.2). Such processing of the experimental data allows one to build dependencies, which can be directly compared with the results of computer modeling. Fig. 24 demonstrates some examples of experimental data on local behavior of the combustion front, in comparison with results of 2D discrete modeling [95]. It can be seen that the cellular 2D model [55,95] adequately describes the variation in the combustion front roughness as a function of media porosity and particle sizes. The discrepancy between the experimental and theoretical critical values of the relative sample density at which the combustion mechanism changes was explained based on the fact that it is a real 3D structure that was analyzed using a 2D model. In 3D-reaction media, the combustion wave is able to propagate not only around inert inclusions or voids (as it does in a plane model), but also above and below them. Hence, some pre-determined values of connectivity will be achieved in the 2D lattice at higher density (less porosity) than in the 3D network of real particles.

Comparison of measured and calculated distributions of local instantaneous velocity were also made [52]. An example presented in Fig. 25 shows a satisfactory fit between model and experiment. Furthermore, an approximate parametric map showing the regions of combustion mechanisms for the Ti–Air system as a function of initial organization of the reaction medium was plotted on the basis of experimental observations (Fig. 26). Comparison of this diagram with the map obtained by computer simulation (see Fig. 22) reveals reasonable agreement in location of the main regions of combustion modes, although some discrepancy is observed between the density scales.

However, we may conclude that the currently available amount of quantitative data on microscopic behavior of

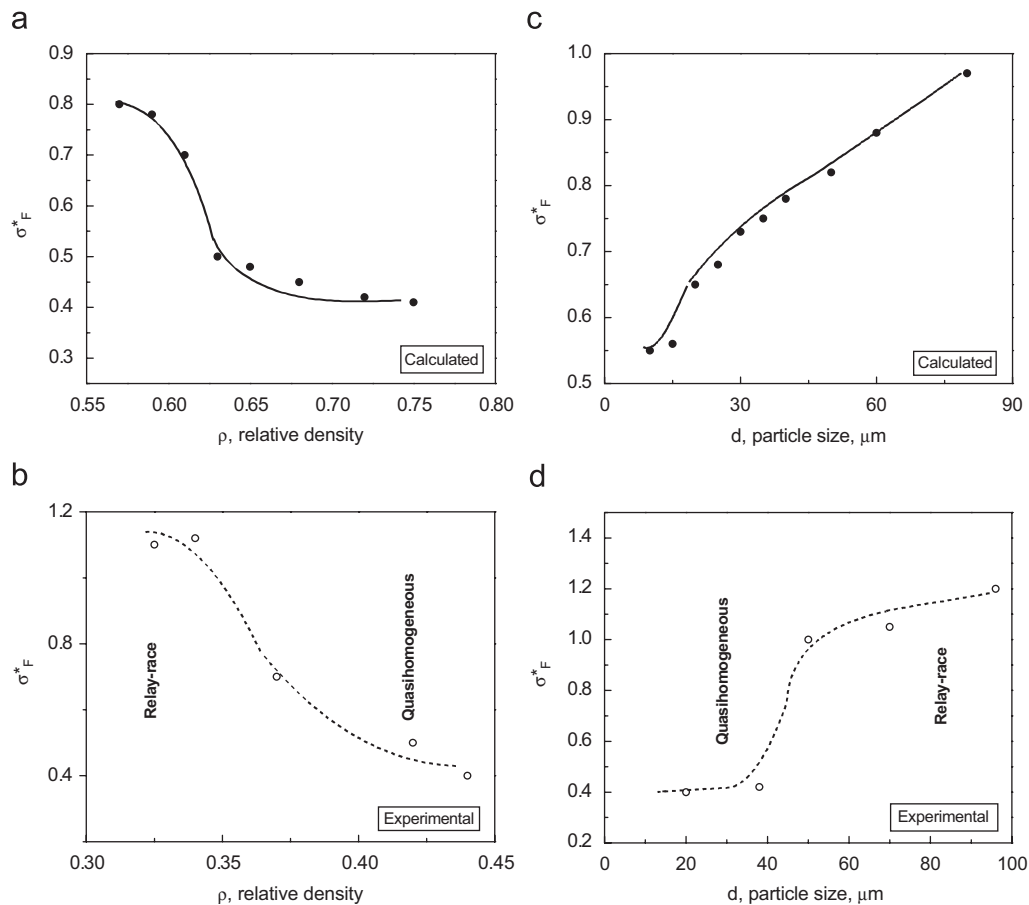


Fig. 24. Roughness of the combustion front as a function of: (a, b) particle size at constant density of the reaction media; (c, d) density at constant particle size.

the combustion front is very limited. This is partly due to the complexity of time-consuming methods, which must be utilized to collect such information. Rapid development of high-speed video recording equipment and computer software for image processing allows us to believe that this obstacle will be overcome in the near future. Another reason for the lack of data is human inertia. Unfortunately, the traditional approaches for combustion research, where macroscopic characteristics, such as average combustion wave propagation velocity or maximum temperature are assumed to be an exhaustive description of the entire process, still prevail.

4.2. Thermal and chemical heterogeneity of the reaction media

As discussed above, the discrete models of combustion waves are based on the assumption of relatively slow rates of heat conduction in porous heterogeneous media, which is the result of high thermal resistivity of the contacts between reaction cells (particles) in the powder mixtures. Let us consider experimental justifications for this assumption. Thermal conductivity in solid porous systems has been extensively investigated [124–127]. In general, such systems consist of a variety of solid particles and pores,

both of different size and complex forms, which make the analysis difficult. However, it was shown that if in the microstructure of such a material some elementary cell (i.e. distinctive structural element with the physico-chemical properties similar to those of the bulk media) can be defined, thermodynamic and hydrodynamic approaches allow one to describe the heat conduction process in these media and carefully predict the effective coefficient of heat transfer (λ_{ef}).

It is well established that λ_{ef} depends on a variety of parameters including media porosity (p), thermal conductivities of solid (λ_s) and gas (λ_g) phases, and contacts between the solid particles (λ_c). It was also shown that at relatively large porosity ($>20\%$) and small particle size ($<100\mu\text{m}$), the *contact particle resistance* to the heat flow defines the heat conduction in such media. The size of the contact spot area (A_{sp}) depends on the physical characteristics of the solid particles (e.g. modulus of elasticity), the applied pressure (P), as well as the roughness of particle surfaces (h_c). Also, in general, contact conduction occurs through different mechanisms including molecular and radiation thermal conductivities in the micro-gaps.

All of the above allow one to clarify the experimental data on effective thermal conductivities of different discrete reactive porous systems. For example, the contact resistance

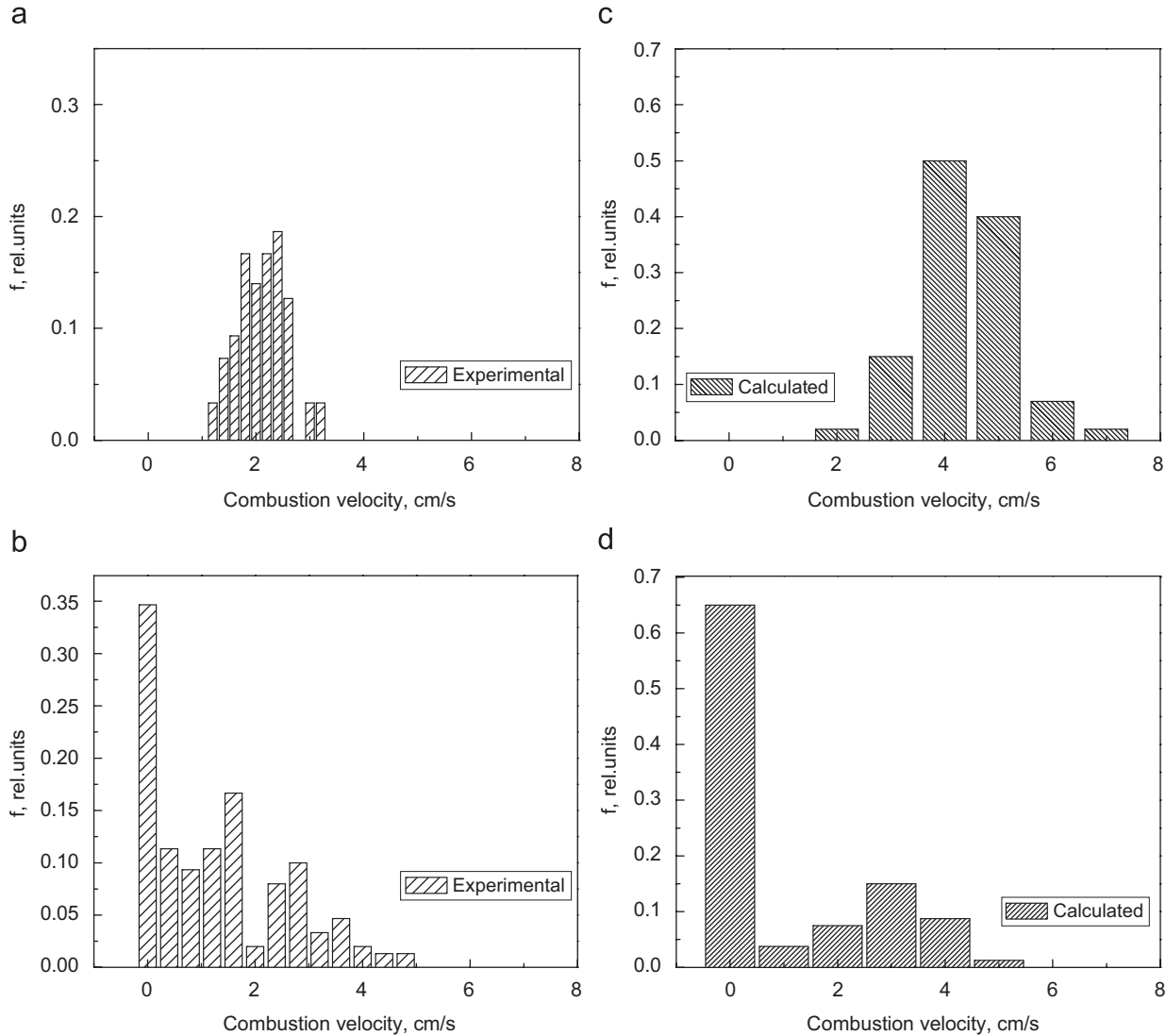


Fig. 25. Measured (a, b) and calculated (c, d) distributions of instantaneous velocities for large (a, c) and small (b, d) reaction media densities (adopted from Ref. [52]).

explains the essentially equal values of λ_{cf} (less than 1 W/mK) for heterogeneous samples consisting of metal particles with high bulk λ_s (~40–200 W/mK) and oxides with relatively low λ_s (1–10 W/mK) [124]. It is more important that it was shown experimentally and confirmed theoretically that λ_{cf} of such solid porous structures may be much lower (10–100 times) than the bulk λ_s for the solid particles which formed these structures.

Despite the large number of publications on combustion of heterogeneous systems, there is a lack of experimental data on their microstructure and transport properties. These systems involve at least two types of solid particles (e.g. A and B) that assume different types of contacts (e.g. A–A, A–B, and B–B). The thermal properties of such media also depend on the ratio between the reagents and may change abruptly at compositions which correspond to the formation of a continuous skeleton (percolation) of sorts of A (or B) particles. This interesting aspect was

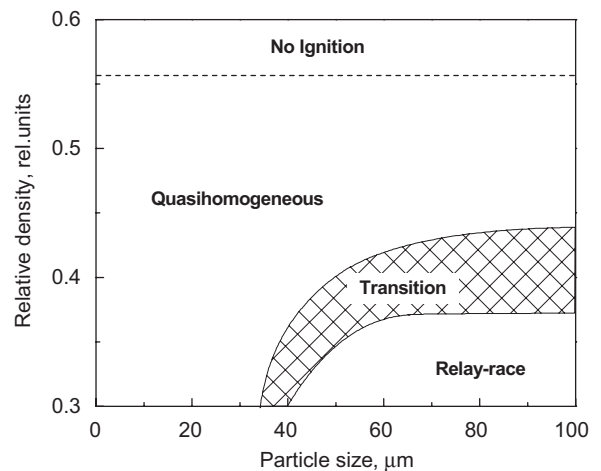


Fig. 26. Parametric map (adopted from Ref. [52]) showing regions of combustion mechanisms for the Ti-air system as a function of initial organization of the reaction medium.

noted by different authors [64], but additional direct measurements of the media thermal conductivity as a function of the length of the continuous clusters are required to make a distinct conclusion.

However, the thermal conductivities of some reaction mixtures were experimentally defined [128–130]. Hard and Phung [128] reported the λ_{ef} for binary (Ti–B; Ti–C Zr–C; Ni–Al) and ternary (Ti–B–Al; Ni–Al–B) systems (Table 5). It can be seen that loose powders have very low λ_{ef} (~ 0.05 W/mK), which is comparable to the thermal conductivity of air (~ 0.027 W/mK). After compaction, for example in the Ti–2B system, λ_{ef} increases on an order of magnitude (0.3–1.2 W/mK) and depends on the sample porosity, as well as the direction of measurement (normal

or parallel to the direction of compression). It is important that the measured λ_{ef} is still much lower than λ_{s} of the individual solid components. Also, a small addition of a third element (e.g. boron in the Ni–Al–B system) leads to a significant decrease in the media thermal conductivity, which may be explained by the percolation effect (note that λ_{s} of Al, 220 W/mK is much higher than for B, 25 W/mK).

Thermal conductivities of binary metal powdered systems (Zr–Al; Ni–Al) were also investigated as a function of media porosity and temperature [129]. It was shown that in the temperature interval 300–500 K, the effective thermal conductivity of these systems is essentially independent of temperature (see Fig. 27a). Also, the absolute values of the measured λ_{ef} are much less than λ_{s} for the bulk metallic

Table 5
Thermo-chemical characteristics for different powder reaction systems (adopted from Ref. [128])

Mixture	Nom. part size (μm)	C (cal/g K)	ρ (g/cm^3)	λ (cal/cm s K)	Q (Cal/g)
Ni–Al	3	0.180	5.11	0.1156	329
With 5 wt% B	3	0.193	4.50	0.053	273
10 wt% B	3	0.217	3.95	0.008	230
25 wt% B	3	0.273	2.82	0.0013	100
Ni–Al	30	0.180	5.11	0.156	329
With 5 wt% B	30	0.193	4.50	0.053	273
10 wt% B	30	0.217	3.95	0.008	230
25 wt% B	30	0.273	2.82	0.0013	100
Ti–2B	60	0.306	2.32	0.0029	1155
Ti–2B	10	0.306	2.32	0.0029	1155
With 30% Al	60	0.292	2.45	0.0043	690
With 60% Al	60	0.282	2.42	0.0085	533
Zr–2B	2	0.171	2.11	0.00081	690
Zr–2B	50	0.171	2.11	0.00081	690
Ti–C ^a	10	0.226	2.50	0.017	737
Ti–C ^b	60	0.226	2.44	0.0014	737
Ti–C ^b	10	0.226	2.44	0.0014	737
Zr–C ^a	2	0.180	3.65	0.0035	461
Zr–C ^b	2	0.180	3.00	0.00067	461
ZR–C ^b	15	0.180	3.00	0.00067	461

^a 1/3-Lampblack + 2/3 graphite.

^b Lampblack.

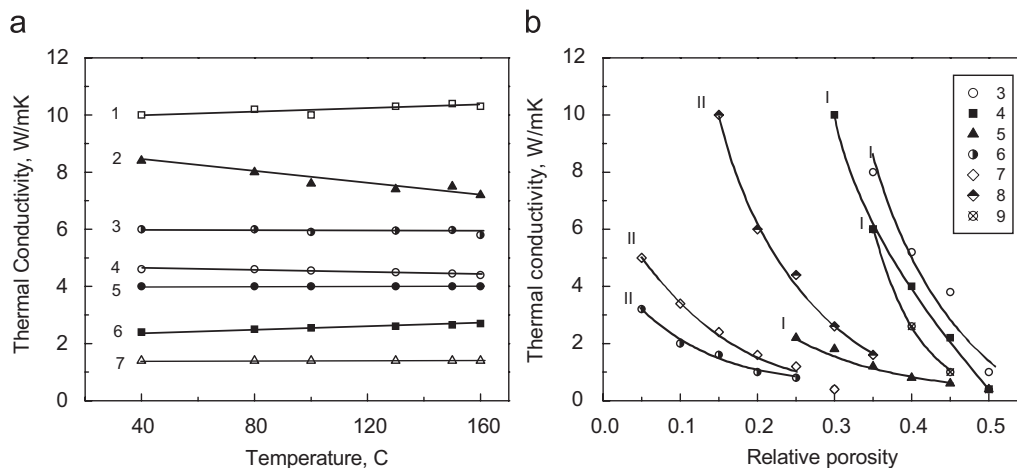


Fig. 27. Dependencies of thermal conductivity in different Zr–Al and Ni–Al powder mixtures as a function of: (a) temperature and (b) media porosity (adopted from Ref. [129]).

components. In addition, at relatively high porosity, λ_{ef} weakly depends on the amount of Al in the system (Fig. 27b), which has a high thermal conductivity (~ 220 W/mK).

Finally, it was reported that λ_{ef} in such systems depends on the nature of the gas environment [130]. More specifically, it was shown that effective conductivity (e.g. in the Ti–C system) increases with an increase in the gas thermal conductivity, λ_g , being 0.34, 0.627, and 1.24 W/mK in vacuum, air, and helium, respectively. Note that these data explained the observed dependence of combustion velocity in heterogeneous systems as a function of the thermal conductivity of the used inert gases [131].

All of the above results, on the one hand, are in qualitative agreement with the trends, which were observed for one-component systems. On the other hand, they confirm the important role of the inter-particle contacts in the mechanism of heat transfer in heterogeneous reaction media. The latter suggests relatively slow rates of heat conduction in such discrete systems as compared to the bulk pore-free media with ideal (no contact heat resistance) inter-particle contacts (e.g. obtained by sputtering of reactants nano-layers [132]).

Unlike the thermal heterogeneity of the reaction media, chemical heterogeneity issue has been discussed in many papers and reviews [60,86]. A variety of mass transfer and reaction mechanisms were suggested and discussed (see also Section 3). Since this concept can be the topic of a separate review, let us consider only two important features.

First, the unique conditions of the combustion wave (extremely high rate of temperature change in the combustion front, up to 10^5 K/s; high reaction temperatures,

typically above the melting point of at least one reagent; and relatively low initial contact area between the reactants) leads to very high rates of chemical interaction. Experiments have shown that because of the high heating rates, there is not enough time to form a continuous layer of the intermediate products owing to solid-solid reactions, i.e. below the melting point of the less refractory reactant [133–135]. Thus when one reactant (e.g. A) melts, it spreads along the “pure” surface of the other reactant particle B, which leads to a significant increase in the direct contact area between the reagents (A and B). The latter effect is known as *chemical homogenization of the reaction media*. Again, an absence of a product layer allows immediate reaction between reagents (so-called reaction spreading [136]) with rates much higher than typically observed at these temperatures under relatively low ($< 10^3$ K/s) heating rates (compare Fig. 28a and c). A similar situation (so-called reaction coalescence [137]) occurs if the combustion temperature is higher than the melting point of both components (Fig. 28b). The detailed studies on kinetics of chemical reactions in such heterogeneous systems allows for the critical heating rates to be obtained, which are required to observe such rapid interaction at high temperatures [135]. Recall that below the critical heating rate, chemical reaction is relatively slow since it proceeds by diffusion of melted reagent through a solid layer of product formed at lower temperatures (Fig. 28c).

The second important observation is that typically reactions in such heterogeneous combustion waves “on-sets” at some specific point, which is related to the temperature of *reagent phase transformation* (e.g. melting, dissociation, etc.). Note that the latter is the *characteristic*

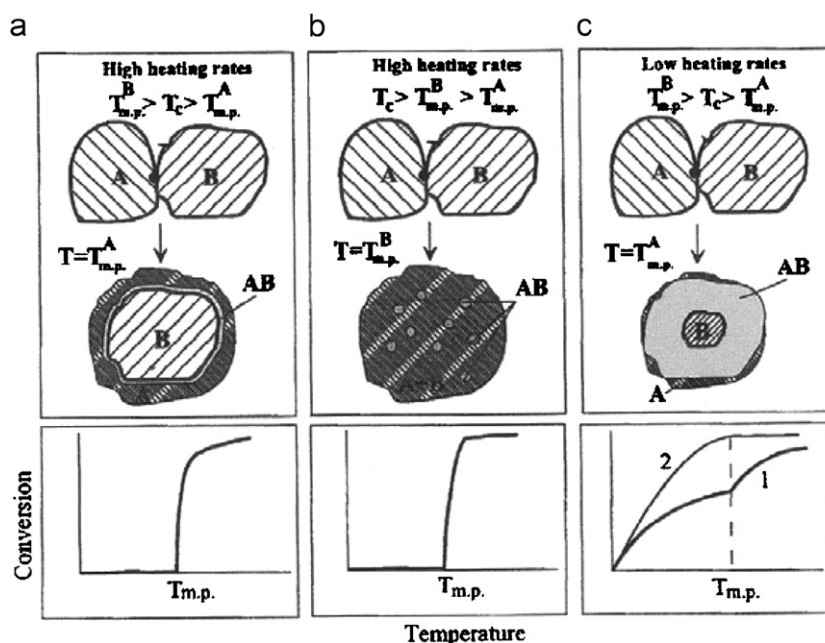


Fig. 28. Schematic representation of the interaction mechanisms for different binary (A,B) reaction systems: (a) reaction spreading—reactant A melts and B remains solid, high heating rate; (b) reaction coalescence—both reactants melt, high heating rate; and (c) solid state reaction diffusion—reactant A melts and B remains solid, low heating rate (adopted from Ref. [53]).

temperature of the system, which does not depend on ambient conditions (heat loss, inert gas pressure, etc.) [52]. This feature follows from the previously discussed mechanisms of interaction in heterogeneous combustion waves. Indeed, melting of particles (or reagents coalescence) leads not only to a rapid increase in reaction surface but also enhances the diffusion processes. Taking into account slow reaction rates by solid diffusion and small contact surface area between reagents in the initial porous media, it becomes clear why the melting point of the less refractory reagent is the “ignition” temperature for most considered reactions. This conclusion was confirmed by numerous studies of the ignition temperatures in a variety of heterogeneous systems [138–141].

Thus, the thermal and chemical heterogeneity of the reaction media are important features that define the specifics of combustion wave propagation in such systems. To develop an adequate model that accurately describes this process, it is important to take into account two factors: (i) the contact thermal resistance in porous discrete media makes this network much less thermally conductive than bulk homogeneous materials; (ii) despite chemical heterogeneity, the rate of chemical interaction in the combustion front of such systems may be extremely high. In another words, experimental studies of the heat and mass transfer mechanisms in the considered heterogeneous reactive systems allow one to conclude that the characteristic reaction time, t_r , in such heterogeneous reactive mixtures is much smaller than the time of heat conduction, t_{hc} . The latter exactly match condition B formulated in Section 3.1 for existence of the discrete combustion waves.

4.3. Global characteristics of combustion processes

The data on the macroscopic characteristics of combustion form a major part of all experimental data available up to date. However, analysis of these data in order to distinguish homogeneous and discrete combustion mechanisms faces certain difficulties. The point is that most of the observed macro effects can be qualitatively explained from the viewpoints of both homogeneous and discrete approaches. Indeed, experimentally observed trends, such as increasing combustion (U_c) velocity with increasing initial temperature and density of the reaction media, or decreasing U_c with increasing reactant particle size, heat losses, inert dilutions, evidently work for both mechanisms.

Quantitative calculations of absolute values of combustion velocities could provide more distinguishing conclusions, however, two obstacles arise: (a) such calculation require knowledge of the characteristics of the reaction medium, which are usually unknown, e.g., thermal resistance of the inter-particle contacts or intrinsic reaction kinetics, and (b) there is no consistency between experimental data reported by different authors even for the same systems (see, for example, review [142]). Thus, we must admit that there are no algorithms, neither homogeneous nor discrete, which allow precise calculation of the

combustion velocity for micro-heterogeneous mixtures without using at least one fitting parameter.

However, other approaches exist, where comparison can be made for a wide variety of experimental data obtained by different research groups. For example, despite the significant scattering of absolute values of combustion velocity, different authors reported consistent data on effective activation energy for the combustion propagation process. The most widespread method for measuring this energy is based on the variation of combustion temperature (by preheating of a green mixture or dilution with inert product), defining a temperature coefficient of combustion velocity K_T (see Eq. (11)) and calculating the value of the activation energy as follows:

$$E \cong 2RT_C^2 K_T. \quad (19)$$

The results of different authors obtained using this approach, are summarized in Fig. 29. According to quasi-homogeneous theory, the E value is equal to the activation energy of the “leading” chemical reaction in the combustion wave. Since the rate of this reaction is commonly assumed to be limited by diffusion, E is usually related to the activation energy of diffusion: a high value is considered as evidence of solid-state diffusion across the layer of refractory product, while a low value ($E < 150$ kJ/mol) is attributed to liquid-phase diffusion in the melts. As a matter of fact, most of the works [143–153] presented in Fig. 29 followed this viewpoint. However, when all results are collected in one plot, the weakness of such an explanation becomes evident.

Indeed, the systems with light elements (boron, carbon) where one may expect the lowest diffusion activation energies actually exhibit the highest E values. The tendency of E to increase with increasing temperature also cannot be rationally explained from the viewpoint of homogeneous theory. Let us briefly discuss this issue. On the one hand, the combustion temperature for a Ti+2B stoichiometric mixture ($T_C = 3200$ K) is much higher than the melting point of Ti (1940 K) or B (~2300 K) and equal to the melting point of the final product, titanium diboride. A similar situation takes place for Zr+2B and Hf+2B mixtures. On the other hand, the T_C for Zr+2Al or Ti+Co mixtures is lower than the melting points of Ti or Zr. Moreover, in the vicinity of the combustion temperature, the solubility of Al in Ti or Zr is much lower than the solubility of B in these metals. Therefore, it can be expected that activation energies will be lower for the diffusion in Ti–B, Zr–B systems compared to intermetallic systems (Zr–Al; Ti–Co, etc.). However, quite opposite results were obtained experimentally (see Fig. 29).

Furthermore, if one assumes (following quasi-homogeneous theory), that the effective activation energies presented in Fig. 29 are equal to the intrinsic activation barriers of elementary diffusion, then these value should coincide with E values obtained by other approaches. The method for determining this parameter based on the treatment of temperature profiles of combustion or thermal

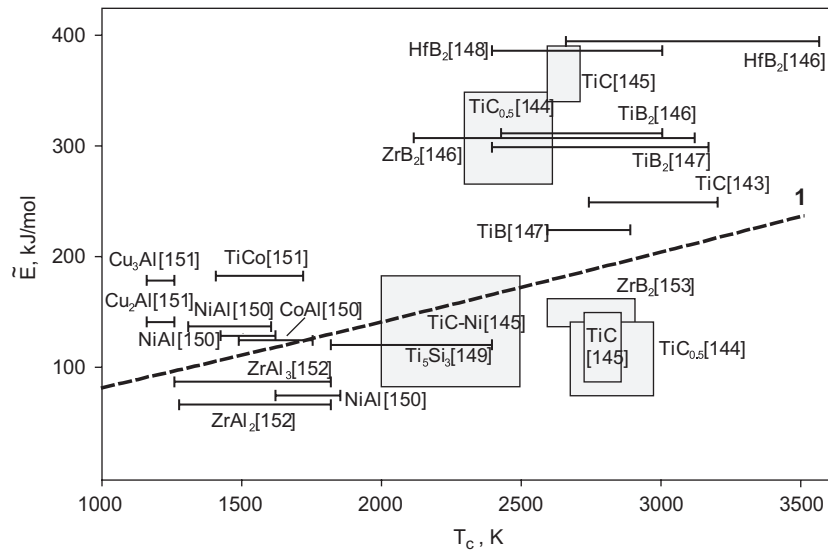


Fig. 29. Summary of the experimental data on activation energies for typical gasless combustion systems (dashed line is calculated using Eq. (20)) (adopted from Ref. [87]).

Table 6

Some effective kinetic parameters of gasless combustion assessed from temperature profiles and thermal explosion experiments

Reaction	Range of T (K)	Range of η	E (kJ/mol)	Kinetic function parameters		Z/B/S	Reference
				m	n		
Ti + C → TiC	< 1940	–	210	–	–	S	[92]
	1940–3000	–	0	–	–		[92]
Ti + x B → TiB + Ti ($x < 1$)	–	–	–	0	2	Z	[26]
Zr + 2B → ZrB ₂	1500–2700	0.3–0.9	142 ± 17	10	0	Z	[26,154]
	< 1500	< 0.3	59	–	–		[154]
Zr + 1.5B + x TiB ₂	–	0.5	89 ± 10	–	–	B	[153]
→ ZrB ₂ + Zr +		0.6	138 ± 13				[153]
TiB ₂		0.7	155 ± 17				[153]
		0.8	140 ± 39				[153]
		0.9	88 ± 77				[153]
		0.5–0.9	122 ± 29				[153]
		0.6–0.8	145 ± 15				[153]
Hf + 2B → HfB ₂	1900–2800	0.5–0.9	168 ± 21	15	0	Z	[26,154]
	< 1900	< 0.5	80	–	–		
Nb + 2B → NbB ₂	1600–2300	0.4–0.9	146 ± 21	12	0	Z	[26,154]
	< 1600	< 0.4	100	–	–		[154]
Nb + B → NbB	1800–2500	0.4–0.8	210 ± 42	23	0	Z	[26,154]
	< 1800	< 0.4	159	–	–		[154]
Ta + 2B → TaB ₂	–	0.4–0.9	210 ± 42	18	0	Z	[26,154]
		< 0.4	138	–	–		[154]
Ta + B → TaB	–	–	285	24	0	Z	[154]
5Ti + 3S → Ti ₅ Si ₃	1100–1790	–	117 ± 8	0	1	Z	[156]
	1790–2400	–	147	0	3		[156]
Zr + x Si → Zr ₅ Si ₃ + Zr	–	0.25–0.5	84	0	1.5	Z	[156]
Si ($0.5 \leq x \leq 1$)		0.7–0.9	126	8	0		[156]

Notes: Z, B, and S denote methods of E determination. Z—temperature profile treatment according to Zenin et al. [26]; B—temperature profile treatment according to Boddington et al. [155]; S—electric-thermal explosion method by Shteinberg et al. [92].

explosion processes is described in the works [26,27,154]. Generally, there are two routes for processing temperature profiles of the combustion wave, one suggested by Zenin et al. [26,56], another by Boddington and Layer [27,155], which allow one to extract kinetic data. Results obtained for gasless heterogeneous systems are shown in Table 6.

Comparison of these data with those shown in Fig. 29 reveals significant discrepancies. Only one system, Ti–Si, demonstrate similar E values obtained by different methods. For the other compositions, values extracted by analysis of temperature profiles are lower than those obtained from velocity measurements.

Finally, activation energies can be derived from the temperature–time history of the thermal explosion process. Data obtained by Knyazik et al. [92] for a Ti+C mixture indicate a highly activated reaction below the melting point of Ti and essentially zero activation energy for reaction above this point. All of the above discrepancies are impossible to explain based on the quasi-homogeneous combustion model.

Let us consider these results from the viewpoint of the discrete model. If the reaction time is shorter than the time of heat transfer between reaction cells, the combustion wave velocity is limited by heat transfer. It means that U_c is less sensitive to the rate of chemical reaction, which allows one to use simplified stepwise kinetics (Eq. (14)). As it was shown above (see Section 3), the temperature coefficient for combustion velocity K_R in this case equals 3.9. It is

important that this coefficient does not depend on any parameter of the model. Utilizing Eqs. (14)–(16), one can obtain the formula for effective activation energy as follows:

$$\bar{E} = -2R \frac{T_c^2}{T_c - T_0} K_R. \tag{20}$$

Calculations according this formula yield the line which is presented in Fig. 29. First of all, it is not a trivial result that the values calculated by formula (20) have the same order of magnitude as the measured values. Indeed, the discrete model based on stepwise kinetics assumes no specific activation energy. Second, this curve demonstrates the tendency of increasing E with increasing temperature. Third, it is in satisfactory agreement with experimental results.

Dependence of the effective activation energy on porosity of the mixture is another distinguishing feature between quasi-homogeneous and discrete models. According to the quasi-homogeneous model, E does not depend on media porosity, because it relates directly to the elemental process of atomic diffusion through the solid layer of product. The discrete model makes the opposite prediction: since propagation of the combustion wave is limited by heat transfer between particles, the effective activation energy must exhibit a noticeable dependence on the contacts properties, which in turn depend on the density (porosity) of the powder mixtures. Evident dependencies of E on the sample density were observed for Ti–Si [156] and T–Si–C [157] systems (see Fig. 30). It was found that the effective value of activation energy decreases with increasing porosity. The fact that E depends on porosity indicates a discrete mechanism rather than a homogeneous one.

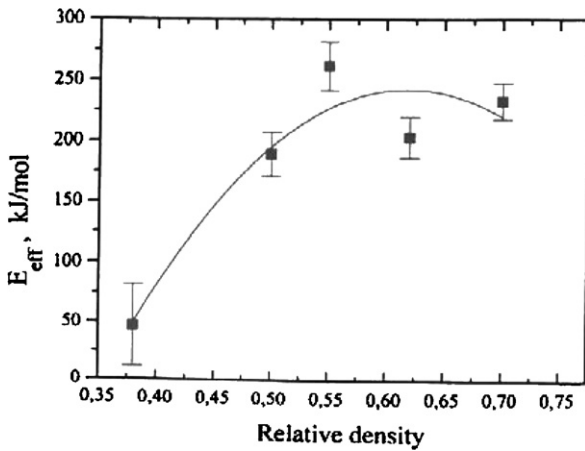


Fig. 30. Dependence of effective activation energy (assessed from the combustion experiments) on initial reaction medium media density for the 5Ti–3Si reaction system (adopted from Ref. [156]).

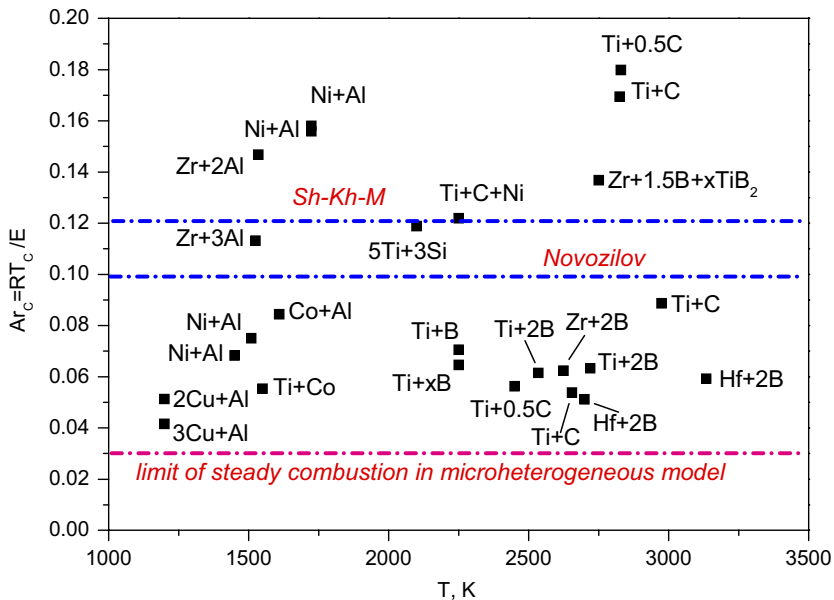


Fig. 31. Summary of the experimental data on stability limits for combustion of various gasless reaction systems (dashed lines = theoretical predictions).

The boundary between steady-state and oscillating regimes is one of the most important combustion characteristics. Two equations were suggested in the frames of quasi-homogeneous theory for calculating this boundary. A stability criterion for steady combustion wave propagation was developed numerically in the form of the approximate relation [158]:

$$\alpha_{st} = \left(9.1 \frac{T_c}{T_c - T_0} - 2.5 \right) \frac{RT_c}{E}$$

and the boundary separating the steady state and oscillation combustion modes is given by the following conditions: $\alpha_{st} > 1$, steady state mode; $\alpha_{st} < 1$, oscillatory mode.

This formula is in good agreement with the analytically derived criterion [159,160]:

$$\frac{E(T_c - T_0)}{2RT_c^2} < (2 + \sqrt{5}).$$

Under closer examination, it becomes evident that these two criteria describe essentially the same condition, i.e. for stable steady-state propagation, the temperature dependence (sensitivity) of combustion velocity must not be too high (relatively low E). Note that the discrete model, as it was shown in Section 3, suggests a notably different criterion: $Ar_c > 0.03$.

Analysis of this criterion indicates that the relay-race mechanism allows the existence of a steady regime for much higher values of the activation energies. Since the effective energies and combustion temperatures were measured for a wide variety of powder mixtures, it is possible to check the applicability of all above criteria directly. Fig. 31 shows values of the stability criteria calculated using published experimental data for the systems known as typical examples of steady-state combustion. A conclusion can be made that the discrete model fits the experimental data on combustion stability much better than the quasi-homogeneous approach.

4.4. Combustion in model heterogeneous systems

Commonly used reactive powder mixtures possess very complicated irregular microstructures, which is a difficult object for mathematical formalization. On the one hand, this gap can be decreased by developing more sophisticated mathematical models taking into account the random distribution of the reaction cells, as considered above (see Section 3). On the other hand, the microstructure of the real reaction media can be modified in order to make it closer to theoretical models. This approach, which allows experimental verification of the basic principles of discrete models, is named *model experiments*.

Several approaches were used to increase the contact surface area between reagents inside the reaction cell, including utilization of so-called clad particles [161,162], composite particles obtained by mechanical activation [163,164], and reactive multi-layer nano-films [165,166]. Each of these methods allowed emphasis on the important

features of heterogeneous combustion, which are briefly discussed below.

The clad particle is a specially prepared “elemental chemical cell”, where one metal (e.g. Al) is uniformly covered by a layer of the other (e.g. Ni) reagent with a desired mole ratio between reactants. The microstructures of the samples compacted from the Ni–Al clad particles and powder mixture (Ni+Al) with the same overall composition are shown in Fig. 32 [141]. These micrographs show that in the case of clad particles, Fig. 32a, the contacts between reactants are more uniform and their area is larger than for mixtures compacted from elemental reactant particles, Figs. 32b and c.

More importantly, absolutely different trends in the dependence of combustion velocity vs. the initial sample density (ρ_0) were observed for these mixtures [162]. It is

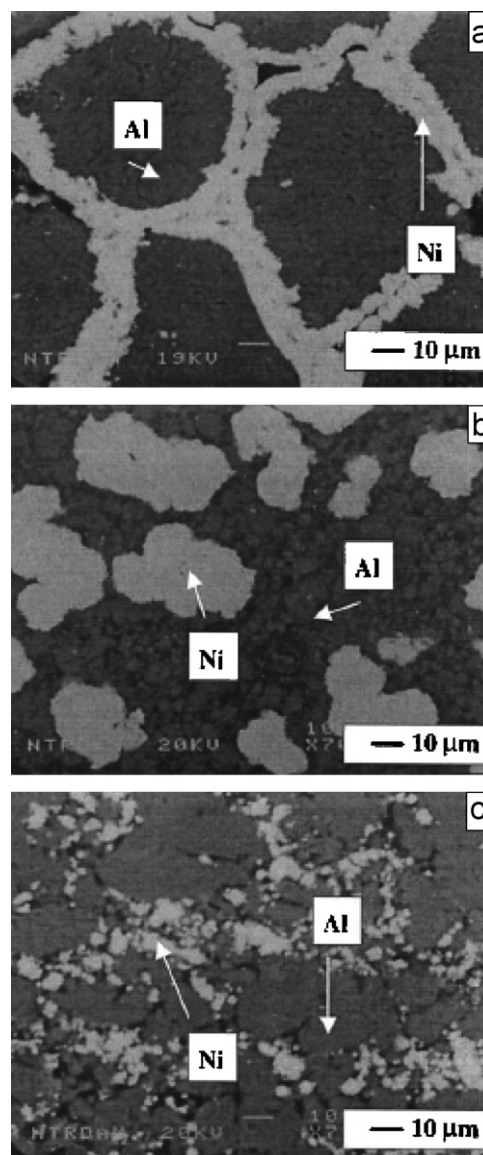


Fig. 32. The microstructures of the samples compacted from: (a) Ni–Al clad particles and (b, c) Ni+Al powder mixtures with the same overall composition (1:1 mole ratio) (adopted from Ref. [141]).

well established that in the Ni–Al system, with increasing ρ_0 , U_c monotonically increases or exhibits a maximum [60,86]. A singular dependence was obtained for combustion of clad particles (Fig. 33). It was shown that within a

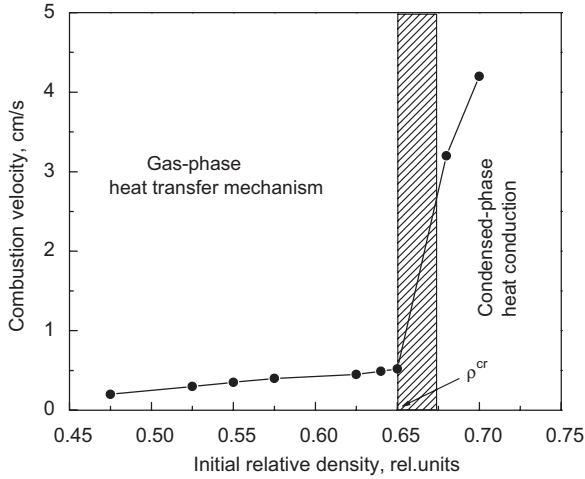


Fig. 33. Dependence of combustion velocity as a function of initial sample density in heterogeneous powder media consisting of clad Ni–Al particles (adopted from Ref. [162]).

relatively wide range of ρ_0 , (0.48–0.65) the combustion front velocity increases monotonically as predicted by classical theory. However, when density was increased by only 3% above the critical value, U_c increases significantly (more than five times). These results were explained by a change in the primary mechanism of heat transfer in the reaction medium. Detailed studies showed that below a critical density (in this system $\rho_{cr} = 0.66$) heat conduction along the porous media occurs primarily because of the gas-phase heat convection mechanism, whereas for $\rho_0 > \rho_{cr}$ the more rapid solid-phase heat conduction predominates. This elucidates the considerable increase in combustion velocity on the right branch of the curve of Fig. 33 and emphasizes the role of heat transport on combustion in such heterogeneous media.

Other remarkable results were obtained on combustion of such systems in microgravity [162] including onboard the MIR Space Station [167,168]. In all cases, both pressed pellets ($\rho_0 < 0.7$) and loose powder ($\rho \sim 0.5$) of Ni clad Al particles were used for the investigation. For the latter, the powders were typically placed in evacuated sealed quartz ampoules with a free space (pores + unoccupied ampoule volume) of 50–70%. Combustion was initiated at the bottom of the quartz ampoule, for example by focused

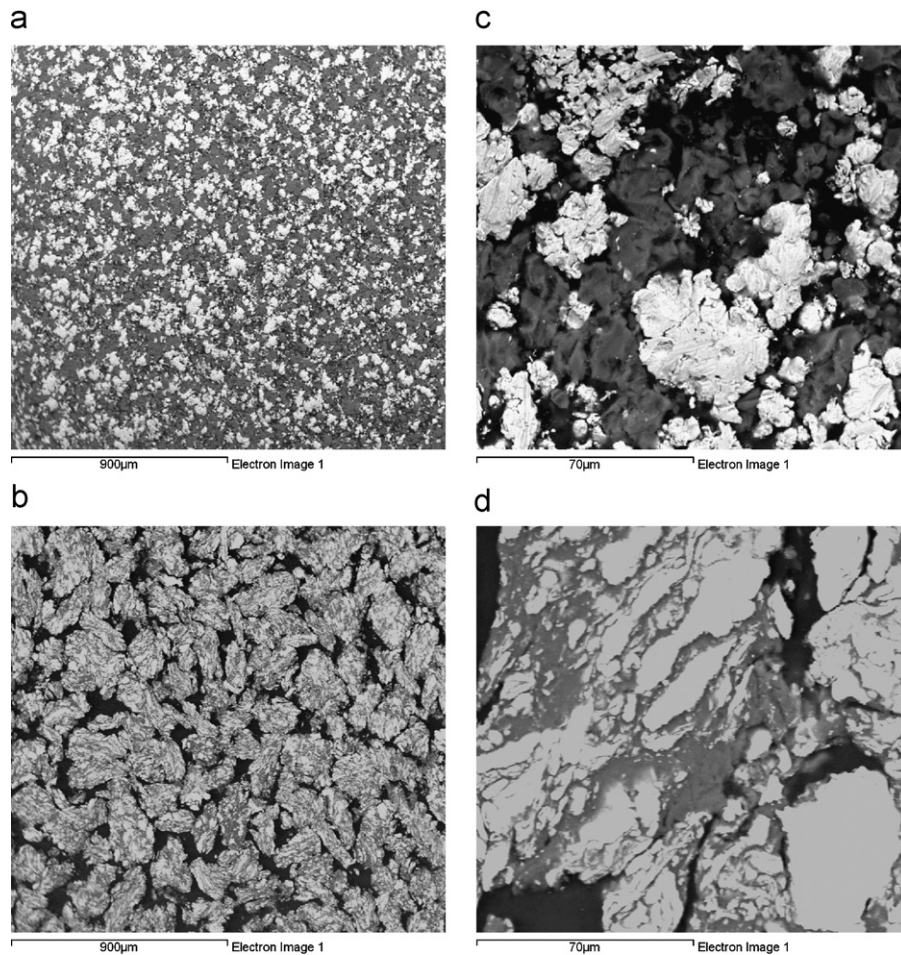


Fig. 34. Typical microstructures of the Ni + Al powder mixtures after different types of mixing procedures: (a, b) conventional mixing; (c, d) high energetic ball milling (adopted from Ref. [172]).

radiation from halogen lamps located around the sample [167]. The video recordings of the process showed that in microgravity conditions, clad particles were initially uniformly distributed throughout the ampoule volume forming a particle cloud in vacuum. After reaction initiation, the combustion front propagates in this *gasless cloud*. It was also suggested that heat transfer in such clouds can occur by *radiation and/or upon particle collisions* [162,168]. In addition, it was reported that the average combustion velocity in such gasless clouds is higher than in loose powder mixtures [169]. The latter suggests that heat transfer is the controlling step of reaction front propagation in such heterogeneous mixtures, and radiation ($T \sim 2000$ K) in *contactless* combustion waves provides higher propagation velocities compared to gas phase convection.

Another type of complex particles, which have even higher surface contact between the reagents, can be obtained by energetic ball-milling [163,170,171]. Fig. 34 represents the microstructures of porous media in the Ni–Al system after conventional (a and b) and energetic (c and d) ball-milling [172]. It can be seen that in the latter case, each particle is pore-free and has a *lamellar structure* that involves thin layers of both reagents (Ni: bright and Al: gray). Note that one can control the ratio between the precursors and the thickness of these layers can be as small as a *few nanometers*. Thus, each particle represents the elemental chemical cell which, as it was discussed above, is frequently used in theoretical models.

High-speed video recording of combustion wave propagation [172] in the reaction media compacted from these complex particles revealed strongly pronounced features of the relay-race mechanism discussed above. The typical distributions of the hesitation (t_h) time and duration of the active phase (t_r) are presented in Fig. 35a. It can be seen that t_h is much (1–2 orders) longer than t_r . The hesitations occur on the boundary between the particles, while during the active stage the reaction propagates along the complex particle. Indeed it was shown that the distributions of reaction front “jump” distances during the active stage is essentially similar to those of the precursor particle diameters (Fig. 35b).

The last “model” system to be considered is combustion of multilayer foils with nano-scale thickness of the reagent layers, which can be used for production of nano-crystalline materials, foils, and coatings [173,174]. The multilayer foils are prepared by means of magnetron sputtering ([174] for details). An example of the microstructure of such a foil prepared from the Ti–Al system [175] is shown in Fig. 36a. A columnar grains with diameters equal to $1 \mu\text{m}$ or less, can be observed at the fracture of the foil (Fig. 36b). The length of these columnar microstructure elements approaches the total thickness of the foil, which is about $18\text{--}20 \mu\text{m}$. Each columnar element consists of many alternating layers of Ti and Al, therefore, it may be considered as one composite Ti/Al grain.

Among the unique features of combustion wave propagation in such media, there are exceptionally high

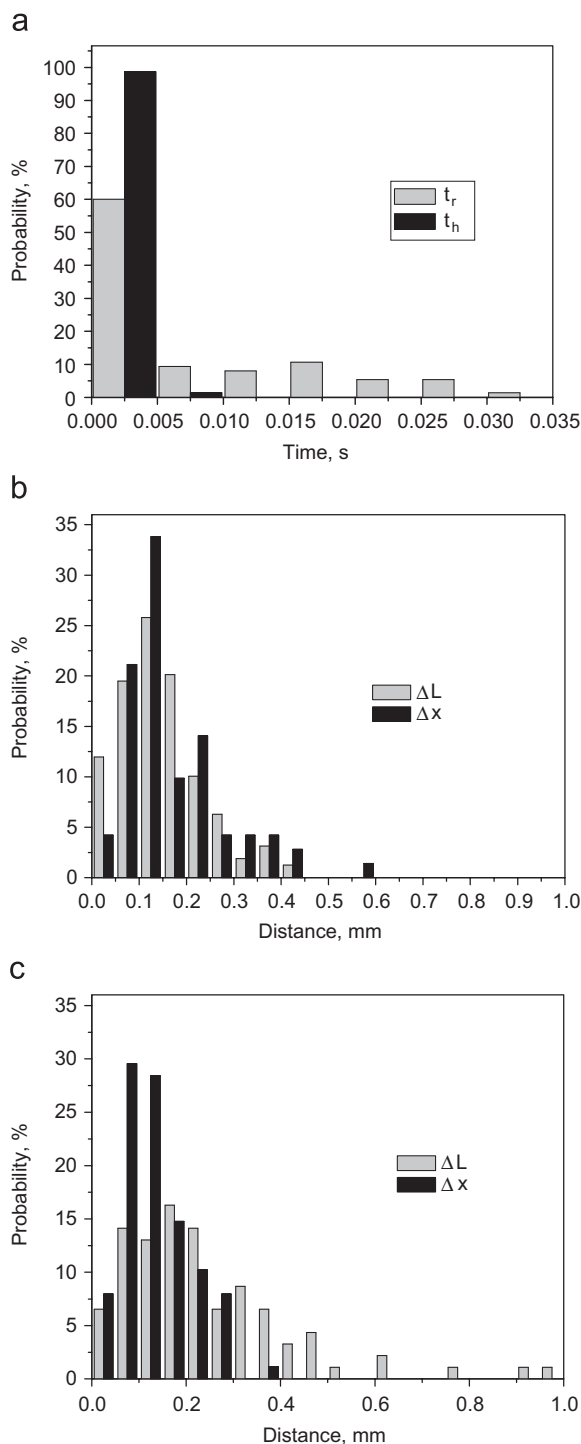


Fig. 35. Statistic treatment of the results of high speed digital micro-video records (adopted from Ref. [172]): (a) distributions of hesitation (t_h) and reaction (t_r) times measured during heterogeneous combustion of mechanically-activated complex Ni–Al particles; (b, c) distributions of distances between composite particles in the green mixture (ΔL) and lengths of the combustion front jumps (Δx). Porosity of the mixture: (a) –30%, (b) –45% and (c) –25%.

velocities of the reaction front and low temperatures of reaction initiation [173,175]. Due to good contact between nano-layered reactants (see Fig. 36), propagation of the combustion wave in this pore-free multi-layer foil is an

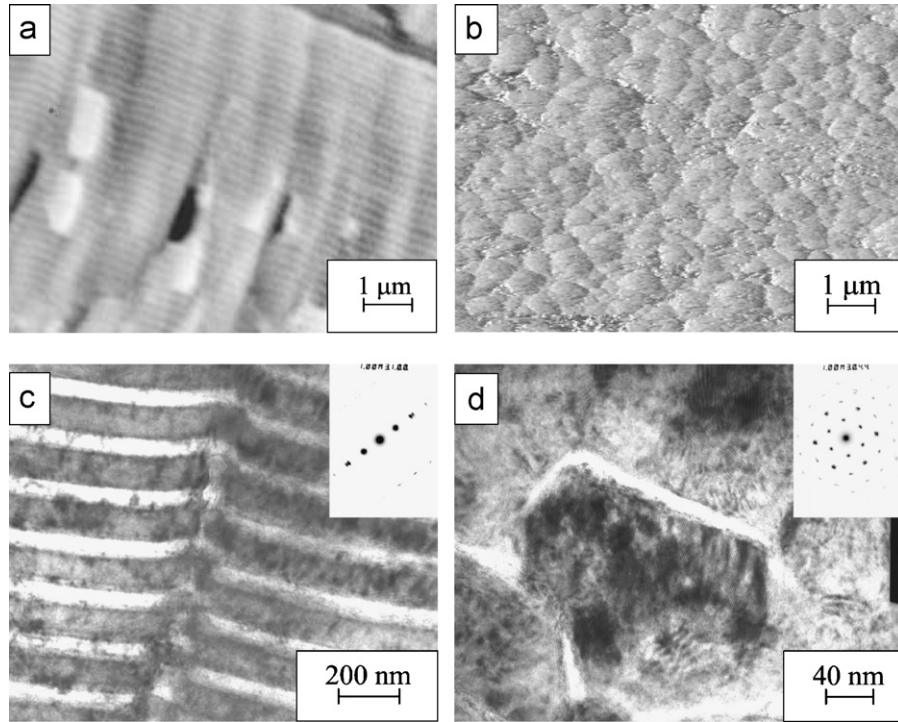


Fig. 36. Microstructure of a multilayer Ti/Al film Ti/Al: (a) SEM picture of the foil fracture; (b) atomic scanning tunneling microscopy of the foil surface; (c, d) TEM and electron micro-diffraction with sample oriented parallel (c) or perpendicular (d) to the electron beam (adopted from Ref. [176]).

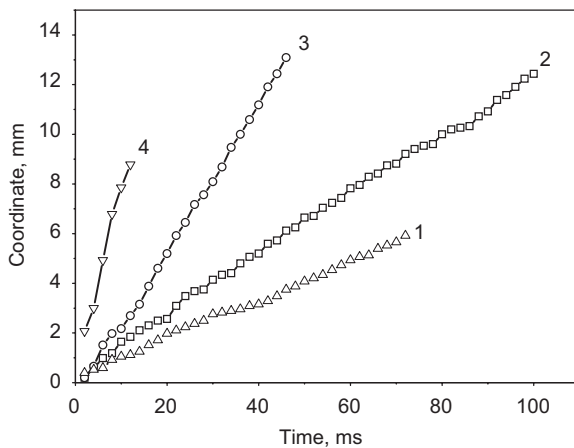


Fig. 37. Dependence of the combustion front coordinate on time: 1—foil Ti/Al, 46 layers, 400 nm each, $T_0 = 700$ K; 2—foil Ti/Al, 190 layers, 100 nm each, $T_0 = 500$ K; 3—foil Ti/Al, 190 layers, 100 nm each, $T_0 = 600$ K; 4—foil Ti/3Al, 400 layers, 50 nm each, $T_0 = 300$ K (adopted from Ref. [178]).

example of “true” *homogeneous* gasless combustion. Fig. 37 shows the position of the combustion front as a function of time for a Ti–Al foil obtained by the HSVR technique under different experimental conditions [177]. In all cases, the coordinate (position) of the front changes linearly with time. Also, distributions of local velocities (Fig. 38) indicate that their instantaneous value never drops to zero, as is typically observed in powder mixtures.

Also, it was suggested that deviation of instantaneous velocities (average value 71 ± 5 cm/s, while instantaneous velocity spreads from 20 to 90 cm/s) is related to the thermal factors, such as heat evolution and heat losses and does not correlate with the fine microstructure of the foils. It was concluded that the combustion process in such Ti–Al multi-layer foils most likely is an example of *quasi-homogeneous* combustion, where the scale of heat conduction (preheating zone) exceeds the size of reactant layers. Combustion velocity of the multilayer foils decreases with increasing layer thickness according to a parabolic law, which indicates that the process is diffusion-limited. However, note that combustion mechanisms in multilayer foils (especially with nano-scale layers) are not yet adequately understood.

Thus, the model experiments confirmed the existence of discrete and quasi-homogeneous modes in the most pronounced form. And it was demonstrated that the experimental approach is a powerful tool for verification of the nature and mechanisms of such complex phenomenon as combustion of heterogeneous systems.

5. Concluding remarks

An overview of recent experimental and theoretical discoveries demonstrates that heterogeneity of the reaction media not only influences the kinetics of chemical reaction (i.e., local rate of heat evolution) but often determines the process of heat transfer. When the governing effect of

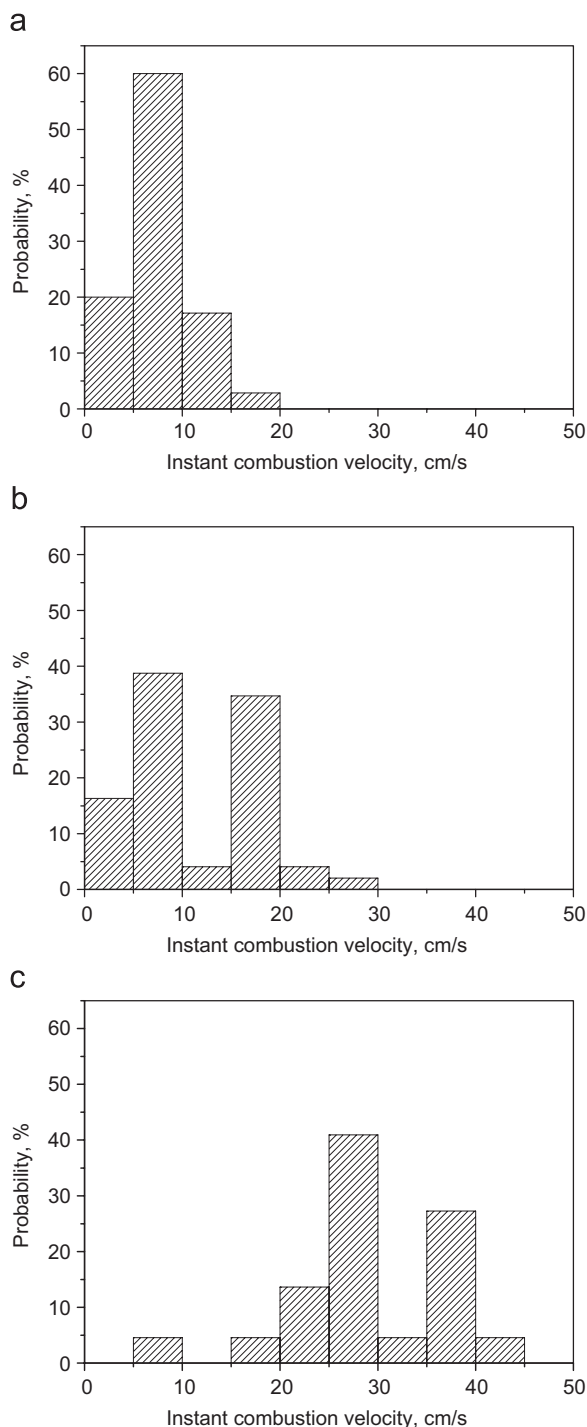


Fig. 38. Distributions of instantaneous combustion velocity: (a) foil Ti/Al, 46 layers, 400 nm each, $T_0 = 700$ K; (b) foil Ti/Al, 190 layers, 100 nm each, $T_0 = 500$ K and (c) foil Ti/Al, 190 layers, 100 nm each, $T_0 = 600$ K (adopted from Ref. [178]).

heterogeneity is limited by a specific form of heat evolution, well-developed theoretical models based on continuous heat transfer equations provide satisfactory description of the combustion process. In the other case, when heat transfer undergoes strong disturbance from the heterogeneous microstructure and non-uniform thermal properties of reactive media (e.g. powder mixtures,

pyrotechnical compositions, etc.), novel discrete models lead to a more adequate description of local and global behavior of the combustion wave. These discrete models, as well as their experimental prerequisites and proofs, have been in the focus of present work.

Detailed analysis of experimental results has shown that, in many cases, the reaction front propagates as a sequence of rapid high-temperature scintillations separated by relatively long periods of hesitation. It was also found that the parameters of such micro-heterogeneous discrete reaction waves closely correlate with the characteristics of the reaction media. Finally, global behavior characteristics of heterogeneous combustion waves, such as the effective energy of activation or limits of steady-state combustion, can be explained and predicted in the frames of the discrete approach.

Despite of the considerable progress in the investigation of discrete reaction waves which was made during last decade, we have to admit that the study of rapid reaction propagation in random media is only in its early stage. Progress in both experimental and theoretical directions is required for deeper understanding of the phenomenon, which will allow for precise control over the combustion processes in complex heterogeneous media. First of all, it is related to the development of the experimental methods, which allow *simultaneous* investigation of the reaction wave propagation and *transformation* of the heterogeneous reactive media on different time and length scales. Also, it is critical to investigate the influence of the reaction media microstructure on important processes which typically accompany combustion, i.e. inhomogeneous transport of melts in porous structures, fluid and gas convection, heterogeneous thermal conductivity. For some applications, such as combustion synthesis of materials, it is important to find out correlations between microstructure of the initial media, characteristics of the reaction front, and microstructure of the final products. The obtained results will allow the development of theoretical approaches which account for a transformation of the reaction media structure in the combustion wave and 3D models which account for the complexity of the heterogeneous media.

Currently, a kind of competition between quasi-homogeneous and discrete paradigms occurs, which helps better understand the combustion processes in heterogeneous systems. As shown above, combustion occurs in quasi-homogeneous or discrete modes depending on the ratio of characteristic times of chemical reaction and heat transfer between the reaction cells. However, direct measuring of this governing parameter represents a real challenge for experimental methods in combustion science. Thus, Table 7 summarizes empirical results, which show the applicability of the competing approaches to some specific combustion processes. Many of the existing theoretical models satisfactorily explain the specific experimental data, but none of them can justify the whole ensemble of observations and provide comprehensive patterns for the

Table 7
Competitive analysis of quasi-homogeneous and discrete approaches to different combustion processes

Type of combustion phenomenon	Applicability of the homogeneous and quasi-homogeneous models	Applicability of discrete models
<i>Combustion synthesis (powder mixtures, solid products)</i>		
Premixed gas flames	Homogeneous theory describes main features of the process	Not applicable
Propellants	Quasi-homogeneous approach that accounts the specific forms of the heat evolution kinetics which inherent to heterogeneous processes gives good approximation of the experimental results	An attempt to use heterogeneous (“relaxation”) model did not succeed
Macroscopic behavior of the combustion wave: velocity dependences on main experimental parameters (porosity, heat losses, specific heat of reaction, etc.)	Qualitatively explain main tendencies. Quantitative calculations require essentially unknown adjustable parameters, such as <i>thermal and mass diffusivities</i> in the combustion front	Qualitatively explain main tendencies. Quantitative calculations require utilization of adjustable parameters, such as <i>heat-transfer coefficients</i> of the contacts between particles in the combustion front
Shape of temperature profiles of the combustion waves	Can explain plateaus but not super adiabatic peaks (treat them as manifestation of oscillating regime)	Explain all known features, including local super-adiabatic peaks
Effective value of the activation energy (E)	Relate each experimentally measured value to the diffusion in solid or liquid phases; suggest no explanation for tendency of increasing E with increasing combustion temperature	Give general explanation of the measured values of E and main tendency, basing only on the heat-transfer process in heterogeneous mixtures
Boundary between steady-state and oscillation regimes	Obvious discrepancy with many SHS-systems	Good agreement with all studied SHS-systems
Microscopic features of the combustion waves: hot spots, random jumps of the local combustion velocity, correlation with microstructure of heterogeneous mixtures	Not applicable	Give explanation for all these phenomena and utilize them as experimental basis of the models

complex process. We hope that the ideas, approaches, and results discussed in this review will induce new fundamental studies of this existing phenomenon, which in turn will lead to numerous novel applications.

Acknowledgments

The Indiana 21st Century Research and Technology Fund, as well as Russian Foundation for Basic Research (RFBR) have partially supported this work. We also thank Mr. J.D.E. White for help in preparation of the manuscript.

References

- [1] Merzhanov AG, Mukasyan AS, Rogachev AS, Sytchev AE, Varma A. Microstructure of combustion wave in heterogeneous gasless systems. *Combust Explos Shock Wave* 1996;32(6):334–47.
- [2] Varma A, Rogachev AS, Mukasyan AS, Hwang S. Complex behavior of self-propagating reaction waves in heterogeneous media. *Proc Natl Acad Sci USA* 1998;95:11053–8.
- [3] Frolov YV, Pivkina AN, Aleshin VV. Structure of HCS and its influence on combustion wave. *Int J Self-Propagat High-Temp Synth* 2001;10(1):31–54.
- [4] Zhang JY, Fu ZY, Wang WM, Zhang QJ. A marco-homogenous and micro-heterogeneous model for self-propagating high temperature synthesis. *Mater Sci For* 2005;475(4):475–9.
- [5] Pivkin NM, Pelych J. High-frequency instability of combustion in solid rocket motors. *Propulsion Power* 1995;11(4):651–6.
- [6] Smirnov VN, Petulov VY, Chuiko SV, Sokolovskii FS, Nechai GV. Specific low-frequency instability of combustion for a micro-heterogeneous charge in a rocket chamber. *Khim Fiz* 1998;17(8):121–30.
- [7] Grabski R, Frank M. Theoretical investigation of flame structures. *Int Ann Conf ICT* 1991;122. 113/1–8.
- [8] Suzuki A, Yamamoto T, Aoki H, Miura T. Percolation model for simulation of coal combustion process. *Proc Combust Inst* 2002; 29:459–66.
- [9] Miccio F. Modeling percolative fragmentation during conversion of entrained char particles. *Korean J Chem Eng* 2004;21(2):404–11.
- [10] Sheng C, Azevedo JLT. Modeling biomass devolatilization using the chemical percolation devolatilization model for the main components. *Proc Combust Inst* 2002;29:407–14.
- [11] Favier C. Percolation model of fire dynamic. *Phys Lett A* 2004;330:396–401.
- [12] Viegas DG. *Philos Trans R Soc Lond A* 1998;356:2907.
- [13] Gardner RH, Romme WH, Turner MG. Predicting forest fire effects at landscape scales. In: Mladenoff DJ, Baker WL, editors. *Spatial modeling of forest landscapes: approaches and applications*. Cambridge: Cambridge University Press; 1999. p. 163–85.
- [14] Scala F, Salatino P, Chirone R. Fluidized bed combustion of biomass char of Robinia pseudoacacia. *Energy Fuels* 2000;14(4):781–90.
- [15] Molerus O. Appropriately defined dimensionless groups for the description of flow phenomena in dispersed systems. *Chem Eng Sci* 1998;53(4):753–9.
- [16] Marban G, Pis JJ. Fuertes AB Characterizing fuels for atmospheric fluidized bed combustion. *Combust Flame* 1995;103(1/2):41–58.
- [17] Kauffman CW, Nicholls JA. Shock-wave ignition of liquid fuel drops. *AIAA J* 1971;9(5):880–5.
- [18] Fedorov AV. Mathematical modeling of the ignition of a cloud of microdrops of a hydrocarbon fuel. *Fiz Goren Vzryva* 2002;38(5):97–100.
- [19] Umamura A, Takamori S. Percolation theory for flame propagation in non- or less-volatile fuel spray: a conceptual analysis to group combustion excitation mechanism. *Combust Flame* 2005;141(4):336–49.
- [20] Zeldovich YB, Frank-Kamenetskii DA. Theory of the thermal flame propagation. *Zh Fiz Khim* 1938;12(1):100–5.

- [21] Mallard E, Le Chatelier HL. Combustion des Melanges Gazeux Explosifs. *Annales des Mines Annales des Mines* 1883;4(208): 274–381.
- [22] Mason EW, Wheller RVJ. The uniform movement during the propagation flame. *Chem Soc* 1917;CXI:1044–58.
- [23] Glassman I. Combustion. New York: Academic Press; 1977.
- [24] Zeldovich YB, Barenblatt GI, Librovich VB, Makhviladze GM. *Mathematic theory of combustion and explosions* [Transl.: D.H. McNeil]. New York: Consultant Bureau; 1985.
- [25] Maltsev VM. Combustion diagnostics in SHS systems. *Int J Self-Propagat High-Temp Synth* 1992;1(4):520–9.
- [26] Zenin AA, Merzhanov AG, Nersisyan GA. Thermal wave structure in SHS processes. *Combust Explos Shock Waves* 1981;17(1): 63–74.
- [27] Dunmead SD, Munir ZA, Holt JB. Temperature profile analysis of combustion synthesis: I. Theory and Background. *Am Ceram Soc* 1992;75(1):175–9.
- [28] Anselmi-Tamburini U, Maglia F, Spinolo G, Munir ZA. Use of two-color array pyrometry for characterization of combustion synthesis waves. *J Mat Res* 2000;15(2):572–80.
- [29] Vol'pe BM, Garkol DA, Evstigneev VV, Milyukova IV, Saigutin GV. Study of interaction in the Ni–Al–Cr self-propagating high-temperature synthesis system by high-temperature radiation pyrometry. *Combust Explos Shock Waves* 1995;31(5):550–4.
- [30] Rogachev AS, Mukasyan AS, Varma A. Quenching of gasless combustion wave: time-resolved thermal vision studies. *Combust Sci Tech* 2003;175(2):357–72.
- [31] Karnatak N, Dubois S, Beaufort MF, Vrel D. Kinetics and mechanisms of titanium carbide formation by SHS using time-resolved X-ray diffraction and infrared thermography. *Int J Self-Propagat High-Temp Synth* 2004;12(3):197–209.
- [32] Bachman NN, Belyaev AF. Combustion of the heterogeneous combustion systems. Moscow: Nauka; 1967.
- [33] Filonenko AK, Bunin VA, Vershinnikov VI. Dependence of the combustion rate on diameter for some gas-free compositions. *Khimich Fizika* 1982;2:260–4.
- [34] Holt JB, Munir ZA. Combustion synthesis of titanium carbide: theory and experiment. *J Mater Sci* 1986;21(1):251–9.
- [35] Vadchenko SG. Gasless combustion of a model multilayer system (combustion of slotted disks). *Fiz Goren Vzryva* 2001;37(2):42–50.
- [36] Levashov EA, Bogatov YV, Milovidov AA. Macrokinetics and mechanism of a self-propagating high-temperature synthesis process in titanium-carbon-based systems. *Fiz Goren Vzryva* 1991;27(1): 88–93.
- [37] Merzhanov AG, Rogachev AS. Structural macrokinetics of SHS processes. *Pure Appl Chem* 1992;64(7):941–53.
- [38] Rogachev AS, Shugaev VA, Khomenko IA, Varma A, Kachelmyer C. On the mechanism of structure formation during combustion synthesis of titanium silicides. *Combust Sci Technol* 1995;109(1–6): 53–70.
- [39] Merzhanov AG, Mukasyan AS, Rogachev AS, Sytchev AE, Varma A. Microstructure of combustion wave in heterogeneous gasless systems. *Combust Explos Shock Waves* 1996;32(6):334–47.
- [40] Mukasyan AS, Hwang S, Rogachev AS, Sytchev AE, Merzhanov AG, Varma A. Combustion wave microstructure in heterogeneous gasless systems. *Combust Sci Technol* 1996;115:335–53.
- [41] Varma A, Mukasyan AS. Combustion synthesis of advanced materials: fundamentals and applications. *Korean J Chem Eng* 2004;21(2):527–36.
- [42] Hwang S, Mukasyan AS, Varma A. Mechanism of combustion wave propagation in heterogeneous reaction systems. *Combust Flame* 1998;115:354–63.
- [43] Kochetov NA, Rogachev AS, Merzhanov AG. Causes of the thermal microheterogeneity of a self-propagating high-temperature synthesis wave. *Doklady RAN* 2003;389(1):65–7.
- [44] Mukasyan AS, Rogachev AS, Varma A. Microstructural mechanisms of combustion in heterogeneous reaction media. *Proc Combust Inst* 2000;28:1413–9.
- [45] Mukasyan AS, Rogachev AS, Mercedes M, Varma A. Microstructural correlations between reaction medium and combustion wave propagation in heterogeneous systems. *Chem Eng Sci* 2004;59: 5099–105.
- [46] Li J, Litzinger TA, Thynell ST. Plasma ignition and combustion of JA2 propellant. *Propuls Power* 2005;21(1):44–53.
- [47] Manai G, Delogu F, Schifflini L, Cocco G. Mechanically induced self-propagating combustions: experimental findings and numerical simulation results. *J Mater Sci* 2004;39(16/17):5319–24.
- [48] Wang W, Fu Z, Wang H, Yuan R. Chemistry reaction processes during combustion synthesis of B₂O₃–TiO₂–Mg system. *J Mater Process Tech* 2002;128(1–3):162–8.
- [49] Dreizin EL, Keil DG, Felder W, Vicenzi EP. Phase changes in boron ignition and combustion. *Combust Flame* 1999;119(3):272–90.
- [50] Mukasyan AS, Rogachev AS, Varma A. Mechanisms of reaction wave propagation during combustion synthesis of advanced materials. *Chem Eng Sci* 1999;54(15–16):3357–67.
- [51] Dacombe PJ, Graville SR, Pourkashanian M, Williams A, Yap L. Study of the fragmentation nature of granular coal particles in a high temperature environment. *Coal Sci Technol* 1995;24(1): 651–4.
- [52] Hwang S. Microstructure of wave propagation during combustion synthesis of advanced materials: experiment and theory, PhD thesis, University of Notre Dame, 1997.
- [53] Davies ER. Machine vision: theory, algorithms. Practicalities. London: Academic Press; 1990.
- [54] Grinchuk PS, Rabinovich OS, Rogachev AS, Kochetov NA. Fast and slow modes of the propagation of the combustion front in heterogeneous systems. *JETP Lett* 2006;84(1):11–5.
- [55] Hwang S, Mukasyan AS, Rogachev AS, Varma A. Combustion wave microstructures in gas–solid system: experiments and theory. *Combust Sci Technol* 1997;123:165–83.
- [56] Zenin AA. The thermal structure of solid flames. *Pure Appl Chem* 1990;62(5):889–97.
- [57] Zenin AA, Nersisyan GA. Zonal structure of self-propagating high-temperature synthesis wave for borides near the critical conditions of extinction. *Khim Fiz* 1982;3:411–8.
- [58] Dunmead SD, Munir ZA, Holt JB. Temperature profile analysis of combustion in the Zr–B system using the Boddington–Laye method. *Int J Self-Propagat High-Temp Synth* 1992;1(1):22–32.
- [59] Wang LL, Munir ZA. Kinetic analysis of the combustion synthesis of molybdenum and titanium silicides. *Metall Mater Trans B* 1995; 26(3):595–601.
- [60] Merzhanov AG. Solid flame combustion. Chernogilovka: ISMAN; 2000. 224p.
- [61] Anselmi-Tamburini U, Campari G, Spinolo G. A two-color spatial-scanning pyrometer for the determination of temperature profiles in combustion synthesis reactions. *Rev Sci Instrum* 1995;66(10): 5006–14.
- [62] Garkol DA, Gulyayev PY, Evstigneyev VV, Mukhachev AB. New method for high-velocity luminance pyrometry for studies of self-propagating high-temperature synthesis processes. *Combust Explos Shock Waves* 1994;30(1):72–7.
- [63] Grabski R. Fractal and chaotic properties of combustion processes. *Proc Int Pyrotech Seminar* 1992;18:335–52.
- [64] Frolov YV, Pivkina AN. Fractal structure and characteristics of energy release (combustion) processes in heterogeneous condensed systems. *Fiz Goren Vzryva* 1997;33(5):3–19.
- [65] Frolov YV. Combustion of heterogeneous condensed systems. *Proc Int Pyrotech Seminar* 2000;27:463–84.
- [66] Umemura A, Takamori S. Percolation theory for flame propagation in non- or less-volatile fuel spray: a conceptual analysis to group combustion excitation mechanism. *Combust Flame* 2005;141:336–49.
- [67] Garner WE. Introduction to part I—Explosive reactions considered generally. *Trans Faraday Soc* 1926;XXII:253–66.
- [68] Belyaev AF. Combustion of explosives. *J Phys Chem* 1938;12:93–9.
- [69] Zeldovich YB. To combustion theory of gun powders and explosives. *J Exp Theor Phys* 1942;12(11/12):498–524.

- [70] Margolin AD. The initial stage of burning propellants. Dokl Akad Nauk SSSR 1961;141:1131–4.
- [71] Williams FA. Combustion theory. Reading, MA: Addison-Wesley; 1965.
- [72] Fur ZI. Relaxation mechanism of propagation of combustion in heterogeneous exothermic systems. Russian J Phys Chem 1960; 34(3):289–93.
- [73] Fur ZI. Relaxation mechanism of propagation of combustion in heterogeneous exothermic systems. Russian J Phys Chem 1960; 34(4):621–5.
- [74] Belyaev AF. About relaxation mechanism of combustion wave propagation in the heterogeneous exothermic systems. Russian J Phys Chem 1961;34(6):1374–8.
- [75] Semenov NN. Thermal theory of combustion and explosion. Uspekhi Fizicheskikh Nauk 1940;23:251–92.
- [76] Frank-Kamenetskii DA. Diffusion and heat transfer in chemical kinetics. Princeton: Plenum Press; 1967. 491p.
- [77] Novozilov BV. The rate of propagation of the front of an exothermic reaction in a condensed phase. Dokl Akad Nauk SSSR 1960;131:1400–3.
- [78] Khaikin BI, Merzhanov AG. Theory of thermal propagation of a chemical reaction front. Combust Explos Shock Waves 1966;2: 22–7.
- [79] Merzhanov AG, Khaikin BI. Theory of combustion waves in homogeneous. Prog Energy Combust Sci 1988;14:1–98.
- [80] Xin J. Front propagation in heterogeneous media. SIAM Rev 2000;42(2):161–230.
- [81] Makino A. Fundamental aspects of the heterogeneous flame in the self-propagating high-temperature synthesis process. Prog Energy Combust Sci 2001;27:1–74.
- [82] Aldushin AP. Steady-state propagation of the front of an exothermic reaction in a condensed medium. Prikladnaya Mekhanika i Fizika 1974;3:96–105.
- [83] Hard AP, Phung PV. Propagation of gasless reactions in solids.1. Analytical study of exothermic intermetallic reaction rates. Combust Flame 1973;21(1):91–7.
- [84] Khaikin BI. Theory of the combustion processes in the heterogeneous condensed media. In: Merzhanov AG, editor. Combustion processes in chemical engineering and metallurgy (Russ.). Chernogolovka, Russia: USSR Academy of Science; 1975. p. 227–45.
- [85] Okolovich EV, Merzhanov AG, Khaikin BI, Shkadinskii KG. Propagation of the combustion zone in melting condensed mixtures. Combust Explos Shock Waves 1977;13(3):264–85.
- [86] Varma A, Rogachev AS, Mukasyan AS, Hwang S. Combustion synthesis of advanced materials: principles and applications. Adv Chem Eng 1998;24:79–226.
- [87] Rogachev AS. Microheterogeneous mechanism of gasless combustion. Fiz Goren Vzryva 2003;39(2):38–47.
- [88] Emel'yanov AN, Shkiro VM, Rogachev AS, Kochetov NA. Thermal conductivity of powder mixtures for gas-free combustion. News of Higher Schools, Nonferrous Metallurgy Transactions 2005;1:60–3 (in Russian).
- [89] Merzhanov AG. Propagation of a solid flame in a model heterogeneous system. Dokl Akad Nauk 1997;353(4):504–7.
- [90] Merzhanov AG, Peregudov AN, Gontkovskaya VT. Heterogeneous model of solid combustion: numerical experiment. Dokl Akad Nauk 1998;360(2):217–9.
- [91] Daniel PJ. The theory of flame motion. Proc Roy Soc 1929; 126:393–6.
- [92] Knyazik VA, Merzhanov AG, Shteinberg AS. On combustion mechanism of titanium-carbon system. Dokl Acad Nauk SSSR 1988;301(4):899–902.
- [93] Rogachev AS. Macrokinetics of gasless combustion: old problems and new approaches. Int J Self-Propagat High-Temp Synth 1997;6(2):215–42.
- [94] Rogachev AS, Merzhanov AG. Theory fast combustion wave propagation in the heterogeneous media. Dokl Akad Nauk 1999; 365(6):788–91.
- [95] Varma A, Mukasyan AS, Hwang S. Dynamics of self-propagating reactions in heterogeneous media: experiments and model. Chem Eng Sci 2001;56:1459–66.
- [96] Cooper MG, Mikic BB, Yovanovih MM. Thermal contact conductance. Int J Heat Mass Trans 1969;12:279–300.
- [97] Rabinovich OS, Grinchuk PS, Khina BB, Belyaev AV. Percolation combustion: is it possible in SHS? Int J Self-Propagat High-Temp Synth 2003;11(3):257–70.
- [98] Grinchuk PS, Rabinovich OS. Percolation phase transition during combustion of heterogeneous mixtures. Fiz Goren Vzryva 2004; 40(4):41–53.
- [99] Armstrong RC, Koszykowski ML. Combustion theory for sandwiches of alloyable materials. In: Munir ZA, Holt JB, editors. Combustion and plasma synthesis of high-temperature materials. New York: VCH Publ.; 1990. p. 88–99.
- [100] Nekrasov EA, Smolyakov VK, Maksimov YM. Mathematical model for the titanium-carbon system combustion. Fiz Goren Vzryva 1981;17(5):39–46.
- [101] Aleksandrov VV, Korchagin MA, Boldyrev VV. Mechanism and macrokinetics of reactions accompanying the combustion of SHS systems. Dokl Akad Nauk SSSR 1987;292(4):879–81.
- [102] Aleksandrov VV, Korchagin MA. Mechanism and macrokinetics of reactions accompanying the combustion of SHS systems. Fiz Goren Vzryva 1987;23(5):55–63.
- [103] Kanury AM. A kinetic model for metal+nonmetal reactions. Metall Trans A 1992;23A(9):2349–56.
- [104] Makino A, Law CK. Burning velocity of the heterogeneous flame propagating in the SHS process expressed in explicit form. Combust Flame 1995;101:551–5.
- [105] Lakshminantha MG, Sekhar JA. Influence of multi-dimensional oscillation combustion fronts on thermal profiles. J Mater Sci 1993;28:6403–8.
- [106] Cao G, Varma A. A new expression for velocity of the combustion front during self-propagating high-temperature synthesis. Combust Sci Technol 1994;102:181–91.
- [107] Oliveira AAM, Kaviany M. Role of inter- and intraparticle diffusion in nonuniform particle size gasless compacted-powder combustion synthesis-I: formulation. Int J Heat Mass Trans 1998;42(6):1059–73.
- [108] Oliveira AAM, Kaviany. Role of inter- and intraparticle diffusion in nonuniform particle size gasless compacted powder combustion synthesis-II: results and comparison with experiment. Int J Heat Mass Trans 1998;42(6):1075–95.
- [109] Zuccaro G, Lapenta G, Maizza G. Particle in cell simulation of combustion synthesis of TiC nanoparticles. Comput Phys Commun 2004;162(2):89–101.
- [110] Nekrasov EA, Maksimov YuM, Ziatdinov MKh, Shteinberg AS. Capillary spreading influence on the combustion wave propagation in gasless systems. Fiz Goren Vzryva 1978;14(5):26–33.
- [111] Shcherbakov VA, Shteinberg AS. Macrokinetics of SHS infiltration. Combust Sci Technol 1995;107(1–3):21–9.
- [112] Smolyakov VK. Melting of an inert component in a gasless combustion wave. Fiz Goren Vzryva 2002;38(5):78–84.
- [113] Astapchik AS, Podvoisky EP, Chebotko IS, Khusid BM, Merzhanov AG, Khina BB. Stochastic model for a wavelike isothermal reaction in condensed heterogeneous systems. Phys Rev E 1993;47: 319–26.
- [114] Goroshin S, Lee JH, Shoshin Yu. Effect of the discrete nature of the heat sources on flame propagation in particulate suspensions. Proc Combust Inst 1998;26:743–9.
- [115] Beck JM, Volpert VA. Nonlinear dynamics in a simple model of solid flame microstructure. Physica D 2003;182:86–102.
- [116] Rashkovskii SA. Ignition center combustion of heterogeneous condensed mixtures. Thermal percolation. Fiz Goren Vzryva 2005;41(1):41–54.
- [117] Firsov AN, Shkadinskii KG. Nonstationary combustion regimes of gasless condensed substances periodically diluted by inert admixtures. Fiz Goren Vzryva 1988;24(6):93–8.

- [118] Krishenik PM, Shkadinskii KG. Regimes of wave transformation of heterogeneous systems with nonlinear heat transfer. *Khim Fiz* 2004;23(8):75–9.
- [119] Krishenik PM, Merzhanov AG, Shkadinskii KG. Conditions for frontal transformation of high-energy structured heterogeneous systems. *Fiz Goren Vzryva* 2005;41(2):51–61.
- [120] Jackson TL, Buckmaster J. Heterogeneous propellant combustion. *AIAA J* 2002;40(6):1122–30.
- [121] Massa L, Jackson TL, Buckmaster J. New kinetics for a model of heterogeneous propellant combustion. *J Propul Power* 2005;21(5):914–24.
- [122] Provatas N, Ala-Nissila T, Martin Grant M, Elder KR, Piche L. Flame Propagation in random media. *Phys Rev E* 1995;51(5):4232–6.
- [123] Provatas N, Ala-Nissila T, Martin Grant M, Elder KR, Piche L. Scaling, propagation, and kinetic roughening of flame fronts in random media. *J Stat Phys* 1995;81(3/4):737–59.
- [124] Luikov AV, Shashkov AG, Vasiliev LL, Fraiman YiE. Thermal conductivity of porous media. *Int J Heat Mass Trans* 1968;11:11–140.
- [125] Fletcher LS. Recent development in contact conductance heat transfer. *J Heat Trans* 1988;110:1059–70.
- [126] Kaviany M. Principles of heat transfer in porous media. New York: Springer; 1991.
- [127] Goel NS, Geroc JS, Lehman G. A simple model for heat conduction in heterogeneous materials and irregular boundaries. *Int Comm Heat Mass Trans* 1992;19(4):519–30.
- [128] Hard AP, Phung PV. Propagation of gasless reactions in solids. 1. Analytical study of exothermic intermetallic reaction rates. *Combust Flame* 1973;21(1):77–89.
- [129] Aleksandrov VV, Gruzdev VA, Kovalenko YA. Thermal conduction of some SHS-systems on the basis of aluminium. *Fiz Goren Vzryva* 1985;21(1):98–104.
- [130] Kochetov NA, Rogachev AS, Emel'yanov AN, Illarionova EV, Shkiro VM. Microstructure of heterogeneous mixtures for gasless combustion. *Fiz Goren Vzryva* 1994;40(5):74–80.
- [131] Vadchenko SG, Gordoplov AY, Mukasyan AS. The effect of molecular and conductive mechanism of heat transfer on the propagation of heterogeneous combustion waves. *Phys Dokl* 1997;42(6):288–90.
- [132] Mann AB, Gavens AJ, Reiss ME, Van Heerden D, Bao G, Weihs TP. Modeling and characterizing the propagation velocity of exothermic reactions in multilayer foils. *J Appl Phys* 1997;82(3):1178–88.
- [133] Deevi SC. Difusional reactions in the combustion synthesis of MoSi_2 . *Mater. Sci Eng A* 1992;149:241–51.
- [134] Philpot KA, Munir ZA, Holt JB. An investigation of the synthesis of nickel aluminides through gasless combustion. *J Mater Sci* 1987;22(1):159–69.
- [135] Kharatyan SL, Chatilyan HA, Mukasyan AS, Simonetti DA, Varma A. Influence of heating rate on kinetics of rapid high-temperature reactions in condensed heterogeneous media: Mo–Si System. *AICHE J* 2005;51(1):261–70.
- [136] Rogachev AS, Mukasyan AS, Merzhanov AG. Structural transitions in the gasless combustion of titanium-carbon and titanium-boron systems. *Dokl Phys Chem* 1987;297(6):1240–3.
- [137] Rogachev AS, Varma A, Merzhanov AG. The mechanism of self-propagating high-temperature synthesis of nickel aluminides. Part I. Formation of the product microstructure in a combustion wave. *Int J Self-Propagat High-Temp Synth* 1993;2(1):25–38.
- [138] Bertolino N, Monagheddua M, Tacca A, Giuliana P, Zanottia C, Anselmi Tamburini U. Ignition mechanism in combustion synthesis of Ti–Al and Ti–Ni systems. *Intermetallics* 2003;11:41–9.
- [139] Shen P, Guo ZX, Hu JD, Lian JS, Sun BY. Study on laser ignition of Ni-33.3at%Al power compacts. *Scripta Mater* 2000;43:893–8.
- [140] Rogachev AS, Mukasyan AS, Varma A. Thermal explosion modes in gasless heterogeneous systems. *Mater Synth Proc* 2002;10(1):29–34.
- [141] Thiers L, Mukasyan AS, Varma A. Thermal explosion in Ni–Al system: influence of reaction medium microstructure. *Combust Flame* 2002;131(1–2):198–209.
- [142] Rice RW. Microstructural aspects of fabricating bodies by self-propagating synthesis. *J Mater Sci* 1991;26:6533–41.
- [143] Shkiro VM, Borovinskaya IP. The study of combustion regularities of titanium and carbon mixtures. In: *Combustion Processes in Chemical Technology and Metallurgy*, Chernogolovka, 1975. p. 253–8.
- [144] Kiriyashkin AI, Maksimov YuM, Nekrasov EA. On the mechanism of titanium interaction with carbon in combustion wave. *Fiz Goren Vzryva* 1981;17:33–6.
- [145] Dunmead SD, Readey DW, Semler ChE, Holt JB. Kinetics of combustion synthesis in the titanium–carbon–nickel system. *Am Ceram Soc* 1989;72(12):2318–20.
- [146] Borovinskaya IP, Merzhanov AG, Novikov NP, Filonenko AK. Gasless combustion of powder mixtures of the transition metals with boron. *Fiz Goren Vzryva* 1974;10(1):4–15.
- [147] Azatyan TS, Mal'tsev VM, Merzhanov AG, Seleznev VL. Propagation mechanism of combustion wave in titanium–boron mixtures. *Fiz Goren Vzryva* 1980;16(2):37–42.
- [148] Andreev VA, Mal'tsev VM, Seleznev VL. Investigation of hafnium and boron mixtures combustion by optical pyrometry. *Fiz Goren Vzryva* 1980;16:18–23.
- [149] Azatyan TS, Mal'tsev VM, Merzhanov AG, Seleznev VL. Some peculiarities of titanium-silicon mixtures burning. *Fiz Goren Vzryva* 1979;15(1):43–9.
- [150] Naiborodenko YS, Itin VI. Gasless combustion process study for the powder mixtures of the different metals. 1. Peculiarities and combustion mechanism. *Fiz Goren Vzryva* 1975;11(3):343–53.
- [151] Itin VI, Bratchikov AD, Lepinskikh AV. Phase transition at combustion of copper and aluminium powders mixture. *Fiz Goren Vzryva* 1981;17(5):31–4.
- [152] Itin VI, Naiborodenko YS. Vysokotemperaturnyi sintez intermetallicheskih soedinenii (High-temperature synthesis of intermetallic compounds). Tomsk: Izd. Tomsk Univ.; 1989. 214p.
- [153] Dunmead SD, Munir ZA, Holt JB. Temperature profile analysis in combustion synthesis: II. Experimental observations. *Am Ceram Soc* 1992;75(1):180–8.
- [154] Zenin AA, Nersisyan GA. The zone structure of the SHS wave for the borides formation near the critical combustion conditions. Chernogolovka: Preprint Inst. Chem. Phys.; 1980.
- [155] Boddington T, Laye PG, Tipping J, Whalley D. Kinetics analysis of temperature profiles of pyrotechnic systems. *Combust Flame* 1986;63:359–86.
- [156] Kachelmyer CR, Varma A, Rogachev AS, Sytschev AE. Influence of reaction mixture porosity on the effective kinetics of gasless combustion synthesis. *Industr Eng Chem Res* 1998;37(6):2246–9.
- [157] Grigoryan HE, Rogachev AS, Sytschev AE. Gasless combustion in the Ti–C–Si system. *Int J Self-Propagat High-Temp Synth* 1997;6(1):29–39.
- [158] Shkadinskii KG, Khaikin BI, Merzhanov AG. Propagation of a pulsating exothermic reaction front in the condensed phase. *Combust Explos Shock Waves* 1971;7(1):19–28.
- [159] Machviladze GM, Novozilov BV. Two-dimensional stability of combustion of condensed systems. *Zhurn Prikl Mekhaniki I Tekhn Fiziki* 1971;5:51–8.
- [160] Matkowsky BJ, Sivashinsky GI. Propagation of a pulsating reaction front in solid fuel combustion. *SIAM J Appl Math* 1978;35:465–9.
- [161] Shafirovich E, Mukasyan AS, Thiers L, Varma A, Legrand B, Chauveau C, et al. Ignition and combustion of Al particles clad by Ni. *Combust Sci Technol* 2002;174(3):125–40.
- [162] Mukasyan AS, Lau C, Varma A. Gasless combustion of aluminum particles clad by nickel. *Combust Sci Technol* 2001;170:67–85.
- [163] Dubois S, Vrel D, Cochevin B, Karnatak N, Heian EM. Recent developments in self-propagating high-temperature synthesis of TiC. *Recent Res Develop Phys* 2004;5(2):569–605.

- [164] Maglia F, Anselmi-Tamburini U, Deidda C, Delogu F, Cocco G, Munir ZA. Role of mechanical activation in SHS synthesis of TiC. *J Mater Sci* 2004;39(16–17):5227–30.
- [165] Blobaum KJ, Reiss ME, Plitzko JM, Weihs TP. Deposition and characterization of a self-propagating CuO_x/Al thermite reaction in a multilayer foil geometry. *J App Phys* 2003;94(5):2915–22.
- [166] Rivero C, Gergaud P, Gailhanou M, Thomas O, Froment B, Jaouen H, et al. Combined synchrotron X-ray diffraction and wafer curvature measurements during Ni–Si reactive film formation. *Appl Phys Lett* 2005;87(4):041904/1–3.
- [167] Merzhanov AG, Rogachev AS, Sytshev AE. Self-propagating high-temperature synthesis: first experiment in space. *Dokl Akad Nauk* 1998;362:217–21.
- [168] Merzhanov AG. SHS process in microgravity activities: first experiments in space. *Adv Space Res* 2002;29:487–95.
- [169] Mukasyan AS, Lau C, Varma A. Influence of gravity on combustion synthesis of advanced materials. *AIAA J* 2005;43(2):225–45.
- [170] Bernard F, Gaffet E. Mechanical alloying in SHS research. *Int J Self-Propagat High-Temp Synth* 2001;10(2):109–32.
- [171] Grigorieva T, Korchagin M, Lyakhov N. Combination of SHS and mechanochemical synthesis for nanopowder technologies. *KONA Powder Particles* 2002;20:144–58.
- [172] Rogachev AS, Kochetov NA, Kurbatkina VV, Levashov EA, Grinshuk PS, Rabinovich OS, et al. Microstructural aspects of gasless combustion of mechanically activated mixtures. I. High-speed microvideorecording of the Ni–Al composition. *Combust Explos Shock Waves* 2006;42(4):421–9.
- [173] Barbee TW, Weihs T. US Patent No. 5538795. Jul. 23, 1996.
- [174] Reiss ME, Esber CM, Van Heerden D, Gavens AJ, Williams ME, Weihs TP. Self-propagating formation reactions in Nb/Si multilayers. *Mater Sci Eng* 1999;A261:217–22.
- [175] Elistratov NG, Nosyrev AN, Khvesyuk VI, Tsygankov PA. The experimental ion-assisted deposition equipment for producing the multilayers materials. *Appl Phys (Russ.)* 2001;3:8–11.
- [176] Gachon JC, Rogachev AS, Grigoryan HE, Illarionova EV, Kuntz JJ, Kovalev D, et al. On the mechanism of heterogeneous reaction and phase formation in Ti/Al multilayer nanofilms. *Acta Mater* 2005;53(4):1225–31.
- [177] Rogachev AS, Grigoryan AE, Illarionova EV, Kanel IG, Merzhanov AG, Nosyrev AN, et al. Gasless combustion of Ti–Al bimetallic multilayer nanofilms. *Combust Explos Shock Wave* 2004;40(2):166–71.
- [178] Rogachev AS, Kochetov NA, Yagubova IY, Grigoryan HE, Sachkova VI, Nosyrev NV, et al. Some features of SHS-process in the multilayer Ti/Al foils. *Int J SHS* 2004;13(4):285–91.